Technische Universität München
III. Medizinische Klinik und Poliklinik
Klinikum rechts der Isar

The role of the deubiquitinase USP9X in lymphomagenesis

Felicia Miranda Katharina Andresen

Vollständiger Abdruck der von der Fakultät für Medizin der Technischen Universität München zur Erlangung des akademischen Grades eines Doktors der Medizin genehmigten Dissertation.

Vorsitzende: Prof. Dr. Gabriele Multhoff

Prüfer der Dissertation: 1. Prof. Dr. Florian Bassermann
2. Prof. Dr. Barbara Wollenberg

Die Dissertation wurde am 23.06.2020 bei der Technischen Universität München eingereicht und durch die Fakultät für Medizin am 01.12.2020 angenommen.

Table of contents

Abbreviations

Akt ..... protein kinase B (PKB)
aaIPI ..... Age-adjusted International Prognostic Index
ABC ..... activated B-cell
APS ..... ammonium persulfate
ATP ..... adenosine triphosphate
ASCT ..... autologous stem cell transplantation
BCL2 ..... B-cell lymphoma 2 protein
BCL6 ..... B-cell lymphoma 6 protein
BES ..... N,N-Bis(2-hydroxyethyl)taurine
BIR ..... baculovirus IAP repeats
bp ..... base pairs
BS ..... bovine serum
BSA ..... bovine serum albumin
$CaCl_2$ ..... calcium chloride
$CaPO_4$ ..... calcium phosphate
cDNA ..... complementary deoxyribonucleic acid
CD3 ..... cluster of differentiation 3
CD5 ..... cluster of differentiation 5
CD10 ..... cluster of differentiation 10
CD19 ..... cluster of differentiation 19
CD20 ..... cluster of differentiation 20
CD23 ..... cluster of differentiation 23
CD45 ..... cluster of differentiation 45
CD79a ..... cluster of differentiation 79a
CDK1 ..... cyclin-dependent kinase 1
CHOP ..... cyclophosphamide, doxorubicin, vincristine, prednisone
dH_2O ..... distilled H_2O (water)
DLBCL ..... diffuse large B-cell lymphoma
DMEM ..... Dulbecco's Modified Eagle's Medium
DMSO ..... dimethyl sulfoxide
DNA ..... deoxyribonucleic acid
dNTP ..... deoxynucleoside triphosphate mix
dsDNA ..... double-stranded DNA
DTT ..... Dithiotheritol
DUB ..... deubiquitinase
ECOG ..... Eastern Cooperative Oncology Group
EDTA ..... ethylenediaminetetraacetic acid

ELISA ..... enzyme-linked immunosorbent assay
EtBr ..... ethidium bromide
FACS ..... fluorescence-activated cell sorting
FBS ..... fetal bovine serum
FDA ..... (U.S.) Food and Drug Administration
FOXP1 ..... forkhead box protein P1
FSC ..... forward scatter
Fw ..... forward
G2P ..... glycerol 2-phosphate disodium salt pentahydrate
GCB ..... germinal center B cell
GCTE1 ..... germinal center B cell expressed transcript 1
GEP ..... gene-expression profiling
h(rs) ..... hour(s)
HBV ..... hepatitis B virus
HCV ..... hepatitis C virus
HD ..... high dose
HDC ..... high-dose chemotherapy
HIV ..... human immunodeficiency virus
IgH ..... immunoglobulin heavy chain
IHC ..... immunohistochemistry
IPI ..... International Prognostic Index
IRES ..... internal ribosomal entry site
IRF4 ..... interferon regulatory factor 4
kb ..... kilobase pairs
kDa ..... kilo Dalton
LDH ..... lactate dehydrogenase
LMO2 ..... LIM domain only 2 (rhombotin-like 1)
MAPK ..... mitogen-activated protein kinase
mRNA ..... messenger ribonucleic acid
mTOR ..... mammalian/mechanistic inhibitor of rapamycin
MYC ..... avian myelocytomatosis viral oncogene homolog
NaF ..... sodium fluoride
NaCl ..... sodium chloride
NaVa ..... sodium orthovanadate
NEAA ..... nonessential amino acids
NF-kB ..... nuclear factor 'kappa-light-chain-enhancer' of activated B-cells
NHL ..... non-Hodgkin lymphoma
OptiMEM ..... phosphate buffered saline

ORR ..... overall response rates
OS ..... overall survival
PBS ..... phosphate-buffered saline
PCR ..... polymerase chain reaction
qPCR ..... quantitative polymerase chain reaction
PFS ..... progression-free survival
PIN ..... peptidylprolyl isomerase inhibitor
PI3K phosphatidylinositol-4,5-bisphosphate 3-kinase
PMSF ..... phenylmethylsulfonylfluoride
P/S ..... penicillin/streptomycin
PI ..... propidium iodide
Puro ..... puromycin
RING ..... really interesting gene
RNA ..... ribonucleic acid
RNAi ..... RNA interference
RPMI-1640 ..... Roswell Park Memorial Institute 1640 Medium
RT ..... room temperature
RT-PCR ..... reverse transcription-polymerase chain reaction
rv ..... reverse
SAC ..... spindle assembly checkpoint
SD ..... standard deviation
SDS ..... sodium dodecyl sulfate
SDS-PAGE ..... sodium dodecyl sulfate-polyacrylamide gel electrophoresis
shRNA ..... small hairpin ribonucleic acid
siRNA ..... small interfering ribonucleic acid
SSC ..... sideward scatter
TBE ..... tris borate EDTA
TEMED ..... tetramethylethylenediamine
TLCK ..... tosyl-L-lysyl-chloromethyl-ketone
TPCK ..... tosyl-phenylalanyl-chloromethyl-ketone
TRC ..... The RNAi Consortium
TRIS ..... tris(hydroxymethyl)aminomethane
UPS ..... ubiquitin-proteasome system
USA ..... United States of America
USP9X ..... ubiquitin-specific protease 9X
V ..... Volt
WB ..... washing buffer
XIAP ..... X-linked inhibitor of apoptosis

1. Introduction

1.1. Diffuse large B-cell lymphoma

1.1.1. Disease characterization, epidemiology, and etiology

Diffuse large B-cell lymphoma (DLBCL) is considered to be the most common aggressive Non-Hodgkin lymphoma in adults (Shaffer, Young, & Staudt, 2012). It arises from malignant B cells and is characterized by rapid clinical onset with a good response to first-line therapy but high relapse rates. The incidence rate of DLBCL is estimated at 3.81 to 7.14 per 100,000 (Morton et al., 2006; Sant et al., 2010). DLBCL amounts to approximately 30% of non-Hodgkin lymphomas (NHL) and 80% of aggressive lymphomas (Campo et al., 2011). It is slightly more common in men than women (Possinger, 2015) and the median age of diagnosis is approximately 66 years (Howlader N, 1975-2013). The etiology of aggressive lymphomas is mostly unknown. Nonetheless, there are several risk factors for the disease, such as immunosuppression (hereditary, pharmacological), infections (e.g., HIV infection, EBV infection), herbicides, pesticides, and indolent lymphomas (Blinder, Fisher, & Lymphoma Research Foundation, 2008).

1.1.2. Disease presentation and classification

DLBCL presents with a rapidly progressing lymphadenopathy or B symptoms. Extranodal involvement is seen in approximately 40% of cases (Martelli et al., 2013) and can present as organ failure (e.g., liver, renal, respiratory failure, etc.) or with signs of bone marrow involvement (cytopenias, infections, e.g.). Some patients also show systemic symptoms like weight loss > 10% in 6 months, fever > 38°C or drenching night sweats, so-called B symptoms. Diffuse large B-cell lymphoma can be classified according to clinical features, morphology, immunophenotype, immunohistochemistry, cytogenetic profiling, and gene expression analysis.

1.1.2.1. Clinical classification

The International Prognostic Index (IPI) is a clinical scoring system to evaluate the prognosis and long-term survival of patients with aggressive NHL (Table 1). It is based on performance status, Ann-Arbor-stage, extranodal involvement, and LDH serum level. The age-adjusted IPI (aaIPI) is used for patients under 60 years, in which the extranodal involvement does not have an impact on the prognosis ("A predictive model for aggressive non-Hodgkin's lymphoma. The International Non-Hodgkin's Lymphoma Prognostic Factors Project," 1993; Ziepert et al., 2010).

International Prognostic Index (IPI)	
Risk factors	- Age > 60 years - Performance status 2-4 - Ann-Arbor-stage III-IV - Extranodal involvement ≥ 2 - LDH elevation

Risk categories	1 Low risk: 0 - 1 (3y-OS: 91%) 2 Low intermediate risk: 2 (3y-OS: 81%) 3 High intermediate risk: 3 (3y-OS: 65%) 4 High risk: 4-5 (3y-OS: 59%)
Age-adjusted International Prognostic Index (aaIPI)	
Risk factors	- Patients ≤ 60 years - Performance status 2 – 4 - Ann-Arbor-stage III - V - LDH elevated
Risk categories	1 Low risk: 0 - 1 (3y-OS: 98%) 2 Low intermediate risk: 2 (3y-OS: 92%) 3 High intermediate risk: 3 (3y-OS: 75%) 4 High risk: 4-5 (3y-OS: 75%)
Table 1. International Prognostic Index (IPI) and age-adjusted IPI (aaIPI) (Tilly et al., 2015).	

1.1.2.2. Morphology, immunophenotype, and immunohistochemistry

DLBCL commonly disrupts the regular lymph node architecture and is composed of medium to large, atypical lymphoid cells with nuclei with at least twice the size of a lymphocyte nucleus and with a diffuse growth pattern (Martelli et al., 2013).

Different morphological variants can be distinguished histologically: centroblastic, immunoblastic, anaplastic DLBCL, and more rarely other morphological variants (Hunt & Reichard, 2008). Most cases are polymorphic, showing a mix of centroblastic and immunoblastic cells (Swerdlow, 2008). B-cell markers like CD20, a mature B-cell marker, and CD79a, a pan-B-cell marker, are usually detected in DLCBL by immunohistochemical staining. The panel of markers usually also includes CD3, CD5, CD10, CD19, CD45, BCL2, BCL6, Ki-67, IRF4/MUM1, MYC, GCTE1, and FOXP1.

Furthermore, flow cytometry (FACS or FCM) is used as a sensitive method to detect DLBCL cells in bone marrow, peripheral blood, cerebrospinal fluid, or effusions. Cellular clonality can be confirmed with kappa or lambda light chain restriction (Hunt & Reichard, 2008).

As mentioned above, DLBCL is usually positive for several B-cell markers, such as CD19, CD20, or CD79a. DLBCL is usually also positive for CD45 and PAX5 (Martelli et al., 2013). The expression of CD10, BCL6, MUM1/IRF4, GCTE1, and FOXP1 varies and different expression combinations are used as gene-expression profile (GEP) substitutes (chapter 1.1.2.3.). De novo CD5-positive DLBCL was recently recognized as a DLBCL subtype, accounting for 5% - 10% of DLBCL (Harada et al., 1999). This subtype has a poorer outcome in comparison to CD5-negative DLBCL and predominately affects elderly patients with a higher IPI (Jain, Fayad, Rosenwald, Young, & O'Brien, 2013; Yamaguchi et al., 2008).

1.1.2.3. Molecular profiling

Three distinct molecular subtypes, that differ biologically and clinically, can be identified by gene expression profiling (GEP) or substitutes (Alizadeh et al., 2000; Rosenwald et al., 2002).

The germinal center B cell (GCB) subtype presumably arises from a germinal center B cell and typically expresses genes such as CD10, LMO2, and BCL6 (Alizadeh et al., 2000; Rosenwald et al., 2002). In contrast, the activated B-cell (ABC) subtype originates from a post-germinal center B-cell that underwent a malignant transformation during plasmacytic differentiation. The ABC subtype commonly expresses targets of the anti-apoptotic nuclear factor-kappaB (NF-κB) signaling pathway (R. E. Davis, Brown, Siebenlist, & Staudt, 2001). Patients with the ABC subtype face a poorer prognosis and inferior outcome after standard chemotherapy than the GCB subtype (Fu et al., 2008; Lenz et al., 2008; Rosenwald et al., 2002). A third unclassifiable group can be recognized that does not express characteristic genes of the GCB nor the ABC subtype and has a poorer outcome, comparable to the ABC subgroup (Rosenwald et al., 2002).

The 2008 WHO (World Health Organization) classification of aggressive lymphomas recognizes these three subtypes. Additionally, the WHO classification (Table 2.) is also based on clinical, morphological, immunophenotypic, immunohistochemical, genetic, and molecular characteristics (Swerdlow, 2008).

Diffuse large B-cell lymphoma (DLBCL)	<u>Morphologic subtypes</u> - Centroblastic - Immunoblastic - Anaplastic - Other rare variants <u>Molecular subtypes</u> - Germinal center B cell-like (GCB) - Activated B-cell-like (ABC)
Other lymphomas of large B-cells	- T-cell/histiocytic large B-cell lymphoma - Primary DLBCL of the CNS - Primary cutaneous DLBCL, leg type - EBV positive DLBCL of the elderly - DLBCL associated with chronic inflammation - Lymphomatoid granulomatosis - Large B-cell lymphoma with IRF4 rearrangement - Primary mediastinal (thymic) large B-cell lymphoma - Intravascular large B-cell lymphoma - ALK (anaplastic lymphocyte kinase)-positive large B-cell lymphoma - Plasmablastic lymphoma - HHV8-positive diffuse large B-cell lymphoma - Primary effusion lymphoma

Borderline lymphomas	- B-cell lymphoma, unclassifiable, with features between DLBCL and Burkitt lymphoma - B-cell lymphoma, unclassifiable, with features between DLBCL and classic Hodgkin's lymphoma

Table 2. Classification of diffuse large B-cell lymphomas and other large B-cell lymphomas. Adapted from – Swerdlow et al. (2008). WHO Classification of Tumors of Haematopoietic and Lymphoid Tissues.

The classification mentioned above can be studied by gene expression profiling (GEP), immunohistochemistry (IHC), or with NanoString® techniques using the Lymph2CX algorithm (Scott et al., 2015). However, GEP is still not a routine clinical test since it requires fresh frozen tissue. Possible GEP substitutes using immunohistochemistry-based methods and formalin-fixed, paraffin-embedded samples were identified (Choi et al., 2009; Hans et al., 2004; Meyer et al., 2011). The Hans et al. algorithm has become the most popular and clinically accepted method. It uses three markers (CD10, Bcl-6, MUM1/IRF4) to differentiate between two groups, the GCB group (CD10+, Bcl-6+, IRF4-) with a 5-year-overall survival (OS) of 76% and the non-GCB group (CD10-, Bcl-6+/-, IRF4+) with a 5-year-OS of 34% (Hans et al., 2004). Choi et al. used five makers (GCTE1, CD10, BCL-6, IRF4, FOXP1) and achieved about 90% concordance with the GEP (Choi et al., 2009).

These available IHC-based algorithms show a variable reproducibility, only conform to GEP in 80%, and have an inconsistent prognostic value in different studies (Colomo et al., 2003; de Jong et al., 2007; Friedberg, 2015; Fu et al., 2008; Moskowitz et al., 2005; van Imhoff et al., 2006; Zinzani et al., 2005). Even the Lunenburg consortium could not show an improvement of the International Prognostic Index (IPI) by including immunohistochemical markers (Salles et al., 2011).

1.1.2.4. Molecular prognostic subtypes

Different genetic aberrations, usually being detected by fluorescence in situ hybridization (FISH), go along with a poor clinical course and prognosis.

Translocations of the MYC oncogene are present in 5-10% of patients with DLBCL and go along with a significantly inferior progression-free survival (PFS) and OS compared to non-rearranged DLBCL (Barrans et al., 2010; Klapper et al., 2008; Savage et al., 2009).

B-cell lymphoma 2 protein (BCL2) is an anti-apoptotic protein family member, which has a strong survival signal to malignant cells. It is over-expressed in approximately 50% and rearranged in about 14% of DLBCL tumors. Before the introduction of rituximab, BCL2 overexpression was associated with a higher relapse rate, worse disease-free and overall survival (Gascoyne et al., 1997; Hermine et al., 1996; M. E. Hill et al., 1996; Horn et al., 2013), which seems to have been improved with the addition of rituximab to standard chemotherapy (Mounier et al., 2003; Shivakumar & Armitage, 2006).

Double-hit lymphoma describes the concurrence of MYC and BCL2 or BCL6 gene rearrangements, which leads to a highly aggressive and chemoresistant phenotype with a poor survival rate (Johnson et al., 2009; Pedersen et al., 2014; Savage et al., 2009; Swerdlow, 2008). Unfortunately, there is still no consensus on which DLBCLs should undergo testing for MYC and BCL2/BCL6 aberrations (Friedberg, 2017).

1.1.3. Diagnostic criteria, staging and assessment of prognostic factors

The diagnosis of high-grade lymphoma is based on a combination of clinical features, histological, and molecular confirmation.

Initially, a detailed medical history (age, sex, B symptoms, pre-existing conditions, history of malignancy, etc.), a physical examination, and an assessment of the performance status according to the Eastern Cooperative Oncology Group (ECOG) scale should be performed. A surgical incision biopsy of a clinically involved whole lymph node is the standard method for further assessment and diagnosis. If lymph nodes are not accessible, a needle-core or endoscopic biopsy can be considered. The morphological diagnosis of DLBCL can be made either by immunohistochemistry or by flow cytometry. An immunohistochemical panel should confirm B-cell origin and differentiate other variant forms (e.g., EBV-positive DLBCL of the elderly, primary cutaneous DLBCL leg-type, CD5+ DLBCL). The diagnostic workup usually includes CD20, CD79a, CD3, CD5, CD10, CD19, CD23, MYC, BCL2, BCL6, Ki67, IRF4/MUM1, CyclinD1, GCTE1, FOXP1, and EBER-1 for Epstein-Barr virus-positive DLBCL subtype (Tilly et al., 2015). As mentioned above, gene expression profiling (GEP) distinguishes between GCB and non-GCB subtype, which is an important prognostic factor in DLBCL (Lenz et al., 2008). However, GEP is not established in clinical practice and further studies are needed to define its role in diagnosis, treatment decision, and prognosis of DLBCL.

A full blood count should be carried out to assess the bone marrow function and a differential blood count with a focus on circulating lymphoma cells. Serum chemistry should include liver and renal function tests and uric acid. Lactate dehydrogenase (LDH) is a marker of tumor activity and is included in the IPI (chapter 1.1.2.). The workup should also include a complete assessment of HIV, HBV & HCV status before any immune-compromising therapy.

A bone marrow biopsy should be performed in every patient to exclude lymphoma infiltration. A lumbar puncture can be performed to check for meningeal involvement. A brain MRI can be helpful in patients with a high risk of central nervous system progression (Martelli et al., 2013). ^{18}Fluorodeoxyglucose positron emission tomography (FDG-PET)/computed tomography (CT) scan is recommended by the clinical and imaging working groups of the international conference of malignant lymphomas (Lugano classification) as the gold standard for staging and response assessment in DLBCL patients (Barrington et al., 2014; Cheson et al., 2014).

The Ann Arbor classification was developed in 1971 for the staging of Hodgkin lymphoma. It was subsequently also employed as an anatomic staging system for non-Hodgkin lymphomas (Lister et al., 1989). The Ann Arbor stages reflect the extent of disease involvement (Table 3.). Besides the Ann Arbor system, other clinical factors influence the outcome in Non-Hodgkin lymphomas. Therefore, the evaluation of patient with a newly diagnosed Non-Hodgkin lymphoma should include the application of the Ann Arbor classification as well as the International Prognostic Index (chapter 1.1.2.1.) (Armitage, 2005).

Stage I	Single lymphatic (I_N) or extralymphatic (I_E) region involved.
Stage II	Two or more lymphatic (II_N) or extralymphatic (II_E) regions on the same side of the diaphragm involved.
Stage III	Lymphatic (III_N) or extralymphatic (III_E) regions on both sides of the diaphragm involved.
Stage IV	Diffuse or disseminated involvement of one or more extralymphatic organs, including any involvement of the liver, bone marrow, or lungs.
Modifying factors	A: absence of B-symptoms B: presence of B-symptoms (drenching night sweats, fever > 38°C, weight loss > 10% in 6 months)
	S: involvement of spleen
	X: largest disease deposit is > 10 cm ("bulky disease"), or mediastinum is wider than 1/3 of the chest on a chest X-ray.
Table 3. Ann Arbor staging classification (Lister et al., 1989).	

1.1.4. Treatment and response evaluation

1.1.4.1. First-line therapy

Current guidelines recommend R-CHOP as first-line therapy for all DLBCL patients, irrespective of the cell of origin (GCB versus non-GCB) (Ghielmini et al., 2013; Zelenetz, 2014). The initial CHOP regimen contained cyclophosphamide, doxorubicin, vincristine, and prednisone (Sehn, 2012). Over ten years ago, the CD20-antibody rituximab was added to the regimen (R-CHOP), which has led to an improvement in progression-free survival and overall survival (Coiffier et al., 2002; Pfreundschuh et al., 2006). Sehn et al. could show that the 2-year OS of all adult DLBCL patients increased from 52% with the CHOP to 78% with the R-CHOP regimen as the first-line therapy (Sehn et al., 2005). In contrast, more intensive chemotherapy combinations did not show any additional benefits (Fisher et al., 1993).

DLBCL treatment is tailored according to the patients age and risk group.

Patients ≤ 60 years with a low-risk aaIPI (aaIPI 0-1) usually receive six cycles of the R-CHOP regimen every 21 days (R-CHOP-21 x6) (Pfreundschuh et al., 2006; Tilly et al., 2015). Another variant is the treatment with six CHOP cycles and eight doses of rituximab every 14 days (R-CHOP-14) that provides comparable results in terms of progression-free survival and overall survival. This treatment variant requires the

administration of G-CSF, but is associated with a lower cumulative dose of cytostatic drugs and shorter total therapy duration (Cunningham et al., 2013). Moreover, the DSHNHL-FLYER study could show that a dose reduction to four cycles of CHOP-21 with two additional rituximab doses in patients with stage I and II DLBCL and a low risk profile (aaIPI 0 and absence of a bulk) led to a reduction of treatment-related side effects while maintaining the same efficacy than the standard R-CHOP 21 regimen (Poeschel et al., 2018). In patients ≤ 60 years with a low intermediate prognosis (aaIPI 2) the R-ACVBP protocol proved to be superior to the R-CHOP protocol. The R-ACVBP protocol consists of an induction with four cycles of a dose-intensified R-CHOP variant and consolidation with two cycles of high-dose methotrexate, followed by four cycles of rituximab, ifosfamide, and etoposide and two cycles of cytarabine (Récher et al., 2011). However, the R-ACVBP protocol has not become generally accepted due to increased toxicity and the need for hospitalization.

Intermediate high-risk or high-risk patients ≤ 60 years (aaIPI 3-5) have a poorer prognosis and 30% of patients have disease progress during first-line therapy or relapse within one year (Martelli et al., 2013). Treatment regimens include six to eight cycles of the standard R-CHOP-21 or six cycles of R-CHOP14 with two additional rituximab doses. More intensive regimens with R-ACVBP or R-CHOEP (rituximab, cyclophosphamide, doxorubicin, vincristine, etoposide, prednisolone) can be considered in selected patients (Tilly et al., 2015). Four randomized phase III trials have been conducted to compare the standard rituximab-based chemotherapy followed by a consolidating high-dose chemotherapy (HDC) and autologous stem cell transplantation (ASCT) to only chemotherapy in the first-line therapy of DLBCL. Two studies showed an improved progression-free survival for the HDC/ASCT group, but no improved overall survival (Chiappella et al., 2017; Stiff et al., 2013), while two studies showed no improvement for the HDC arm(Gouill et al., 2011; Schmitz et al., 2012). Therefore, a consolidating high-dose chemotherapy (HDC) with autologous blood stem cell transplantation is not recommended as a concept for first-line therapy. In addition, intermediate high-risk and high-risk patients should be enrolled in ongoing clinical trials.

Elderly patients over 60 years of age receive six to eight cycles of CHOP and eight doses of rituximab every 21 days (R-CHOP21 x 6-8). Treatment with R-CHOP-14 did not show a survival advantage (Cunningham et al., 2013; Delarue et al., 2013; Pfreundschuh et al., 2008). The R-CHOP-21 regimen can additionally be dose-reduced if patients are unfit or have cardiac dysfunction (Spina et al., 2012).

In case of bulky disease, consolidation by radiotherapy to the involved sites can be added (Pfreundschuh et al., 2006). Due to a 5% overall risk of central nervous system (CNS) involvement (Feugier et al., 2004; Q. A. Hill & Owen, 2006), CNS prophylaxis can be considered for patients with intermediate-high and high-risk IPI (Tilly et al., 2015). A standard CNS prophylaxis is intrathecal methotrexate or one to two cycles of systemic methotrexate interspersed with the other chemotherapy cycles (J. S.

Abramson et al., 2010; Cheah et al., 2014). The necessity of CNS prophylaxis in DLBCL is still controversial because clear evidence is lacking (Kridel & Dietrich, 2011).

1.1.4.2. Relapse therapy

Between 30% and 40% of patients with DLBCL will relapse or be refractory after first-line therapy and have a very poor outcome (Feugier et al., 2005; Friedberg, 2011; Pfreundschuh et al., 2006; Sehn, 2012). Additionally, 10% of patients have an upfront refractory DLBCL (Martelli et al., 2013). Most relapses occur early, mostly in the first two years, but late relapses after five years are possible (Larouche et al., 2010). Patients can be categorized into three groups according to their survival outcome: Patients who have a DLBCL relapse after achieving complete remission have the best prognosis. Patients with a partial response and persistent disease can sometimes benefit from non-cross-salvage regimens and high-dose chemotherapy plus autologous stem cell transplantation (HDC-ASCT). Patients, who are refractory to initial treatment, can benefit from salvage regimens, but generally have a poor outcome (Friedberg, 2011).

Initially, patients with clinical or radiological signs of a relapse or refractory disease should receive a biopsy to confirm the recurrent lymphoma and reveal the current histology. It should be noted that a relapse might recur with more indolent histology, such as follicular lymphoma. A full restaging evaluation similar to the initial staging (chapter 1.1.3.) should be performed.

The salvage treatment in patients less than 65 to 70 years of age with good performance status and no major organ dysfunction, includes salvage regimens with rituximab and chemotherapy followed by HDC and ASCT (Gisselbrecht et al., 2010; Horwitz et al., 2004; Kewalramani et al., 2004; Tilly et al., 2015). The salvage chemotherapy regimens R-DHAP (rituximab, cisplatin, cytarabine, dexamethasone) and R-ICE (rituximab, ifosfamide, carboplatin, etoposide) show similar outcomes (Gisselbrecht et al., 2010). The BEAM regimen containing carmustine, etoposide, cytarabine, and melphalan, is most frequently used as a high-dose regimen before ASCT (Tilly et al., 2015). Several phase II trials have shown the benefit of HDC-ASCT in patients with relapsed/refractory DLBCL (Bosly et al., 1992; Petersen et al., 1990; Philip et al., 1987; Phillips et al., 1990; Vose et al., 2002). Patients, who are not eligible for ASCT, can be treated with salvage regimens like R-DHAP (rituximab, dexamethasone, high-dose cytarabine, cisplatin) or R-GEMOX (rituximab, gemcitabine, oxaliplatin) (Mounier et al., 2013).

Furthermore, chimeric antigen receptor (CAR) T-cell therapy might be an option for relapsed or refractory DLBCL. CAR T-cell therapy is an immunotherapy that genetically alters a patient's T-cells to target a specific protein (e.g. CD19 or CD20) and thereby destroy tumor cells. To date, three large multicenter studies have reported on anti-CD19 CAR T-cell therapy in aggressive B-cell lymphomas. The ZUMA-1 trial included 101 patients with relapsed or refractory lymphoma (DLBCL, primary

mediastinal B-cell lymphoma, or transformed follicular lymphoma) that had received CAR T-cell therapy. The objective response rate (ORR) was 83% and complete remission was achieved in 54% (Neelapu et al., 2017). The JULIET trial reported on 99 adult patients with relapsed or refractory lymphomas (DLBCL, transformed lymphoma) that had received CAR T-cell therapy with an ORR of 53% and a CR of 40% (Schuster et al., 2017). The TRANSCEND-001 study included relapsed or refractory lymphomas (DLBCL, marginal zone lymphoma, primary mediastinal B-cell lymphoma, follicular lymphoma 3B). The study included 67 patients with DLBCL, transformed follicular lymphoma, and high-grade B-cell lymphoma. Of this subgroup, 55 patients had more than three months of follow-up and an ORR of 57% and CR of 52% (J. Abramson et al., 2017; Chavez & Locke, 2018). These reports are promising, but further work is needed to improve the efficacy and safety of CAR T-cells.

1.1.4.3. Novel therapies

Several new chemotherapeutic agents have been investigated in patients with DLBCL.

Immunomodulating agents (IMiDs) such as lenalidomide are well tolerated and induce durable responses and an improvement of overall response rates (ORR) in patients with relapsed/refractory DLBCL (Chiappella et al., 2013; Hernandez-Ilizaliturri et al., 2011; Vitolo et al., 2014; Wiernik et al., 2008; Zinzani, Pellegrini, Argnani, & Broccoli, 2016; Zinzani et al., 2011). Interestingly, the response to lenalidomide treatment was higher in DLBCL of non-germinal center (non-GCB) origin (Hernandez-Ilizaliturri et al., 2011; Nowakowski et al., 2015).

MTOR inhibitors such as everolimus have been investigated in patients with DLBCL due to the importance of the PI3K/Akt/mTOR pathway in lymphoma pathogenesis (Panwalkar, Verstovsek, & Giles, 2004). Studies in relapsed DLBCL could show a single-agent activity of everolimus with an ORR of 30% but without complete responses (Witzig et al., 2011). Other studies found that a combination of everolimus and rituximab induces responses and improves the OS in pre-treated and untreated patients with DLBCL (Barnes et al., 2013; Johnston et al., 2016; Witzig et al., 2017).

Bortezomib is a proteasome inhibitor and is thought to improve the molecular dysregulation in NF-κB activation and regain cell cycle control. This mode of action is particularly interesting in patients with the ABC subtype (Bu et al., 2014). A study of 40 untreated patients with DLBCL showed that a combination of bortezomib and R-CHOP improved the outcome with no difference in non-germinal center B cell (non-GCB) versus GCB subtypes (Ruan et al., 2011). In relapsed/refractory patients, a combination of bortezomib and gemcitabine given bi-monthly showed an ORR of 10% and complete remission in 10% of patients (Evens et al., 2013). A regimen of bortezomib with ifosfamide, cisplatin, etoposide, rituximab, and dexamethasone (VIPER) showed a comparable response (Elstrom et al., 2012). A European phase III trial (REMoDLB) is underway to evaluate the benefits of the addition of bortezomib to standard R-CHOP therapy in DLBCL. A recent study from 2017 evaluated the

combination of bortezomib and R-CHOP (called VR-CHOP) in newly diagnosed patients with non-GCB DLBCL. However, the outcome for patients with non-GCB DLBCL was not significantly improved by adding bortezomib (Leonard et al., 2017). The REMoDL-B trial, a randomized controlled phase III trial performed in the UK and Switzerland, confirmed these findings. The study included 918 adult patients with DLBCL, who received either R-CHOP or R-CHOP and bortezomib (called RB-CHOP). 27% of patients had an ABC subtype, 52% had a GCB subtype, and 22% an unclassified DLBCL. Davies et al. did not find a difference in PFS between the R-CHOP and the RB-CHOP group (Davies et al., 2019).

Another recently tested agent is ibrutinib, an inhibitor of Bruton's tyrosine kinase that mediates B-cell receptor signaling and can lead to NF-κB activation (Kuppers, 2005; Lenz & Staudt, 2010). Ibrutinib showed an improvement in response rates in patients with DLBCL (Advani et al., 2013; Younes et al., 2014). A randomized phase III trial of R-CHOP +/- ibrutinib is ongoing in de novo DLBCL. A recent double-blind phase III trial investigated the addition of ibrutinib to the R-CHOP regimen in newly diagnosed patients with non-GCB DLBCL. R-CHOP and ibrutinib did not improve OS, EFS, or PFS in the overall non-GCB population and ABC subpopulation. However, a subgroup analysis showed that patients younger than 60 years had a prolonged EFS, PFS, and OS with the addition of ibrutinib. In contrast, in older patients (≥60 years), the addition of ibrutinib increased rates of adverse events and lead to treatment discontinuation (Younes et al., 2019).

The agents mentioned above and many more have been investigated and have shown different degrees of activity. Despite their improvement in outcome and survival, these agents do not target individualized tumor-specific aberrations. In order to improve the treatment of DLBCL, studies also need to investigate prospective biomarkers to guide treatment decisions and to predict therapy response.

1.1.4.4. Response evaluation

An ^{18}FDG-PET/CT should be performed for post-treatment assessment, preferably six to eight weeks after completion of therapy (Cheson et al., 2007; Juweid et al., 2007). Using the Deauville five-point scale (5-PS), the ^{18}FDG-PET/CT divides patients into three response groups: complete remission (CR), partial remission (PR), stable disease (SD) or progressive disease (PD) (Table 4.) (Barrington et al., 2014; Cheson et al., 2014). The results of the post-treatment scan seem to predict disease outcome, more precisely higher relapse rates in positive PET scans (Mikhaeel, Timothy, Hain, & O'Doherty, 2000; Spaepen et al., 2001).

Several studies have investigated interim PET imaging after one to three cycles of chemotherapy in order to identify DLBCL patients who are at high risk for relapse after standard treatment. Unfortunately, the data has not shown any significant benefit and is currently not recommended outside of clinical trials (Friedberg, 2010).

Status	Response criteria
Complete remission (CR)	- ^{18}FDG-PET is completely negative or only shows residual, but PET negative sites - No hepatosplenomegaly, regression of enlarged lymph nodes - No clinical evidence of disease and related symptoms if present before therapy - Bone marrow infiltrate cleared (via morphology or immunohistochemistry)
Partial remission (PR)	- ^{18}FDG-PET shows ≥ 50% decrease of previously involved sites, no new lesions - No increase of the size of liver, spleen, or lymph nodes
Stable disease (SD)	- Patients fail to achieve CR and PR and do not fulfill the PD criteria - ^{18}FDG-PET is usually positive at previously involved sites but does not show new areas of involvement
Progressive disease (PD)	- ^{18}FDG-PET/CT shows new, usually PET-positive lesion(s) or an increase ≥ 50% of previously involved sites - 50% increase of hepatic or splenic lesions - New or recurrent bone marrow infiltration
Table 4. Post-treatment evaluation criteria (Cheson et al., 2007).	

DLBCL treatment response and prognosis are thought to vary depending on the molecular subtype (GCB vs. non-GCB subtype) and clinical criteria (e.g., IPI) (Alizadeh et al., 2000; Lenz et al., 2008; Rosenwald et al., 2002). However, GEP is not available as a clinical routine test and IHC-based algorithms are currently no adequate substitutes. Molecular subtypes currently have no impact on clinical treatment decisions and are only a subject of clinical trials.

1.2. The ubiquitin-proteasome-system

1.2.1. The ubiquitin-proteasome-system

The ubiquitin-proteasome system (UPS) regulates the degradation of numerous proteins by tagging proteins with ubiquitin. The UPS regulates cell growth, cell cycle progression, cell signaling, intracellular trafficking, apoptosis, and gene expression by controlling the cellular lifetime of eukaryotic proteins and the cellular localization of many critical proteins (Weissman, Shabek, & Ciechanover, 2011).

The initial step for protein degradation is the attachment of ubiquitin to the target protein. Ubiquitin is a 76-amino-acid, highly conserved polypeptide with seven lysine residues (K6, K11, K27, K29, K33, K48, and K63). Ubiquitylation is performed in three steps: The E1 enzyme activates ubiquitin in an ATP-consuming reaction. Ubiquitin is then passed on to the E2 enzyme, which associates with the E3 ubiquitin ligase enzyme. The E3 ligase binds the target protein and transfers the glycine residue of

ubiquitin to the lysine residue of the target protein (Ciechanover, Elias, Heller, & Hershko, 1982; Hershko & Ciechanover, 1998; Hershko, Heller, Elias, & Ciechanover, 1983). The human genome contains more than 600 different E3 ligases that are highly specific to their target proteins. Additionally, different combinations of E2 and E3 enzymes provide selective tagging for protein degradation. Monoubiquitination is involved in regulating membrane trafficking, gene transcription, DNA repair, and DNA replication (Chen & Sun, 2009). The binding of ubiquitin molecules by its glycine residue to the lysine residue of the preceding ubiquitin forms polyubiquitin chains (Jacobson et al., 2009). K48-linked polyubiquitin chains are the target signal for proteasomal degradation. Polyubiquitin chains linked through other lysines have proteolytic and non-proteolytic functions. The 26S-proteasome degrades polyubiquitylated proteins to oligopeptides in an ATP-dependent manner and recycles free ubiquitin. It consists of two subunits: the 20S core particle (CP) with the catalytic activity, and a regulatory 19S regulatory particle (RP) (Ciechanover, 2013). Deubiquitinases (DUBs) can reverse ubiquitylation and are necessary for balancing proteolysis and maintaining the amount of free ubiquitin in cells (Amerik & Hochstrasser, 2004).

Mutations in the UPS genes can change the levels of their substrates dramatically, which can be associated with disease (Nalepa, Rolfe, & Harper, 2006).

1.2.2. The spindle assembly checkpoint and the ubiquitin-proteasome-system

Mitosis aims to produce genetically identical, euploid daughter cells. On the other hand, aneuploidy can result in cell death or even malignant transformation (Kops, Weaver, & Cleveland, 2005). Cells have evolved checkpoint controls in the somatic cell cycle to ensure two genetically identical daughter cells. These checkpoints delay the cell cycle progression into S-phase, the entry into mitosis as well as the exit from mitosis.

The restriction point, a cell cycle checkpoint, controls the transition from the late G_1-phase to the S-phase via the CDK4/6-cyclin D complex and the CDK2-cyclin E complex, which enables DNA replication (Shaltiel, Krenning, Bruinsma, & Medema, 2015). The next checkpoint guards the entry into mitosis (G2/M transition) and delays cell cycle progression by inhibiting the activation of cyclin B and CDK1 (Rieder & Maiato, 2004). Once in mitosis, the spindle assembly checkpoint (SAC) ensures the proper chromatid separation at the metaphase-to-anaphase-transition and controls the exit from mitosis. The SAC effector is called the mitotic checkpoint complex (MCC), which is a protein complex consisting of CDC20 and the SAC proteins MAD2, BUBR1/Mad3, and BUB3. The MCC is activated during prometaphase when the kinetochores are not attached to the microtubules (Musacchio & Salmon, 2007). It inhibits the anaphase-promoting complex/cyclosome (APC/C) by acting as a competitive substrate. As a result, cyclin B and securin are kept active. Cyclin-dependent kinase-1 (CDK1) is bound to cyclin B and securin inhibits the protease

separase (Pines, 2011). At this point, the sister-chromatids are kept linked and the cell remains in mitosis until the SAC is satisfied.

Cyclin B promotes the creation of the spindles, decomposition of the nuclear envelope, the end of gene transcription, and condensation of chromosomes and blocks the exit from metaphase (Bassermann, Eichner, & Pagano, 2014). The protease separase can cleave the kleisin subunit of the cohesin ring structure and opens the ring to allow the separation of the sister chromatids (Lin, Luo, & Yu, 2016). APC/C is an E3 ubiquitin ligase that ubiquitylates cyclin B and securin. Once all kinetochores are correctly attached to the spindles, the MCC is inactivated and disassembles. Consequently, CDC20 activates APC/C, which leads to the degradation of cyclin B and securin via ubiquitin-mediated proteolysis. Degradation of securin enables separase to resolve the cohesin ring between the sister chromatids and allows the separation of the sister chromatids (anaphase). During the last step of mitosis (telophase), the degradation of cyclin B inactivates CDK1 leading to the exit from mitosis (Figure 1.) (Lara-Gonzalez, Westhorpe, & Taylor, 2012; Musacchio & Salmon, 2007; Peters, 2006).

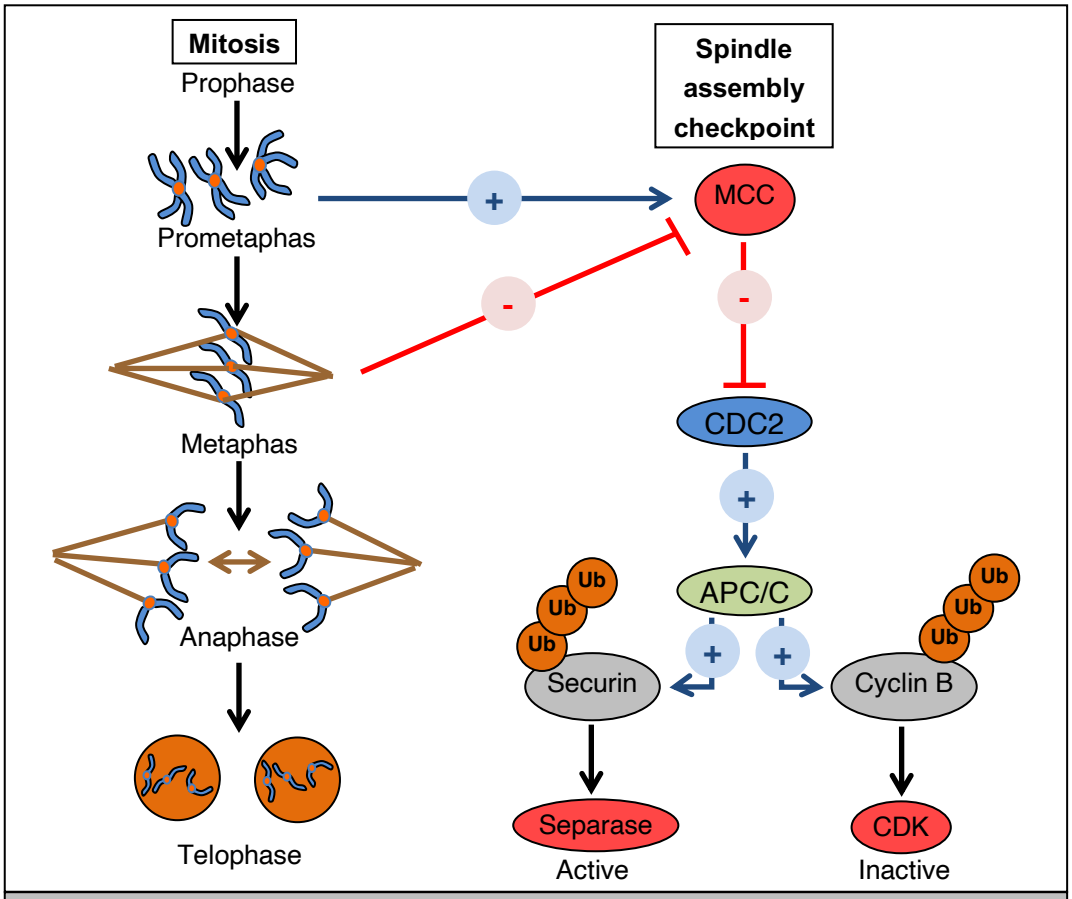

Figure 1. Spindle assembly checkpoint.

If mitosis is delayed, cells have two potential fates: Cells can die in mitosis ('mitotic cell death') or can escape mitosis and return to the G1 phase in a tetraploid state ('mitotic slippage'). The term 'mitotic catastrophe' is often used in this context and refers to cell

death caused by a disturbed mitosis (Chan, Koh, & Li, 2012). Mitotic cell death can be executed by caspase-dependent apoptosis via the intrinsic apoptotic pathway. Apoptotic stimuli (e.g., irradiation, cytotoxic drugs) activate pro-apoptotic proteins of the BH3-only family proteins (e.g., BAD, BIM). These pro-apoptotic proteins inhibit anti-apoptotic Bcl2 family proteins (e.g., Bcl2, Bcl-xL, Mcl1). This step allows the formation of pores in the mitochondrial membrane and the release of cytochrome C, which activates apoptosis and the caspase cascade. Additional mechanisms of mitotic cell death such as necrosis-like, caspase-independent cell death (Jonathan, Bernhard, & McKenna, 1999), and autophagy (Xi et al., 2011) have been described. Although the SAC is fully active during delayed mitosis, a residual APC/C activity will gradually degrade cyclin B to levels that cannot maintain the mitotic state. The cell can eventually exit mitosis and return to the G1 phase in a tetraploid state, which is referred to as mitotic slippage (Brito & Rieder, 2006; Topham & Taylor, 2013).

In summary, the ubiquitin-proteasome system (UPS) assists in the SAC signaling process via ubiquitin-triggered proteolysis and proteolysis-independent mechanisms and degrades cyclins, CDK inhibitors, and other cell cycle regulating proteins at specific times of the cell cycle. The SAC aims to maintain genome stability by ensuring correct mitotic chromosome segregation and prevents aberrant chromosome separation and aneuploidy (Glotzer, Murray, & Kirschner, 1991; Lara-Gonzalez et al., 2012; Skaar & Pagano, 2009).

1.2.3. X-linked inhibitor of apoptosis (XIAP)

X-linked inhibitor of apoptosis (XIAP) is a member of the inhibitor-of-apoptosis protein (IAP) family. Eight IAPs are encoded in human genome. The IAP family shares one to three baculovirus IAP repeats (BIR), which are ~70 amino acid long, and zinc-ion-binding domains. IAPs also contain additional domains such as the C-terminal RING finger domain, that has ubiquitin ligase (E3) activity (Gyrd-Hansen & Meier, 2010). Most prominently, IAPs are negative regulators of caspases and, therefore, cell death. Additionally, they control ubiquitin-dependent signaling pathways that regulate activation of NF-kB and MAPK pathways that promote expression of genes involved in inflammation, immunity, cell migration, cell differentiation, cell survival, and cell cycle progression (Gyrd-Hansen & Meier, 2010; Silke & Vucic, 2014).

The XIAP gene is found on chromosome Xq25 (Rajcan-Separovic, Liston, Lefebvre, & Korneluk, 1996) and consists of 6 exons (Rigaud et al., 2006). XIAP has three BIR domains, a ubiquitin-associated (UBA) domain, and a RING domain. XIAP negatively regulates apoptosis by inhibiting caspases 3, 7, and 9. The linker region between its BIR1 and BIR2 domain and the BIR2 domain directly bind caspase 3 and 7 (Chai et al., 2001; Deveraux, Takahashi, Salvesen, & Reed, 1997; Riedl et al., 2001). Caspase 9 is inactivated, when bound to the BIR3 domain (Deveraux et al., 1999; Shiozaki et al., 2003). The RING finger domain has ubiquitin E3 ligase activity and promotes autoubiquitylation and ubiquitylation of XIAP binding partners (MacFarlane, Merrison, Bratton, & Cohen, 2002; Morizane, Honda, Fukami, & Yasuda, 2005; Nakatani et al.,

2013; Vaux & Silke, 2005). XIAP also seems to activate the pro-survival NF-κB pathway via its BIR1 domain (Lu et al., 2007). Studies have shown that XIAP is frequently expressed in B-cell NHL and Hodgkin's lymphoma (Akyurek, Ren, Rassidakis, Schlette, & Medeiros, 2006). Until now, the biological importance of these findings has not been completely clarified. Additionally, high XIAP expression has been found in acute myeloid leukemia (Tamm et al., 2000), esophageal carcinoma (Zhang et al., 2007), non-small cell lung cancer (Hofmann, Simm, Hammer, Silber, & Bartling, 2002), ovarian carcinoma (Mansouri, Zhang, Ridgway, Tian, & Claret, 2003), and clear cell renal cancer (Ramp et al., 2004). In contrast, XIAP deficiency causes X-linked lymphoproliferative syndrome (XLP), a hereditary immunodeficiency characterized by lymphohistiocytosis, hypogammaglobinemia, and a predisposition to lymphomas (Rigaud et al., 2006).

1.2.4. Ubiquitin-specific protease 9X (USP9X)

The ubiquitylation of proteins is a reversible post-translational modification. Ubiquitin can also be removed by deubiquitinating enzymes (DUBs), which hydrolyze the amide bond of ubiquitin. DUBs help to maintain the homeostasis of free ubiquitin and recycle ubiquitin. They affect the stability of the ubiquitin-conjugated proteins by removing ubiquitin chains (Glickman & Ciechanover, 2002). DUBs can also remove ubiquitin signals and reverse cell signaling. Thirdly, DUBs seem to be able to edit the form of ubiquitin modification by trimming ubiquitin chains (Komander, Clague, & Urbe, 2009). The human genome encodes approximately 80 DUBs (Nijman, Luna-Vargas, et al., 2005). In contrast to the ubiquitin ligases, the role of DUBs in mitosis is not fully understood yet.

USP9X is a member of the ubiquitin-specific protease (USP) family. This family has two characteristic catalytic motifs, a cysteine box and a histidine box. The size of the catalytic motifs varies from 300 to 800 amino acids (Nijman, Luna-Vargas, et al., 2005). USP9X has a size of over 2,550 amino acids and has one USP-defining cysteine, a histidine box catalytic motif, and a ubiquitin-like module (Ubl) in the N-terminal extension (Murtaza, Jolly, Gecz, & Wood, 2015). USP9X is known to remove mono-ubiquitin and poly-ubiquitin chains (e.g., K48-, K63-linkages) from a substrate (Dupont et al., 2009; Marx, Held, Gibson, & Benz, 2010). Various cellular functions are known: It regulates protein trafficking (Azakir & Angers, 2009), is essential for embryonic development (Pantaleon et al., 2001), and also stabilizes pro-survival factors such as beta-catenin (Murray, Jolly, & Wood, 2004; Taya, Yamamoto, Kanai-Azuma, Wood, & Kaibuchi, 1999) and MCL1 (Schwickart et al., 2010). USP9X also ensures a correct chromosome alignment and segregation at the end of mitosis by deubiquitylating the inhibitor of apoptosis survivin and Aurora B (Vong, Cao, Li, Iglesias, & Zheng, 2005).

2. Aim of the study

Diffuse large B-cell lymphoma (DLBCL) is the most common aggressive non-Hodgkin lymphoma in adults. Initial treatment usually consists of cyclophosphamide, doxorubicin, vincristine, prednisone, and rituximab (R-CHOP). However, up to one third of patients is refractory to initial therapy or has a relapse after standard therapy (Friedberg, 2011; Larouche et al., 2010). Several risk factors associated with a poorer outcome and unfavorable genetic and morphological subtypes with a more aggressive clinical course have been described (Pasqualucci & Dalla-Favera, 2015; Shaffer et al., 2012; Ziepert et al., 2010). However, the mechanisms of treatment resistance and relapse are unknown. This work aimed to study the role of USP9X and XIAP in human DLBCL cell lines. Secondly, we wanted to investigate the role of XIAP stabilization by USP9X in B-cell lymphomas. Additionally, USP9X and XIAP could be used as diagnostic markers in DLBCL patients as well as a therapeutic target.

3. Materials and methods

3.1. Materials

3.1.1. Chemicals

Product	Manufacturer
Acetone	Roth, Karlsruhe, Germany
Acrylamide/Bis Rotiphorese 40%	Roth, Karlsruhe, Germany
Agarose powder	Roth, Karlsruhe, Germany
Ammonium persulfate (APS)	Roth, Karlsruhe, Germany
Ampicillin	Roth, Karlsruhe, Germany
Aqua ad injectabilia, sterile	Braun, Melsungen, Germany
β-Mercaptoethanol	Sigma-Aldrich, Taufkirchen, Germany
Bacto agar	BD Bioscience, Franklin Lakes, USA
Bacto tryptone	BD Bioscience, Franklin Lakes, USA
Bacto yeast extract	BD Bioscience, Franklin Lakes, USA
Bovine serum albumin	Roth, Karlsruhe, Germany
Bromophenol blue	Sigma-Aldrich, Taufkirchen, Germany
Calcium Chloride ($CaCl_2$)	Sigma-Aldrich, Taufkirchen, Germany
Deoxynucleotide triphosphate mix	Thermo Fisher Scientific, Waltham,
Dimethyl sulfoxide (DMSO)	Roth, Karlsruhe, Germany
Ethanol 70%	Merck Millipore, Darmstadt, Germany
Ethanol 96%	Merck Millipore, Darmstadt, Germany
Ethidium bromide	Roth, Karlsruhe, Germany
Ethylenediaminetetraacetic acid (EDTA)	Sigma-Aldrich, Taufkirchen, Germany
Glycerol	Sigma-Aldrich, Taufkirchen, Germany
Glycine	Roth, Karlsruhe, Germany
Isopropanol 70%	Roth, Karlsruhe, Germany
Kanamycin	Sigma-Aldrich, Taufkirchen, Germany
Methanol	Merck Millipore, Darmstadt, Germany
Nonidet-P40 Substitute (NP40)	Roche, Grenzach-Wyhlen, Germany
N,N-Bis(2-hydroxyethyl)taurine (BES)	Sigma-Aldrich, Taufkirchen, Germany
Polybrene (Hexadimethrine bromide)	Sigma-Aldrich, Taufkirchen, Germany
Propidium iodide (PI)	Thermo Fisher Scientific, Waltham,
Puromycin	Sigma-Aldrich, Taufkirchen, Germany
Skim milk powder	Sigma-Aldrich, Taufkirchen, Germany
SOC medium	NEB, Ipswich, USA
Sodium chloride (NaCl)	Roth, Karlsruhe, Germany
Sodium dodecyl sulfate (SDS)	Roth, Karlsruhe, Germany
Sodium fluoride (NaF)	Sigma-Aldrich, Taufkirchen, Germany

SuperSignal West Femto Maximum Sensitivity Substrate	Thermo Fisher Scientific, Waltham, USA
SuperSignal West Pico Chemiluminescent Substrate	Thermo Fisher Scientific, Waltham, USA
Tris/Borate/EDTA (TBE) Buffer, UltraPure 10X	Thermo Fisher Scientific, Waltham, USA
Tetramethylethylenediamine (TEMED)	Sigma-Aldrich, Taufkirchen, Germany
Tris(hydroxymethyl)aminomethane (TRIS)	Roth, Karlsruhe, Germany
Triton X-100	Sigma-Aldrich, Taufkirchen, Germany
Trypan blue	Thermo Fisher Scientific, Waltham,
Tween 20	Sigma-Aldrich, Taufkirchen, Germany
Table 5. List of chemicals.	

3.1.2. Cell culture media and supplements, cell cultures dishes and bench

Product	Manufacturer
Dulbecco's Modified Eagle's Medium (DMEM)	Thermo Fisher Scientific, Waltham, USA
DMEM, no phenol red medium	Thermo Fisher Scientific, Waltham, USA
RPMI 1640 GlutaMAX medium	Thermo Fisher Scientific, Waltham, USA
RPMI 1640, no phenol red medium	Thermo Fisher Scientific, Waltham, USA
Fetal Bovine Serum (FBS) Superior	Biochrom, Berlin, Germany
Opti-MEM, reduced serum media	Thermo Fisher Scientific, Waltham, USA
Phosphate buffered saline (PBS)	Thermo Fisher Scientific, Waltham, USA
Penicillin/Streptomycin (100X)	Thermo Fisher Scientific, Waltham, USA
Trypsin-EDTA (10X) solution	Biochrom, Berlin, Germany
Trypsin-EDTA (10X) solution	Thermo Fisher Scientific, Waltham, USA
Glutamine (100X)	Thermo Fisher Scientific, Waltham, USA
0.2ml, 1.5ml, 2ml Eppendorf tubes	Sarstedt, Nümbrecht, Germany
15ml, 50ml Falcon tubes	Greiner Bio-One, Krems, Austria
1ml, 250µl, 20µl tips	Sarstedt, Nümbrecht, Germany
Gel-loading tips	Roth, Karlsruhe, Germany
T25, T75, T175 cell culture flasks	Sarstedt, Nümbrecht, Germany
6cm, 10cm, 15cm cell culture plates	TPP, Trasadingen, Switzerland
6-well, 12-well, 96-well plates	TPP, Trasadingen, Switzerland
Syringe-Filters 0.45µm, 0.2µm	TPP, Trasadingen, Switzerland
Immobilon-P Membrane, PVDF, 0.45µm	Merck Millipore, Darmstadt, Germany
Microcon 30kDa Centrifugal Filter	Merck Millipore, Darmstadt, Germany

X-Ray Films for Western Blot, CL-XPosure	Thermo Fisher Scientific, Waltham, USA
Table 6. List of cell culture media, supplements, cell culture dishes, and bench.	

3.1.3. Transfection reagents & enzymes

Product	Manufacturer
HiPerFect Transfection Reagent	Qiagen, Hilden, Germany
Lipofectamine® 2000 Transfection Reagent	Thermo Fisher Scientific, Waltham, USA
Pfu II Ultra DNA Polymerase	Agilent Technologies, Santa Clara, USA
Restriction Enzymes: AgeI, BamHI, DpnI, EcoRI, HindIII, KpnI, XbaI, XhoI	Thermo Fisher Scientific, Waltham, USA
SuperScript III Reverse Transcriptase	Thermo Fisher Scientific, Waltham, USA
Table 7. List of transfection reagents & enzymes*.	

All enzymes were used with appropriate reaction buffers.

3.1.4. Inhibitors

Inhibitor	Manufacturer
DL-Dithiotheritol (DTT)	Sigma-Aldrich, Taufkirchen, Germany
β-Glycerol 2-phosphate disodium salt pentahydrate (βG2P)	Sigma-Aldrich, Taufkirchen, Germany
Phenylmethylsulfonylfluoride (PMSF)	Sigma-Aldrich, Taufkirchen, Germany
Peptidylprolyl isomerase inhibitor (PIN)	Sigma-Aldrich, Taufkirchen, Germany
Sodium orthovanadate (NaVa)	Sigma-Aldrich, Taufkirchen, Germany
Tosyl-L-lysyl-chloromethyl-ketone (TLCK)	Sigma-Aldrich, Taufkirchen, Germany
Tosyl-phenylalanyl-chloromethyl-ketone (TPCK)	Sigma-Aldrich, Taufkirchen, Germany
Table 8. List of inhibitors.	

3.1.5. Molecular weight standards for DNA and proteins

Product	Manufacturer
GeneRuler 1kb DNA Ladder	Thermo Fisher Scientific, Waltham, USA
6X DNA Loading Dye	Thermo Fisher Scientific, Waltham, USA
PageRuler Prestained Protein Ladder	Thermo Fisher Scientific, Waltham, USA
Table 9. List of protein/DNA molecular weight standards.	

3.1.6. Molecular Biology Kits

Product	Manufacturer
Amaxa® Cell Line Nucleofector® Kit V	Lonza Cologne AG, Cologne, Germany

Bio-Rad DC Protein Assay	Bio-Rad, Munich, Germany
GeneJET Gel Extraction Kit	Thermo Fisher Scientific, Waltham, USA
GeneJET PCR Purification Kit	Thermo Fisher Scientific, Waltham, USA
LightCycler 480 SYBR Green I Master	Roche, Grenzach-Wyhlen, Germany
peqGOLD Plasmid Mini Kit I	PEQLAB Biotechnologie GmbH, Erlangen, Germany
QIAGEN Plasmid Maxi Kit	Qiagen, Hilden, Germany
QIAprep Spin Miniprep Kit	Qiagen, Hilden, Germany
QIAshredder Kit	Qiagen, Hilden, Germany
QIAGEN RNeasy extraction Kit	Qiagen, Hilden, Germany
Rapid DNA Dephos and Ligation Kit	Roche, Grenzach-Wyhlen, Germany
SuperScript III Reverse Transcriptase	Invitrogen, Karlsruhe, Germany

Table 10. List of molecular biology kits.

3.1.7. Buffers

Lysis buffer	250mM NaCl, 50mM Tris (pH 7.5), 0.1% Triton X-100, 1mM EDTA, 0.1% NP40, 5mM $MgCl_2$, 5% Glycerol, protease inhibitors (1000X PIN, 1000X TPCK, 1000X TLCK, 1000X NaVa, 1000X DTT, βG2P)
Inhibitors	- 1µg/ml Aprotinin - 1mM DTT - 10mM G2P - 1µg/ml Leupeptin - 0.1mM PMSF - 0.1mM Na_3VO_4 - 10µg/ml Soybean Trypsin Inhibitor - 5µg/ml TLCK - 5µg/ml TPCK
Erythrocyte-lysing buffer	0.15M NH_4Cl, 0.02M HEPES, 0.1M EDTA
Hank's Buffer	10% FBS, 1% P/S, 1% Hepes, 1% NEAA
Mouse Buffer	Hank's Buffer (1X), 1:50 with H_2O
Running Buffer (10X)	250mM Tris (pH 7.5), 1.92M Glycine, 1% SDS
Transfer Buffer (10X)	250mM Tris (pH 7.5), 1.5M Glycine, 1% SDS For 1X: 2vol methanol + 7vol H_2O + 1vol Buffer
Stripping Buffer	62.5mM Tris (pH 6.8), 0.867% β-Mercaptoethanol, 2% SDS
Washing Buffer	PBS (1X), 0.1% Tween 20
Blocking Buffer	PBS (1X), 0.1% Tween 20,5% Skim milk powder
Laemmli Buffer (5X)	300mM Tris (pH 6.8), 50% Glycerol, 10% SDS + 5% β-Mercaptoethanol + 0.05% Bromophenol blue
FACS Sample Buffer	PBS (1X), 1% FBS
Freezing medium	90% FBS + 10% DMSO

LB-agar plates	1% Bacto trypton, 0.5% Bacto yeast extract, 1% NaCl,
Luria-Bertani (LB) medium	1% Bacto trypton, 0,5% Bacto yeast extract, 1% NaCl
Separating Gel Buffer	1.5M Tris/HCl (pH 6.8)
Stacking Gel Buffer	0.5M Tris/HCl (pH 6.8)
Oligo annealing buffer	500mM NaCl + 100mM Tris-HCl + 100mM MgCl2
Table 11. List of buffers.	

All Buffers were prepared with dH_2O (aqua dest.), if not indicated otherwise.

3.1.8. Antibodies

Antibody	Mouse/	Primary/	Dilution	Manufacturer
Anti-mouse IgG, horseradish peroxidase		Secondary		GE Healthcare, Chalfont St. Giles, UK
Anti-rabbit IgG, horseradish peroxidase		Secondary		GE Healthcare, Chalfont St. Giles, UK
β-Actin	Mouse	Primary	1:10000	Sigma-Aldrich, Taufkirchen, Germany
Cleaved caspase-3	Rabbit	Primary	1:300	Cell Signaling, Danvers, USA
Cul 1	Mouse	Primary	1:500	Life Technologies, Carlsbad, USA
PARP1/2	Rabbit	Primary	1:1000	Santa Cruz Biotechnologies, Dallas,
USP9X	Rabbit	Primary	1:4000	Bethyl Laboratories, Montgomery, USA
XIAP	Mouse	Primary	1:1000	BD Bioscience, Franklin Lakes, USA
XIAP	Rabbit	Primary	1:1000	Cell Signaling, Danvers, US
XIAP	Mouse	Primary	1:1000	R&D Systems, Minneapolis, USA
Table 12. List of primary and secondary antibodies.				

3.1.9. Plasmids

Plasmid	Origin	Antibiotic
pMI-dsRed	Kind gift of T. Brummer	Ampicillin
pMD2G	Kind gift of U. Keller	Ampicillin
psPAX	Kind gift of U. Keller	Ampicillin
pVSV-G	Clontech, Saint-Germain-en-Laye, France (Cat. No. 631530)	Ampicillin
pcDNA_MLV_GAG/POL	Kind gift of Dr. A. Krackardt	Ampicillin

pLKO.1 puro TRC cloning vector	AddGene, Cambridge, USA	Ampicillin
pLKO.1 puro scramble shRNA	AddGene, Cambridge, USA	Ampicillin
pLKO.1 GFP scramble shRNA	Cloned by F. Loewecke	Ampicillin
pLKO.1 GFP USP9X shRNA	Cloned by F. Loewecke	Ampicillin
pLKO.1 shXIAP	Kind gift of L. Nilsson	Ampicillin
pLKO.1 GFP XIAP shRNA	Cloned by F. Loewecke	Ampicillin
USP9X siRNA	Thermo Fisher Scientific	
XIAP siRNA	Thermo Fisher Scientific	
Table 13. List of plasmids.		

3.1.10. Oligonucleotides (cloning, sequencing, qPCR, shRNA)

All oligonucleotides were ordered from Eurofins MWG GmbH, Ebersberg. A 'salt-free' purity was used for oligonucleotides of less than 30 base pairs. ShRNA oligonucleotides longer than 30bp were purified by high-performance liquid chromatography (HPLC).

Oligonucleotides	Sequence	Use
sh-scramble_fw	5'-CCGGCCTAAGGTTAAGTCGCCCTCGCTCGAGCGAGGGCGACTTAACCTTAGGTTTTTG-3'	Control shRNA
sh-scramble_rv	5'-AATTCAAAAACCTAAGGTTAAGTCGCCCTCGCTCGAGCGAGGGCGACTTAACCTTAGG-3'	Control shRNA
pLKO.1 dsred sequence	5'-CGCACGTCGGCAGTCGGCTCC-3'	Seq.
pLKO.1 sh-insert sequence	5'-GATACAAGGCTGTTAGAGAGATAATT-3'	Seq.
pLKO.1 shUSP9X, sh-insert sequence	5'-GAT GAG GAA CCT GCA TTT CCA-3'	Seq.
XIAP_XhoI_fw	5'-CCGCTCGAGGCCACCATGACTTTTAAC-3'	Seq.
XIAP_BamHI_rv	5'-CCGGGATCCTTAAGACATAAAAATTTTTTG-3'	Seq.
Table 14. List of oligonucleotides.		

3.1.11. Mice

Mice	Supplier
Wild type C57BL/6 inbred mice (female, ten weeks old)	Harlan Laboratories, Horst, Netherlands
Table 15. List of mice.	

Experiments were performed by Felicia Loewecke with the assistance of Dr. med. Katharina Engel in accordance with the local ethical guidelines and approved by the responsible regional authorities (Regierung von Oberbayern).

3.1.12. Cell lines

Cell line	Type	Medium	Obtained from
Eμ-Myc	Murine lymphoma cells	RPMI-1640 + 10% fetal bovine serum (FBS) + 1% penicillin/streptomycin (P/S) + 1% non-essential amino acids (NEAA) + 0.1% β-mercaptoethanol	Kind gift of U. Keller
HEK 293T	Human embryonic kidney cell-line (CRL-3216)	DMEM + 10% bovine serum (BS) + 1% P/S	ATCC, Virginia, USA
HeLa	Human cervix carcinoma cell-line (CCL-2)	DMEM + 10% FBS + 1% P/S	ATCC, Virginia, USA
NIH 3T3	Murine embryonic fibroblast cells	DMEM + 10% FBS	ATCC, Virginia, USA
Phoenix Eco	Human epithelial kidney cell-line, retrovirus	DMEM + 10% FBS	ATCC, Virginia, USA
RIVA	Human B-cell lymphoma cell-line	RPMI-1640 + 20% FBS + 1% P/S	DSMZ, Braunschweig, Germany
SuDHL 4	Human B-cell lymphoma cell-line	RPMI-1640 + 20% FBS + 1% P/S	ATCC, Virginia, USA
SuDHL 6	Human B-cell lymphoma cell-line	RPMI-1640 + 20% FBS	ATCC, Virginia, USA
Oci-Ly 3	Human B-cell lymphoma cell-line	IMDM + 20 % FBS + 1% P/S + 0.1% β-mercaptoethanol	DSMZ, Braunschweig, Germany
Oci-Ly 10	Human B-cell lymphoma cell-line	IMDM + 20% FBS + 1% P/S + 0.1% β-mercaptoethanol	DSMZ, Braunschweig, Germany

Table 16. List of cell-lines.

3.1.13. Bacteria

Bacteria	Supplier
NEB 5-alpha Competent E. coli (High Efficiency)	New England BioLabs, Ipswich, USA

Table 17. List of bacteria.

3.1.14. Devices, machines, and instruments

Object	Manufacturer
Agarose electrophoresis chamber Mini-Sub Cell GT	Bio-Rad, Munich, Germany
Analytical balance ABJ	Kern & Sohn, Balingen, Germany
Bacterial shaker/incubator innova 40	Eppendorf, Hamburg, Germany
Cell Culture CO_2-Incubator Hera cell 150i	Thermo Fisher Scientific, Waltham, USA
Centrifuge Heraeus Multifuge 3SR+	Thermo Fisher Scientific, Waltham, USA
Chamber for ready gels	Invitrogen, Karlsruhe, Germany
Cobas 8000 modular analyzer series	Roche, Grenzach-Wyhlen, Germany
Cooling-Centrifuge 5417R	Eppendorf, Hamburg, Germany
Cooling-Centrifuge 5430R	Eppendorf, Hamburg, Germany
FACS Calibur	BD Biosciences, Franklin Lakes, USA
Magnetic Thermo Stirrer RCT basic	IKA, Staufen, Germany
Microplate Reader Sunrise	Tecan Group, Männedorf, Switzerland
Microscope Axiovert 40 CFL	Carl Zeiss AG, Oberkochen, Germany
Microscope PrimoStar	Carl Zeiss AG, Oberkochen, Germany
Nano-Photometer	Implen, Munich, Germany
Neubauer hemocytometer	Marienfeld, Lauda-Königshofen, Germany
Nucleofector™ 2b Device	Lonza Cologne GmbH, Cologne, Germany
PCR peqSTAR 2x Gradient Thermocycler	Peqlab, Erlangen, Germany
pH-meter pH720 InoLab	WTW, Weilheim, Germany
Pipetboy acu 2	Integra Biosciences, Zizers, Switzerland
Pipettes PIPETMAN Neo P2, P10, P20, P100, P200, P1000	Gilson, Middleton, USA
Power Supply PowerPac Basic	Bio-Rad, Munich, Germany
Power Supply PowerPac HC High Current	Bio-Rad, Munich, Germany
Precision Balance 572	Kern & Sohn, Balingen, Germany
Rotating wheel L29	Fröbel Labortechnik, Lindau, Germany
Rotating wheel, horizontal, RM10W	Fröbel Labortechnik, Lindau, Germany
RT-PCR System LightCycler 480	Roche, Grenzach-Wyhlen, Germany
Safety hood, Herasafe KS	Thermo Fisher Scientific, Waltham, USA
Scanner V750 Pro	Epson, Meerbusch, Germany
SDS-gel electrophoresis chamber Mini-Protean	Bio-Rad, Munich, Germany
Sorvall Superspeed Centrifuge RC5B	Thermo Fisher Scientific, Waltham, USA

Tabletop centrifuge 5424	Eppendorf, Hamburg, Germany
Thermomixer	Eppendorf, Hamburg, Germany
Vortexer MS3 basic	IKA, Staufen, Germany
Waterbath Aqualine AL 18	Lauda, Lauda-Königshofen, Germany
Waving platform shaker Polymax 2040	Heidolph Instruments, Kelheim, Germany
Western Blotting Chamber Tetra Blotting Module	Bio-Rad, Munich, Germany
Western Blot Developer SRX-101A	Konica Minolta, Munich, Germany
Table 18. List of devices, machines, and instruments.	

3.1.15. Software

Software	Supplier
FlowJo cytometry analysis software, Version 10 OSX	Tree Star, Ashland, USA
GraphPad Prism 8 for statistical analysis	GraphPad Software Inc., La Jolla, USA
MacVector Sequence analysis software, Version 14	MacVector, Cary, USA
QuantPrime, qPCR primer design tool	QuantPrime, AG Bioinformatics, Potsdam, Germany
Table 19. List of software.	

3.2. Methods

3.2.1. Eukaryotic Cell culture

3.2.1.1. Culturing of cell lines

All used cell lines (see 3.1.14.) were cultured at 37°C, 95% humidity and 5% CO_2.

Adherent human embryonic kidney cell line HEK293T DMEM was cultured on 6-15 cm plates with Dulbecco's modified Eagle's medium (DMEM) and 10% bovine serum (BS) and 1% penicillin/streptomycin (P/S). The cell line HeLa, an adherent human cervix carcinoma cell line, was cultured on 6 - 15 cm plates with Dulbecco's modified Eagle's medium (DMEM) and 10% fetal bovine serum (FBS) and 1% penicillin/streptomycin.

The DLBCL cell lines SuDHL 4 and SuDHL 6 were kept in suspension culture with RPMI-1640 and 20% FBS and 1% P/S in cell culture flasks or 6-well plates, depending on the experimental setting. The DLBCL cell lines Oci-Ly 3 and Oci-Ly 10 were cultured as suspension cells in IMDM and 20% FBS and 1% P/S + 0.1% β-mercaptoethanol in cell culture flasks or 6-well plates.

The cell culture media was exchanged at least every 2 to 3 days or earlier if the phenol red in the medium changed its color to orange, which indicates a more acidic medium. Besides, cells were split according to density to achieve cell densities of 1.5 - 5 x 10^5 cells/ml for suspension cells and 40 - 80% cell density for adherent cells. The suspension cells were transferred to falcons, centrifuged for 3 - 4 minutes at 1200 rpm,

and the supernatant was discarded. The cells were resuspended in a larger volume of fresh medium and returned to the flask. New flasks were used at least 1 - 2 times per week. The medium of adherent cells (HEK293T, HeLa) was removed and the plates of flasks were briefly washed with PBS. After that, 1 - 2 ml of 1X Trypsin-EDTA solution was put on the plate and gently rocked and then incubated at 37°C for 3 - 5 minutes to detach the cells from the plate. Trypsin was inactivated by adding twice to the volume of Trypsin-EDTA of fresh medium to the plate and transferred to falcons for centrifugation (4 minutes, 1200 rpm). The cell pellet was resuspended in fresh medium (6 ml for 6 cm-, 10 ml for 10 cm-, 20 ml for 15 cm-plates) and transferred to new plates. All used media and cell culture plastic were disposed of in bleach containers for at least 48 hours to inactivate viral residues and transferred to regular waste. Cells were considered virus-free 14 days post-infection and therefore treated as above. Lentivirus-infected cells were handled differently.

3.2.1.2. Storage of cells

For long-term storage, the cells were frozen in liquid nitrogen at -196°C. The freezing agent dimethyl sulfoxide 10% (DMSO) was supplemented with FBS to prevent cell damage. The cells (approximately 1 x 10^6) were collected from the growing culture, then centrifuged (4 minutes, 1200 rpm), suspended in 1 ml of freezing medium, and transferred to cryotubes. After that, the cells were cooled down to -80°C (1°C per minute) using freezing containers containing isopropanol. The cryotubes were stored in a liquid nitrogen tank. For defrosting, the cells were resuspended in fresh medium and centrifuged (4 minutes, 1200 rpm). The supernatant was quickly removed to prevent DMSO-mediated cytotoxicity and the cells were transferred to plates or flasks in a new medium.

3.2.1.3. Harvesting cells

The adherent cells were detached by using Trypsin-EDTA as described above (chapter 3.2.1.2.) and transferred to falcons. Suspension cell cultures were transferred to falcons. After centrifugation (4 minutes, 1200 rpm), the supernatant was removed, the remaining cell pellet was washed with PBS, and transferred to 1.5 ml tubes. After a quick-spin (10 seconds, 14000 rpm), the PBS was removed, and the cell pellet was temporarily frozen at -80°C.

3.2.2. Proliferation analysis

For assessment of cell proliferation, cultured cells were counted twice with the Trypan Blue exclusion method and the Neubauer hemocytometer. The cells were thoroughly mixed and 50 µl Trypan Blue was added to a tube with 50 µl of the cell-containing medium. A Neubauer hemocytometer was used under the microscope to count viable cells, which have a bright shimmer and an intact membrane (Figure 2.). The cells were

counted in the four 4 x 4 squares and the final cell number was calculated using the following equation: $cells/ml = \frac{(cell\ count)}{2} \times 10^4$.

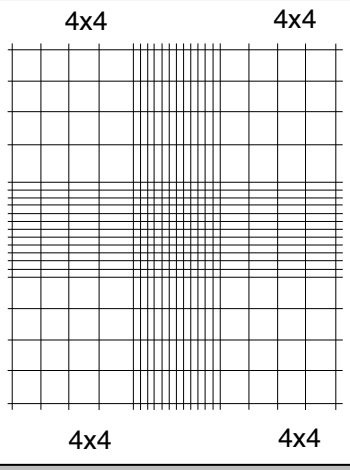

Figure 2. Schematic of a Neubauer hemocytometer under the microscope.

3.2.3. Transient transfection

3.2.3.1. Calcium phosphate transfection

To transiently express genes in adherent cells (e.g., HEK293T-cells), the cells were transfected with the calcium phosphate ($CaPO_4$) method (Kingston, Chen, & Rose, 2003). Therefore, 40 µg of plasmid DNA (20 µg of shRNA, 15 µg of gag-pol and 5 µg of env DNA) was added to 450 µl of dH_2O. 50 µl of 2.5M calcium chloride ($CaCl_2$) was gently added into the DNA solution to achieve a final concentration of 0.25M $CaCl_2$. After 5 minutes of incubation at room temperature (RT), 500 µl of 2X N,N-Bis(2-hydroxyethyl)taurine (BES) was slowly added to the solution, while gently shaking the tube. After that, the mixture was incubated for 20 minutes at RT to allow DNA-complex formation. The solution was added dropwise onto a 10 cm dish of adherent cells at 60-80% confluence. After incubation for 4 - 5 hours, the culture medium was changed and incubation continued for another 24 - 48 hours. Transfection efficiency could be assessed under the fluorescent microscope when fluorescent vectors (e.g., plkO.1 with dsredExpress2, pLKO.1 GFP vector).

3.2.3.2. Lipofectamine® 2000 transfection

Lipofectamine® 2000 transfection is used to transfect RNA or plasmid DNA into eukaryotic cells by lipofection. The Lipofectamine® reagent can form liposome complexes with nucleic acid molecules in an aqueous medium. The nucleic acid-containing liposomes can reach the cytoplasm and the nucleic acid is available to the cell for replication or expression (Dalby et al., 2004). Lipofectamine® 2000 transfection was performed according to the manufacturer's description: For a 96-well plate of adherent cells, 100 µl of the OptiMEM medium was diluted with 40 µl of

Lipofectamine® 2000 reagent and incubated for 5 minutes at RT. Then, 1,6µg of shRNA was added to 100 µl of OptiMEM medium. The diluted Lipofectamine® 2000 reagent was added to the diluted DNA in a 1:1 ratio and incubated for 20 minutes at RT. Before transfection, the medium was changed to a P/S-free medium and the transfection solution was put on the cells. After 5 hours, the fresh cell medium was put on the cells. On the third day after transfection, the cells were harvested for further investigation or the virus-containing medium was used for lentiviral transduction.

3.2.3.3. Amaxa™ Nucleofection™ transfection

The Nucleofector™ technology is a ready-to-use method to transfer nucleic acids (plasmid DNA or siRNA) directly into the nucleus of non-dividing cells. This method aims to maintain the viability of the transfected cells and induce a transgene expression after 2-4 hours after the transfection.

A total of 10^6 suspension cells were put into a 15 ml Falcon tube. The tubes were centrifuged for 10 minutes at 90xg at RT. The supernatant was discarded and 82 µl of the Nucleofector solution V and 1 µg of plasmid DNA or 1,5 µg siRNA were added to the tube. The mix was then put into certified cuvettes while avoiding bubbles. The cuvettes were placed into the Nuclefector® device using the Nucleofector® program T-019. Immediately after that, 500 µl of the medium was added to the cuvette and the sample was gently transferred into a 6-well plate. The cells were incubated for 6 - 8 hours and then analyzed.

3.2.4. Lentiviral DNA transduction

Lentiviral transduction was used to integrate shRNA into the genome of target cells. It offers a way to transfer genes into dividing and non-dividing cells in a stable manner (Naldini et al., 1996). A lentivirus contains a genome (RNA) and virus replication enzymes (*pol* gene proteins = protease, reverse transcriptase, integrase) inside a viral protein core (*gag* gene proteins = matrix, capsid and nucleocapsid proteins). The core is surrounded by the viral envelope, which is made of the host cell membrane and viral-encoded envelope glycoproteins (*env* gene proteins). The viral genome always contains the *gag, pol,* and *env* genes, which encode for the different components of the lentivirus. After the viral core has infected a host cell, the reverse transcriptase catalyzes the reaction of RNA to double-stranded DNA (dsDNA). After that, the enzyme integrase places the viral dsDNA into the host DNA. From thereon, the replication of new viruses can be initiated (Buchschacher & Wong-Staal, 2000).

3.2.4.1. Lentivirus production

Phoenix eco cells were used to produce the lentivirus. 2 x 10^6 Phoenix cells per 6 cm plate were seeded at 24 hours before transfection and transfected using the Lipofectamine method (see above). The transfection solution contained the lentiviral plasmid with the gene of interest, the packaging plasmid, and the envelope plasmid

(Table 20.). The medium was changed with 3.0 ml of fresh, P/S free medium after 4.5 hours of transfection. Lentivirus containing medium was harvested 24 and 48 hours after transfection and filtered through a 0.45 µm syringe-filter to remove cellular debris. The lentivirus-containing medium was used for immediate infection.

Construct	Purpose	Amount
plKO.1-construct	shRNA	20 µg
psPAX	Packaging and integrase vector	15 µg
psMD2.G	Envelope vector	5 µg

Table 20. Plasmid-mix for lentivirus production.

3.2.4.2. Lentiviral infection

For lentiviral infection, 2 x 10^6 Eµ-Myc cells per well were put into 6-well-plates with fresh medium. The lentivirus-containing medium and 8 µg/ml polybrene (250µg/µl polybrene diluted in 1X PBS to 4 µg/µl) were added to the Eµ-Myc cells 24 hours and 48 hours after Phoenix eco transfection. Control Eµ-Myc cells were cultured in 3 ml virus-free medium, 8 µg/ml polybrene was added, and the cells were spun with the infected Eµ-Myc cells. Polybrene is a cationic polymer, which increases the efficiency of virus transduction by neutralizing the charge repulsion between the virus and the cell surface (H. E. Davis, Morgan, & Yarmush, 2002). After adding the lentivirus, the plates were spun (1200 rpm, 50 minutes, 32°C). Fresh Eµ-Myc medium was added to each plate and cells were left to incubate with the lentivirus medium 4.5 hours after each spin-infection. 12-20 hours after the second spin infection, the old cell medium was carefully removed and the new medium was added. Fluorescence microscopy was used to determine the infection rate. The Eµ-Myc cells were used for protein analysis or taxol tests 48 hours after the second spin infection.

3.2.5. Flow cytometry

Fluorescence-Activated Cell Sorting (FACS) enables quantitative analysis of cell surface markers, cell size, cell granularity, and intracellular proteins of single cells. It is used to sort heterogenic cell populations according to desired parameters. When a cell passes through the capillary of the flow cytometer, it scatters light and absorbs the incident light and emits photons in a range of wavelengths. Before the analysis, cells can be stained with fluorescent substances or antibodies. These stains emit photons, which can be detected by specific lasers in the flow cytometer. The FACS machine can simultaneously measure different emission wavelengths for one cell. Besides, the forward scatter (FSC) can measure the cell size, because bigger cells produce a lighter scattering. The sideward scatter (SSC) can determine cell granularity. The flow cytometer repeats this process for each passing cell (Herzenberg, Sweet, & Herzenberg, 1976). FACS analysis was used to determine the infection rates of Eµ-Myc cells after lentiviral infection with plKO.1 shRNA constructs containing a GFP sequence. Cell viability after lentiviral transduction was monitored by staining with

propidium iodide with an excitation and emission maxima of 554 nm and 591 nm, respectively. Forty-eight hours after the second spin-infection, 1 ml of Eμ-Myc cells was harvested, washed with 1X PBS once, and centrifuged for 4 minutes at 1200 rpm. The cell pellet was washed with 1X PBS followed by another spin (4 minutes, 1200 rpm), resuspended in 250 μl FACS-Buffer, and analyzed with the FACSCalibur machine. FACS data were analyzed using the Flow-Jo software. Firstly, cells were pre-gated in a FSC against SSC plot to exclude cell debris. Infected and viable Eμ-Myc cells were gated against the channel FL3-H, which detects green fluorescence at 591 nm wavelengths.

3.2.6. Cell lysis

For protein analysis and Western Blotting, cells were lysed on ice in a 150 mM lysis buffer. Inhibitors were added to the lysis buffer in order to inhibit proteases, kinases, and other enzymes. Cell suspensions were mixed with 30 - 80 μl of lysis buffer and incubated on ice for 10 minutes, followed by centrifugation for 10 minutes at 1300 rpm and 4°C. The supernatant with the proteins was transferred to fresh tubes on ice and protein concentration was measured using the Bio-Rad DC protein assay. 500 μl reagent A and 12.5 μl reagent S were mixed according to the manufacturer's protocol and 52 μl of this mixture was mixed with four μl of the protein sample. 444 μl of Reagent B was then added to the samples to start the reaction. The protein concentration was measured after 10 minutes of incubation on a nano-photometer at a wavelength of 750 nm. 5X Laemmli buffer was added to the samples in order to use them for gel separation or store them at -20°C.

3.2.7. Protein analysis

3.2.7.1. SDS-Polyacrylamide Gel-Electrophoresis (SDS-PAGE)

Protein analysis was performed as described in previous studies (Bassermann et al., 2008; Fernandez-Saiz et al., 2013). SDS-Polyacrylamide Gel-Electrophoresis (SDS-PAGE) is an analytical method to separate proteins based on their molecular weight and was discovered by Laemmli (Laemmli, 1970). Proteins usually have positive and negative charges. SDS-containing Laemmli buffer denatures the proteins and the sodium dodecyl sulfate (SDS) covers the proteins with a negative charge. When an external charge is applied to the proteins in the polyacrylamide gel, the linear and negatively charged proteins move towards the positively charged anode and are separated according to their length, which is proportional to their molecular mass.

The polyacrylamide gel was prepared using 40% acrylamide, 0.5 M Tris-HCl buffer with pH 6.8 for stacking gel or 1.5 Tris-HCl buffer with a pH 8.8 for separating gel, 10% SDS, 10% ammonium persulfate (APS) and Tetramethylethylenediamine (TEMED). Changing the concentration of acrylamide changes the resolution of the separating gel. The protein samples were denatured with Laemmli buffer at 95°C for 10 minutes and then added into the gel pockets. A protein ladder with colored bands at specific

molecular weights was used as a marker. A charge of 60 V was applied for 20 minutes, while samples passed the stacking gel, which assembles all proteins on the same line. The voltage was increased to 150 V for another 60 minutes for migration through the separating gel to separate the proteins regarding their size.

3.2.7.2. Western Blotting

Size separated protein samples were then transferred ('blotted') on a polyvinylidene difluoride (PVDF) membrane by wet Western Blotting. The Western Blot set up is illustrated in Figure 3. When an electric field perpendicular to the polyacrylamide gel is applied, the negatively charged proteins move towards the anode (+) and are separated according to their size, charge or other properties (Goldman, Ursitti, Mozdzanowski, & Speicher, 2015).

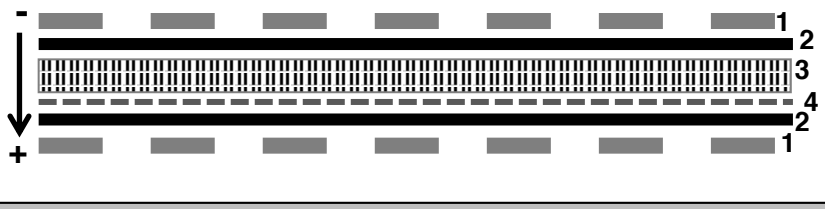

Figure 3. Illustration of a Western Blot set-up.
1: Sponge pads; 2: Whatman paper; 3: Polyacrylamide gel; 4: PVDF membrane; +: anode; -: cathode.

PVDF membranes were activated in methanol. The Western Blot set-up was put into a cassette and placed into a blotting chamber filled with blotting buffer. A charge of 100 V was applied for one hour or at least six hours at 30 V. Since the blotting process generates heat, the transfer was carried out in a cold room to avoid band smearing. After blotting, the PVDF membranes were stained with Ponceau S solution to check equal loading and transfer quality. The membranes were then cut into strips according to the different molecular weights of proteins of interest. The Ponceau S solution was then rinsed off with three washes with washing buffer (WB). Blocking of the membranes was performed with 5% milk in washing buffer for 30 minutes to prevent unspecific binding of antibodies. After that, the membranes were incubated with the primary antibodies overnight at 4°C in 5% milk. Antibodies were washed off three times for 15 minutes with WB and incubated with the matching secondary antibody diluted in 5% milk (1:5000) for one hour at RT. The secondary antibodies are linked to horseradish peroxidase. After three washes with WB and one wash with 1X PBS, the membranes were developed using enhanced chemiluminescent substrates pico and femto by Pierce on photosensitive X-ray films. The intensities of the resulting signals were evaluated using publicly available ImageJ159 program

3.2.7.3. Stripping and reprobing of samples

If the reprobing of membranes was necessary, the membranes were activated with methanol for one minute and washed in distilled water for one minute. The membrane was put into stripping buffer (SB) in a closed container at 65°C for 15 minutes and at RT for another 10 minutes on a platform shaker. The membrane was then washed four times with 1X PBS and blocked in 5% milk for 20 minutes and was then incubated again with a primary antibody of choice.

3.2.8. Quantitative PCR

The polymerase chain reaction (PCR) is a widely used method to amplify DNA sequences of interest. The PCR is a three-step process: Firstly, the DNA is denatured to separate the two DNA strands at 95°C. Secondly, the PCR primers anneal to the DNA single-strand at 55 - 65°C. Thirdly, the selected DNA section is amplified by the elongating enzyme DNA polymerase at 72°C. This cycle is repeated 25 - 30 times and amplifies the amount of initial DNA product exponentially.

Quantitative PCR (qPCR) or real-time PCR (RT-PCR) combines PCR amplification and quantification of the PCR product in real-time with a fluorescent probe. The higher the starting copy number of the nucleic acid target, the sooner a significant increase in fluorescence is observed. The qPCR instrument contains a thermal cycler with an integrated excitation light source, a fluorescence detection system, and software that converts the recorded fluorescence data into a DNA amplification curve (Higuchi, Fockler, Dollinger, & Watson, 1993; Navarro, Serrano-Heras, Castano, & Solera, 2015).

Quantitative PCR was used to evaluate mRNA levels of USP9X and XIAP levels in DLBCL cell lines. The PCR primers for the qPCR were designed using the internet-based free software QuantPrime. The mRNA is purified from a cell culture and then used to synthesize complementary DNA (cDNA) via reverse transcription. The cDNA is then amplified via qPCR exponentially (Figure 4.).

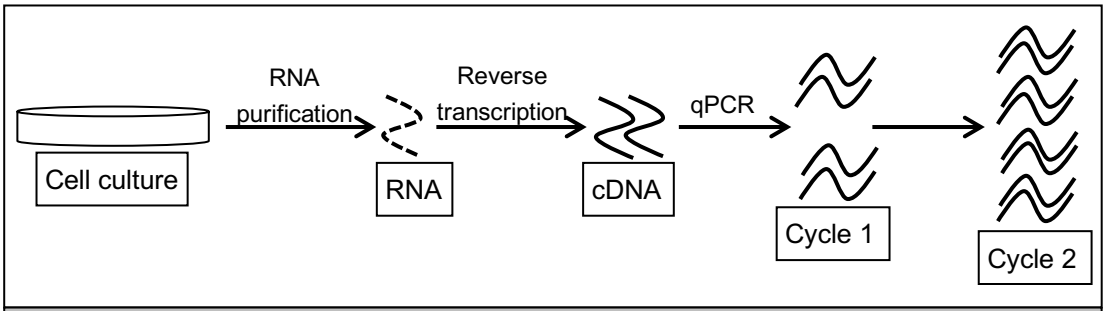

Figure 4. Illustration of quantitative PCR (qPCR).

3.2.8.1. RNA purification

After cell harvesting and cell lysis (chapter 3.2.1.3. and 3.2.6.), RNA was purified from cultured cells using the QIAshredder columns and the Qiagen RNeasy extraction kit. First, 350 µl RLT buffer was added to disrupt the cell membrane and the samples were

vortexed for one minute. The lysates were transferred into the QIAshredder columns placed in a 2 ml tube and centrifuged for 2 minutes at full speed. Then, 350 µl ethanol (70%) was added to each lysate and mixed by pipetting. 700 µl of the sample was put into an RNeasy spin column placed in a 2 ml tube and centrifuged for 15 seconds at 10000 rpm. The flow-through was discarded. Next, 700 µl Buffer RW1 was added to the RNeasy spin column and centrifuged for 15 seconds at 10000 rpm. The flow-through was discarded again. 500 µl Buffer RPE was added to the RNeasy spin column and centrifuged for 15 seconds at 10000 rpm twice. Lastly, the RNeasy spin columns were put in new tubes and 30 µl RNase-free water was added directly to the membrane. The tubes were centrifuged for one minute at full speed to elute the RNA. The RNA concentration was measured using the nano-spectrophotometer. The samples were either temporarily stored at -80°C or used immediately for reverse transcription.

3.2.8.2. Reverse transcription

Reverse transcription is the process of generating complementary DNA (cDNA) by the enzyme reverse transcriptase using RNA as a template. At first, a mix of 1 µg of RNA, 1 µl of Hexamers, 1 µl of dNTP was filled up with RNase-free, distilled water (dH_2O) to add up to 13 µl. Random Hexamers is a mix of oligonucleotides with random base sequences and was used as a primer. The mix was incubated for 5 minutes at 65°C to allow the annealing. The samples were then incubated on ice for one minute. A mix of 4 µl of 5X First-Strand buffer, 3 µl 0.1 M DTT, 0.5 µl of RNAseOut™ recombinant RNase inhibitor, and 1 µl SuperScript™ III reverse transcriptase were added to each sample by gently pipetting. After that, the samples were incubated at 50°C for one hour. The reaction was inactivated at 70°C for 15 minutes. The cDNA concentration of each sample was measured by a nano-spectrophotometer.

3.2.8.3. Quantitative PCR (qPCR)

The quantitative PCR was performed using the LightCycler® SYBR Green I kit according to the manufacturer's instructions. SYBR green contains FastStart Taq DNA Polymerase, a reaction buffer, dNTP mix, SYBR Green I dye, and $MgCl_2$. The SYBR Green I dye is a fluorescent dye that intercalates with DNA, which increases the fluorescence. The increase of DNA during each qPCR cycle correlates with the intensity of fluorescence, which is then detected by the LightCycler®.

Firstly, the synthesized cDNA was diluted 1:10 with dH_2O. Ten µl SYBR Green master mix, 1 µl of both forward and reverse target sequence-specific primers (10 pmol/µl), 3 µl dH_2O and 5 µl of diluted cDNA were pipetted into a well of a 96-well plate. The plate was sealed and shortly centrifuged and put into the LightCycler® for the reaction. An LC480 LightCycler® was used to run 30 PCR cycles. Each sample was pipetted and measured in duplicates, and results were normalized to ARPPA primers as a control using advanced relative quantification.

3.2.9. Design and cloning of shRNA constructs

RNA interference (RNAi) is a method to silence specific target genes transiently. It is mediated by small RNAs, including microRNA (miRNA), small interfering RNA (siRNA), short hairpin RNA (shRNA) (Hannon, 2002). Short hairpin RNA (shRNA) contains 21 - 25 bp with a small terminal loop that can silence target gene expression via RNA interference. Delivery of shRNA into cells is executed by plasmids, viral, or bacterial vectors. Short hairpin RNA is transcribed by polymerase II or III in the nucleus and processed by the ribonuclease III Drosha. The resulting pre-shRNA is exported to the cytoplasm by Exportin 5 and processed by ribonuclease III Dicer and incorporated into RNA-induced silencing complex (RISC). The RISC then uses the antisense “guide” strand to cleave and silence the mRNA (Couto & High, 2010; Paddison, Caudy, Bernstein, Hannon, & Conklin, 2002). The knockdown of specific proteins by shRNA was performed according to the instructions of The RNAi Consortium (TRC), based at the Broad Institute, Cambridge, Massachusetts, USA.

3.2.9.1. General information

For the following experiments, two types of vectors were used: pLKO.1 and MIGR1.

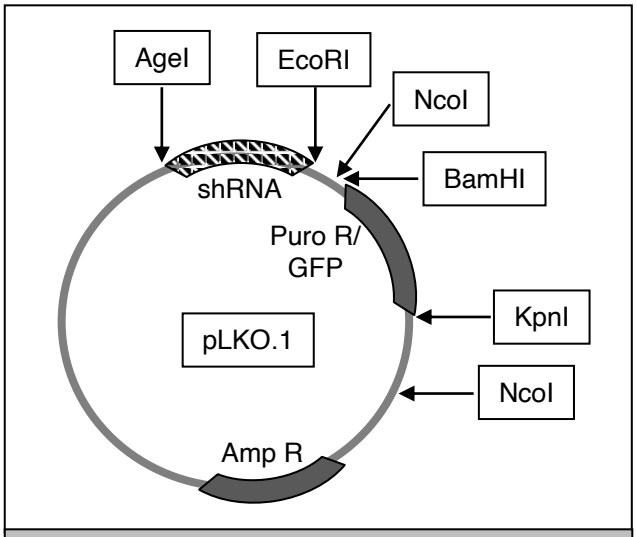

Figure 5. Simplified vector map of pLKO.1 shRNA plasmid. → = Restriction site of cutting enzyme, R = resistance, Puro = Puromycin, Amp = Ampicillin.

The pLKO.1 GFP puro vector is a lentiviral vector, which has a 7000 bp long backbone (Figure 5.). The vector is used to express shRNA in mammalian cells. A 1.9 kb spacer, which needs to be removed before inserting the shRNA sequence, sits between the AgeI and EcoRI cutting sites. The vector also has a puromycin resistance between the BamHI and KpnI cutting sites, as well as an ampicillin resistance. The original puromycin resistance gene of the pLKO.1 plasmid was replaced by a sequence of GFP green fluorochrome to assess the rate of shRNA-infected cells immediately via fluorescence microscopy. The GFP sequences codes for the green fluorescent protein (GFP), which can emit a green fluorochrome upon excitation by a laser line at a

maximum of 591 nm. Agarose gel electrophoresis, purification, ligation, and transformation were carried out as described in the following sections. Test restrictions were performed by double digestion with EcoRI and NcoI. The exchange of the puromycin resistance with GFP resulted in a new NcoI cutting site. The positive clones showed three fragments of 5000 bp, 1250 bp, and 750 bp lengths after test restriction. The MIGR1 vector is a retroviral vector with a 6200 bp long backbone (Figure 6.). It is used to express shRNA in mammalian cells. The vector has an internal ribosome entry site (IRES), which sits between the insert and the GFP green fluorochrome sequence and allows the co-expression of two proteins from a single mRNA. A GFP green fluorochrome sequence follows the IRES. The plasmid also contains an ampicillin resistance.

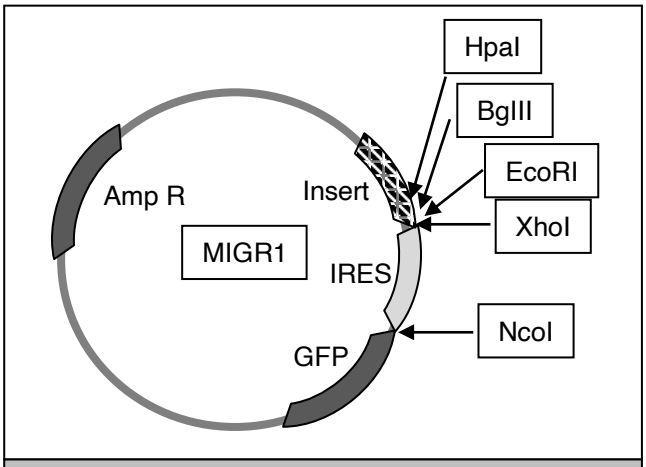

Figure 6. Simplified vector map of MIGR1 plasmid. → = Restriction site of cutting enzyme, R = resistance, Amp = Ampicillin, IRES = internal ribosome entry site.

3.2.9.2. Design of shRNA oligonucleotides

Short hairpin RNA (shRNA) constructs consist of a 21 bp sense and antisense sequence with a loop between and restriction overhangs on both sides and resembles a hairpin (Figure 7.).

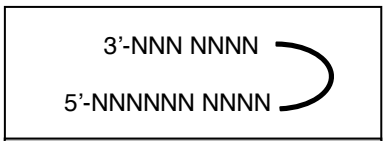

Figure 7. shRNA schematic.

The restriction overhangs are flanks to prime a reaction (Paddison et al., 2004). The oligonucleotides were ordered and dissolved in dH_2O to a final concentration of 100 pmol/µl by gentle shaking for 60 minutes at RT. The details on the oligonucleotide sequences are listed in table 14 (chapter 3.1.10.).

3.2.9.3. Annealing of shRNA oligonucleotides

The shRNA oligonucleotides need to be annealed before cloning into a vector: 1 µl of both forward and reverse oligonucleotides, 5 µl of 10X annealing buffer and 43 µl of dH_2O were mixed and incubated at 95°C for 5 minutes, then at 80°C for 10 minutes and then slowly cooled down to RT in 1 L of 70°C warm water for at least 4 hours.

3.2.9.4. Amplification of genes of interest

The gene of interest (e.g., shXIAP, USP9X, GFP green fluorochrome sequence) was amplified by polymerase chain reaction (PCR). 2.5 µl of the template (100 ng/µl, see 3.1.11. for all templates), 1.5 µl of the forward and reverse primers (10 pmol/µl), 1 µl dNTPs, 5 µl 10X Pfu buffer were mixed with 36.5µl dH_2O. The reaction was started by adding 2 µl of the Pfu II ultra DNA polymerase to the mix. For the separation the DNA-double helix, the temperature was set at 95°C for 30 seconds, the primers annealed at 55°C for 30 seconds, and elongation carried out at 72°C for 3 minutes. This process was repeated for 30 cycles to amplify the amount of DNA product.

3.2.9.5. DpnI digestion

DpnI is an enzyme that degrades bacterially methylated or hemimethylated DNA sites. The DpnI digestion is used to remove the template plasmid and plasmid fragments after amplification via PCR. The DpnI digestion helps to keep the background in transformations low. The digestion with DpnI was performed for one hour at 37°C.

3.2.9.6. Purification of DNA

After PCR amplification and between DNA restrictions, the DNA was purified using the Thermo Scientific GeneJET PCR Purification kit, which removes primers, dNTPs, unincorporated labeled nucleotides, enzymes, and salts.

A 1:1 volume of Binding Buffer was added to the PCR mix and was then mixed thoroughly until the cords disappeared. The mix was then transferred into the purification column and centrifuged for one minute at full speed. The flow-through was discarded. The column was washed by adding 700 µl of Wash Buffer and centrifuging for one minute at full speed. The flow-through was discarded and the column was centrifuged again for a one minute to remove any residual wash buffer. The DNA containing column was placed into a clean 1.5 ml tube, 30 µl of Elution Buffer were added to the center of the column membrane, and centrifuged for one minute.

3.2.9.7. DNA restriction

Restriction enzymes recognize palindromic DNA sequences and can cut the DNA while producing overhanging single-stranded ends. Every restriction enzyme detects a specific palindromic recognition site of the DNA. The amplified PCR product and the vector were cut using a double digest method. The recommended reaction conditions

can be found on the Thermo Fisher Scientific homepage for all combinations of common restriction enzymes.

In general, 1 µg vector and 1 µg insert were mixed with 3 µl of restriction enzyme and 4 µl of recommended buffer and 3 µg dH_2O and incubated at 37°C for 2 hours. After a DNA purification step, the process was repeated with the second restriction enzyme.

3.2.9.8. Ligation

The purified vector and insert were ligated using the rapid ligation kit (Fermentas) according to the manufacturer's instructions. Two µl vector, 6 µl insert, 10 µl T4 DNA ligation buffer were diluted in dH_2O to a final volume of 13.5 µl. The reaction was started by adding 1.5 µl of T4 DNA ligase and incubating for 5 minutes at RT. The ligated DNA was either stored at -20°C or used for the transformation immediately.

3.2.9.9. Agarose gel electrophoresis

The production of agarose gels included the following steps: 0.5 g agarose and 100 ml Tris/Borate/EDTA (TBE) buffer were boiled, 7.5 µl ethidium bromide (EtBr) was added, and the mix was cast into desired forms with sample pockets. Digested DNA samples with 6X DNA loading dye were put into sample pockets. By applying a 120 V charge for 20 minutes, DNA was separated according to size due to the negative charge of the DNA molecule. Ethidium bromide intercalates in nucleic acids (e.g., DNA) and thereby changes its absorption spectrum. By intercalation with DNA, the intensity of fluorescence of Ethidium bromide increases and can be visualized under UV light. The illumination of DNA is proportional to its concentration and length (LePecq & Paoletti, 1967).

The fragments of interest were excised according to size. DNA was extracted from the gel and purified using the gel extraction kit according to the manufacturer's instructions. DNA concentrations were measured on a nano-spectrophotometer.

3.2.9.10. Bacterial transformation and culture

The plasmid DNA was amplified in NEB5α competent high-efficiency Escherichia coli bacteria. Twenty-five µl bacteria were thawed from -80°C, supplemented with 5 µl ligation product, and incubated for 10 minutes on ice. A heat shock for 30 seconds at 42°C was performed, followed by incubation on ice for 2 minutes. For recovery, 200µl of SOC medium was added to the samples and incubated at 37°C for one hour while gently shaking. Samples were plated onto LB agar plates, supplemented with antibiotics specific to the resistance of the plasmid (100 µg/ml ampicillin or 50 µg/ml kanamycin) and incubated at 37°C overnight. The next day, single colonies were picked and cultured overnight in 5 ml LB medium at 37°C under vigorous shaking. Plasmid DNA was extracted from 2 ml bacteria medium using the peqGOLD plasmid mini extraction kit. The samples were centrifuged at 10000 rpm for 4 minutes and the supernatant was discarded. The pellet was resuspended with 250 µl Solution I. 250 µl

of Solution II was added and mixed by inverting 6 - 8 times. Then, 250µl of Solution III was added and inverted 6 to 8 times until a white, flaky precipitate appears. The samples were centrifuged at full speed (FS) for 10 minutes. The plasmid containing supernatant was pipetted into the PerfectBind DNA column in a 2 ml tube and centrifuged at FS for one minute. After the flow-through was discarded, 600 µl of Washing Buffer was added, and the samples centrifuged at FS for 1 minute. The columns were put in new 1.5 ml tubes, 30 µl of Elution Buffer was added to the column, and after 3 minutes, the samples were centrifuged at FS for 1 minute. Plasmid DNA was produced on a larger scale by incubating bacteria in 300 ml LB medium at 37°C overnight. DNA was extracted using the QIAGEN Maxi prep kit according to the manufacturer's instructions.

3.2.9.11. Test restriction

After bacterial transformation, a test restriction via agarose gel electrophoresis was performed to verify the integrity of the vector. In a double digest, 3 µl of ligation product was restricted with 1.5 µl of both restriction enzyme with 1.5 µl buffer and 8.5 µl dH_2O for one hour at 37°C. For the insertion of GFP into a USP9X shRNA vector, BamHI and Kpn were used. GFP is an 800 bp long sequence, while the pLKO.1 vector has 9000 bp. The exchange of the puromycin resistance sequence of the pLKO.1 vector with GFP resulted in a new NcoI cutting site and positive clones showed three fragments (5000 bp, 1250 bp, 750 bp length) after test restriction (Figure 8.).

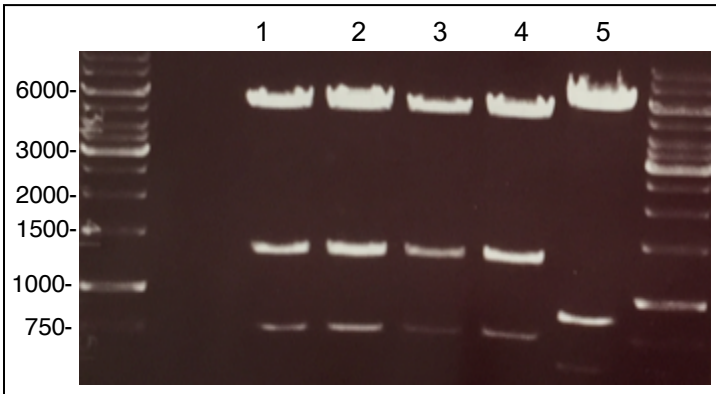

Figure 8. Image of test restriction and electrophoresis on 0.7% agarose gel. The left and right marker represent the size in bp. Positive clones show three fragments (750 bp, 1250 bp, 5000 bp). Therefore, clones 1, 2, 4 were sent for sequencing.

DNA of positive clones was sent for sequencing (Eurofins MWG GmbH, Ebersberg) with corresponding primers to ensure appropriate integration of the insert. Sequences were confirmed using the aligning function of MacVector.

3.2.10. Studies in mice

Lentiviral IRES-GFP shRNA constructs against non-relevant mRNA (non-targeted shRNA/sh_Ctrl) or USP9X mRNA (sh_USP9X) or XIAP mRNA (sh_XIAP) together with IRES-linked GFP were produced in Phoenix eco cells (see 3.2.3.). The murine Eμ-Myc lymphoma cells were spin-infected with the lentivirus twice. After 48 hours, the Eμ-Myc cells were sorted by FACS (see 3.2.5) and injected into syngeneic C57BL mice (5×10^4 cells per mouse). All mice were female, the same size, and 10 weeks old. They were randomly distributed into the experimental groups and equally housed and fed. The mice were checked for lymph node status by weekly palpation. Disease state was defined by the presence of palpable enlarged lymph nodes as well as poor performance status (less movement, dull fur, limping, dyspnea). An independent member of the mouse facility, who did not have any insight into the experiment, determined the time of sacrifice. The lymph nodes and bone marrow were passed through 70-lm cell strainers to obtain single-cell suspensions and assess cell immunophenotype and GFP content. An erythrocyte-lysing buffer (NH4Cl 0.15 M, HEPES 0.02 M, and EDTA 0.1 M) was added to the samples, if necessary. Samples for immunohistochemistry (IHC) were fixed in 5% PFA. Survival data in each approach was analyzed using the Kaplan–Meier method, applying the log-rank (Mantel-Cox) test for statistical significance. Animals were censored from analyses when sacrificed for non-tumor reasons. For the survival and tumor growth studies, a group size of at least five animals per group was chosen, which allowed the detection of twofold differences in survival with a power of 0.89, assuming a two-sided test with a significance threshold of 0.05 and a standard deviation of less than 50% of the mean.

Experiments were performed in accordance with the local ethical guidelines and approved by the responsible regional authorities (Regierung von Oberbayern).

3.2.11. Statistical analysis

Statistical analysis was performed using the GraphPad Prism software. One-sample t-tests were used to assess the statistical significance of relative ratios. Regular Student's t-tests were used in case of absolute values. Most graphs show means ± SD. Significant results are shown by using the following most commonly used representation: *: $P < 0.05$; **: $P < 0.01$; ***: $P < 0.001$; **** < 0.0001.

4. Results

This study covers the biological aspects of the USP9X-XIAP axis in DLBCL cells and an Eμ-myc mouse model. The study is part of a collaborative project and its results are presented in the introduction and discussion sections. However, data in Figure 9, 17, 18, and 25 were obtained by Dr. med. Katharina Engel and are integrated into the results section in order to improve the comprehension of the study.

4.1. Introduction

Initially, our group analyzed cell cycle profiles of different USP family members and found a significant enrichment of USP9X in mitotic cells. We wondered if USP9X exerted mitotic pro-survival activity by stabilizing other IAP family members apart from Survivin. Therefore, different IAP proteins were analyzed under the condition of RNAi-mediated USP9X knockdown.

X-linked inhibitor of apoptosis (XIAP) was decreased upon USP9X knockdown in mitosis (Figure 9.). XIAP expression could be rescued by treating the cells with the proteasome inhibitor MG132. XIAP also accumulated parallel to USP9X during mitosis. These findings indicated that USP9X had a potential role in the stabilization of XIAP during mitosis. To note, Baculoviral IAP repeat-containing protein 8 (BIRC8) also showed reduced expression in USP9X-silenced cells during mitosis. BIRC8 is similar to the C-terminal region of XIAP. However, Shin et al. reported that BIRC8 was an unstable protein due to a conformational instability of its BIR domain and cannot inhibit caspase 9 in vivo (Shin et al., 2005). Other proteins like ML-IAP, NAIP, cIAP2, cIAP1, and cyclin B1 did not show an altered expression level in the USP9X-silenced cells (Engel et al., 2016).

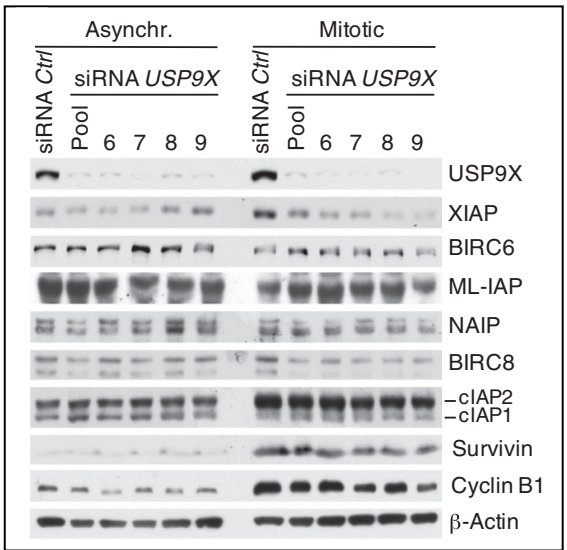

Figure 9. Immunoblot of HeLa cells after siRNA transfection - untreated or synchronized in mitosis with sequential thymidine and nocodazole treatment. From Engel K et al. (2016).

Our group found that the ubiquitin-specific protease 9X (USP9X) has a mitosis-specific function by deubiquitylating and stabilizing XIAP in order to promote mitotic survival. An overexpression of USP9X and subsequent high expression of XIAP causes a poorer prognosis and therapy resistance in DLBCL.

4.2. Design and production of lentiviral IRES-GFP shRNA constructs

We wanted to test five different conditions to investigate the role of USP9X and XIAP in human DLBL cell lines and, consequently, in an Eμ-myc mouse model: an XIAP knockdown, a USP9X knockdown, a knockdown control, an XIAP overexpression, and an overexpression control. For the knockdown conditions, a pLKO.1-based vector carrying shRNA directed against the human XIAP gene (sh_XIAP), a USP9X shRNA vector (sh_USP9X), and a non-targeted shRNA vector control (sh_Ctrl) was used. We wanted to directly assess the rate of transduction of the shRNA constructs into the DLBCL cell lines and Eμ-myc cells by fluorescence microscopy and FACS sorting. Therefore, we exchanged the original puromycin gene of all three pLKO.1-based vectors for a GFP green fluorochrome sequence (sh_Ctrl, sh_USP9X, sh_XIAP). The restriction enzymes BamHI and KpnI were used to insert the GFP into the pLKO.1 vector. The general method of designing and cloning a vector was carried out, as described in section 3.2.9. For the overexpression conditions, the XIAP gene was cloned into a MigR1 vector (MigR1_XIAP). The sole MigR1 vector was used as a control (MigR1_Ctrl).

4.2.1. Non-targeted shRNA pLKO.1 GFP vector

The non-targeted shRNA pLKO.1 puro vector was used as a negative control for the sh_USP9X and sh_XIAP vector. The vector has a 7032bp backbone and a 60bp scramble shRNA sequence. The original puromycin resistance gene was replaced by a sequence of GFP green fluorochrome using restriction enzymes BamHI and KpnI to assess infection rates immediately with fluorescence microscopy. Test restrictions were also performed using BamHI and KpnI.

4.2.2. XIAP shRNA pLKO.1 GFP vector

Our group was kindly gifted five different shRNA plasmids against XIAP in a pLKO.1-based vector from L. Nilsson. Firstly, we tested the efficiency of each plasmid to knockdown XIAP. Each XIAP shRNA plasmid was separately transduced into NIH cells via Lipofectamine® 2000 transfection (chapter 3.2.3.2). Western blotting was used afterward to assess the XIAP protein expression levels (Figure 10.). Construct number 4 showed a clear and total knockdown of XIAP, while the USP9X expression was normal. Therefore, construct number 4 was chosen for the following experiments. As mentioned above, the puromycin resistance in the shRNA-carrying vectors was replaced by a GFP green fluorochrome sequence.

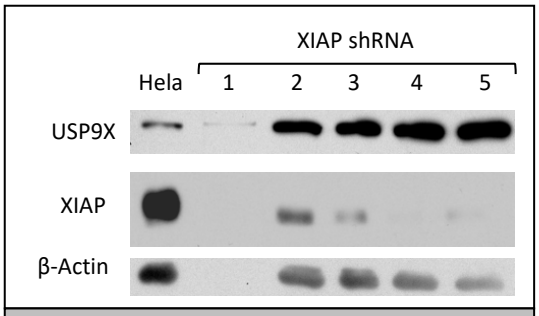

Figure 10. Western Blot of five different XIAP shRNA constructs in NIH cells and Hela cells as a control.

Figure 11 shows representative flow cytometry data of transduced Eμ-Myc cells, which were plotted against FL1-H, which measures green fluorescence emitted by GFP sequence (see 3.2.9.1.), and FL3-H, which measures PI, which is a marker for apoptosis. An appropriate border range was applied to separate the cells into four groups (Figure 11.): PI-negative and GFP-negative cells (quadrant Q4) are viable cells that were not successfully transduced. PI-positive and GFP-negative cells (quadrant Q3) are cells that are apoptotic and do not contain the shRNA vector. PI-positive and GFP-positive cells (quadrant Q2) have successfully been transduced, but are apoptotic. Lastly, the cells of interest are the PI-negative and GFP-positive cells (quadrant Q1) that are viable and contain the shRNA-carrying vector. The infection rate of the sh_Ctrl vector (non-targeted shRNA) into Eμ-Myc cells was 26.8% with a rate of apoptosis of 21.8%. Respectively, the rate of infection of the sh_XIAP vector was 19,0% with an apoptosis rate of 20.8% (Figure 11.).

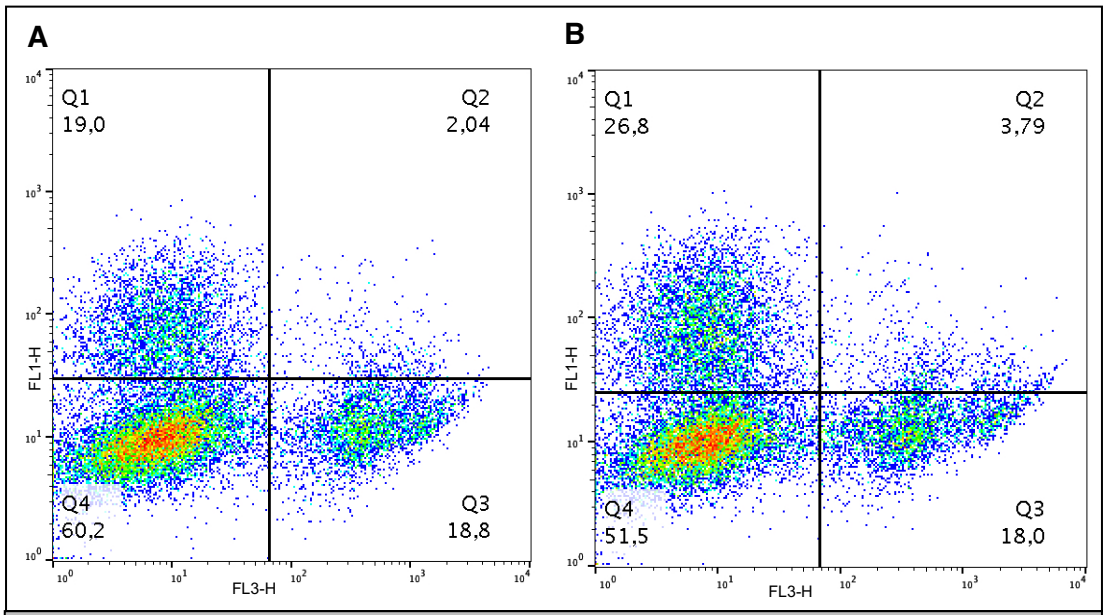

Figure 11. Lentiviral transduction rates of Eμ-Myc cells assessed by flow cytometry analysis. (A) sh_XIAP GFP vector, (B) shRNA_Ctrl (scramble shRNA). FL1-H represents the GFP green fluorochrome gate indicating successful transfection; FL3-H axis is the PI gate indicating apoptosis.

4.2.3. USP9X shRNA pLKO.1 GFP vector

The shRNA sequence of USP9X was derived from a previous publication (Perez-Mancera et al., 2012) using the target sequence 5'-GAT GAG GAA CCT GCA TTT CCA-3'. The USP9X shRNA sequence was cloned into the pLKO.1 GFP vector. NcoI and EcoRI enzymes were used for restriction. The new USP9X shRNA plasmid was amplified via bacterial transformation, five bacteria colonies were picked, and plasmid DNA was extracted. These five constructs with different sequences were tested regarding their USP9X expression. Construct number 4 was selected for further experiments due to the lowest USP9X expression (Figure 12.).

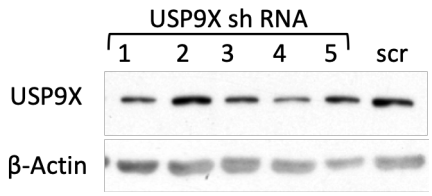

Figure 12. Immunoblot of five USP9X shRNA constructs and a non-targeted (scr) shRNA control in NIH cells.

Eμ-Myc cells were transduced with the UPS9X shRNA plasmid or control shRNA plasmid (sh_UPS9X vs. sh_Ctrl) and assessed regarding their transduction and apoptosis rate using flow cytometry (Figure 13.). The cells were plotted against FL1-H measuring green fluorescence emitted by the GFP sequence and FL3-H measuring the apoptosis marker PI. The transduction rate was 30.6% for the sh_USP9X vector with an apoptosis rate of 24.3%. The transduction rate for the sh_Ctrl vector (non-targeted shRNA) was 26.8% and the rate of apoptosis 21.79%.

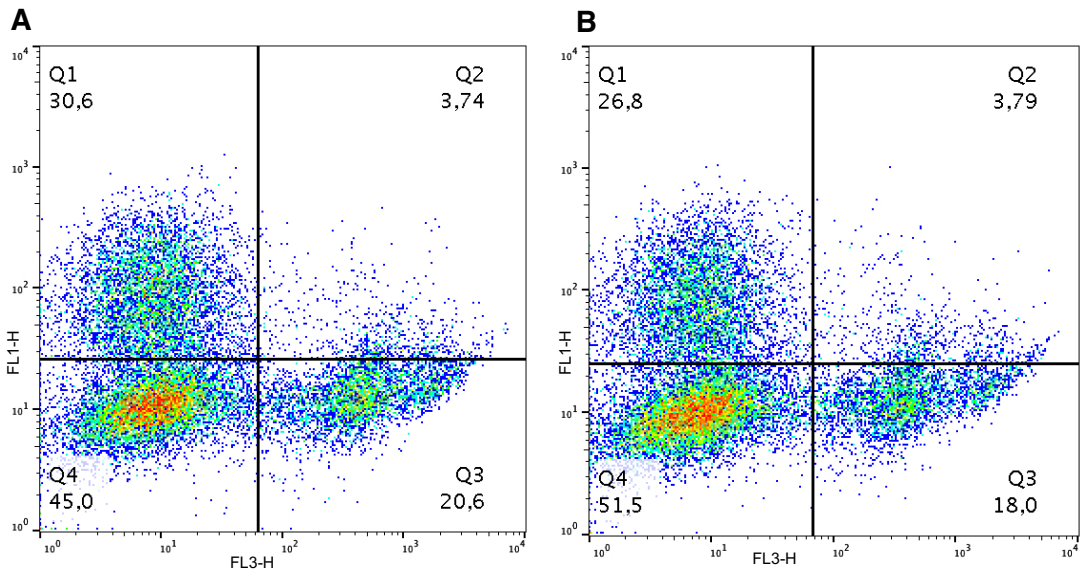

Figure 13. Lentiviral transduction rate of Eμ-Myc cells transduced with sh_USP9X (A) and shRNA_Ctrl (B) assessed by flow cytometry. FL1-H is the GFP green fluorochrome gate indicating successful transfection; FL3-H is the PI gate indicating apoptosis.

4.2.4. MIGR1_XIAP vector

The MigR1_XIAP vector was employed to assess the role of XIAP overexpression in lymphomagenesis. As described above (chapter 3.2.9.1.), the MigR1 is a retroviral vector that contains an internal ribosome entry site (IRES) between the insert and the GFP green fluorochrome sequence. The IRES allows the co-expression of both sequences. The XIAP overexpression sequence was inserted using the BamHI and XhoI enzyme. Test restrictions were performed by double digest with BamHI and XhoI enzymes as well. Figure 14 shows NIH cells that have been transfected with the MigR1_XIAP vector and MigR1_Ctrl vector. Empty NIH cells (Ctrl) were used as control. The NIH cells show a sufficient overexpression of the XIAP protein in comparison to the NIH cells transfected with the MigR1-Ctrl cells.

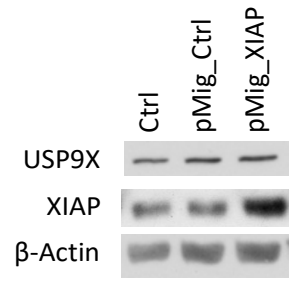

Figure 14. Immunoblot of not transfected NIH cells (Ctrl) and NIH cells transfected with the MigR1_XIAP vector and the MigR1_Ctrl vector.

Flow cytometry was used to assess the rate of transduction of the MigR1_XIAP and MigR1_Ctrl vector in Eμ-myc cells. A transduction rate of 12.7% was achieved using the MigR1_XIAP vector and 36.4% for the MigR1_Ctrl vector (Figure 15.).

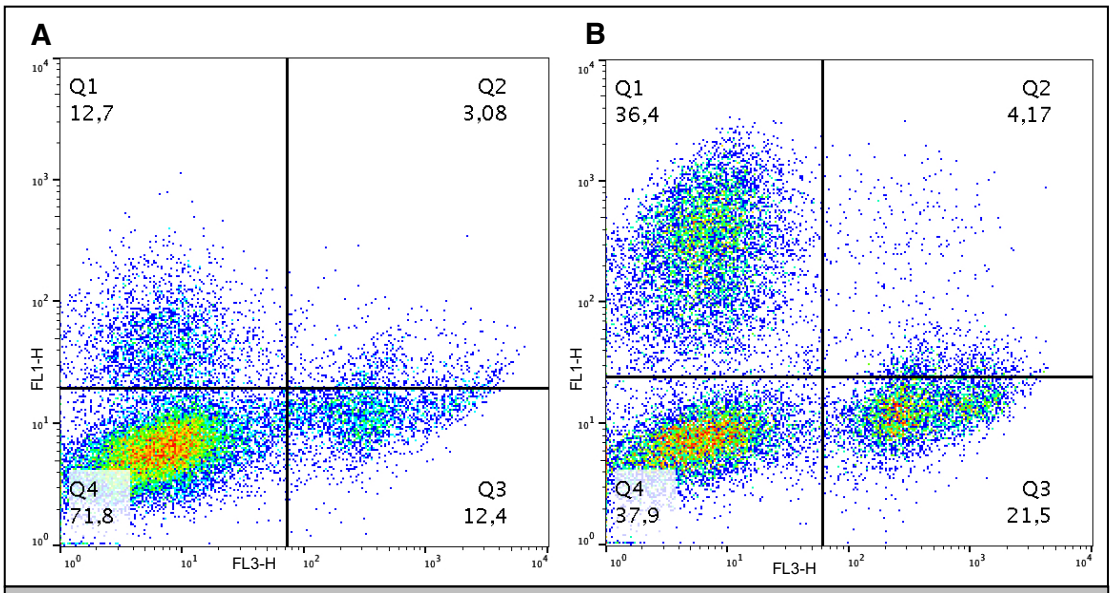

Figure 15. Flow cytometry of Eμ-Myc cells after transduction with a MigR1_XIAP vector (A) and the MigR1_Ctrl control (B). FL1-H represents the GFP green fluorochrome gate indicating successful transduction; FL3-H axis is the PI gate indicating apoptosis.

4.3. XIAP and USP9X expression in human DLBCL cell lines

Since our group had already highlighted the interaction of USP9X and XIAP, we wanted to further investigate the role of XIAP and UXP9X in human DLBCL cell lines. Eight human DLBCL cell lines were characterized regarding their XIAP and USP9X expression levels. Hela cells were used as control. The cell lines SuDHL 6 and Oci-Ly 3 cells had a low USP9X expression and a low XIAP expression. SuDHL 4 cells showed a moderate USP9X expression and low XIAP expression. SuDHL 8 cells showed a high USP9X and, consequently, a higher XIAP expression (Figure 16.).

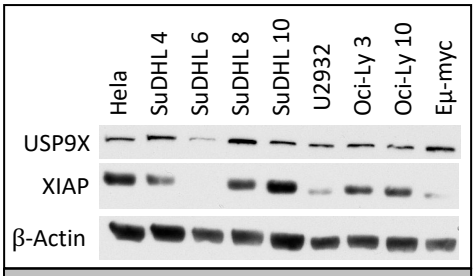

Figure 16. Immunoblot of different DLBCL cell lines regarding the USP9X and XIAP expression. Hela cells were used as a control.

Our group also found that the cell lines RIVA and RT had a high USP9X and XIAP expression (Figure 17.). These cell lines were also tested regarding their response to the taxol. Taxol (or: Paclitaxel) stabilizes the microtubules by binding to tubulin. The microtubule stabilization activates the spindle assembly checkpoint (SAC), which delays the exit from mitosis. Upon delayed mitosis, cells can die via a caspase-dependent apoptotic pathway (mitotic apoptosis) or exit mitosis and return to the G1 phase in a tetraploid state (mitotic slippage). Cells with an anti-apoptotic advantage such as USP9X and consecutive XIAP overexpression might be able to prevent mitotic cell death by mitotic slippage (Topham & Taylor, 2013). Our group found that Oci-Ly 10, RIVA, and RT cells had an increased resistance towards taxol treatment, indicating that USP9X and XIAP are promoting mitotic cell survival (Figure 18.).

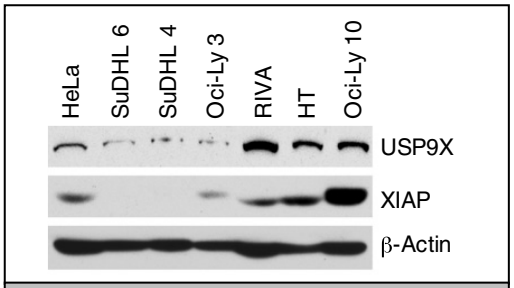

Figure 17. Immunoblot of HeLa cells (control) and six human DLBCL lines. From Engel K et al. (2016).

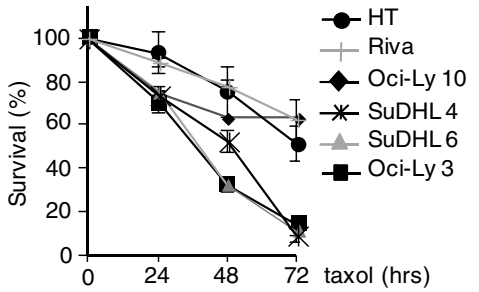

Figure 18. FACS analysis (propidium iodide, PI) of DLBCL cells after treatment with taxol to determine cell survival. From Engel K et al. (2016).

4.4. XIAP- and USP9X-silenced Eμ-Myc cells show increased chemosensitivity

After the confirmation that DLBCL cell lines with high levels of USP9X have an increased chemoresistance towards taxol, the second part of the work was dedicated to the investigation of whether Eμ-myc lymphoma cells showed altered chemosensitivity upon knockdown of XIAP and USP9X in a mouse model.

The Eμ-myc mouse carries the c-myc oncogene that is under the control of the Ig heavy chain (IgH) enhancer. This transgene mimics the t(8;14) translocation of c-myc and the IgH enhancer, which is characteristic for human Burkitt lymphoma (Adams et al., 1985). Eμ-Myc mice develop B-cell leukemia or lymphoma with a 100% penetrance. However, Eμ-Myc lymphomas arise through the acquisition of additional mutations and that the tumors are heterogeneous in their latency of onset and clinical features (Mori et al., 2008). Therefore, the Eμ-Myc mouse model offers a reproducible system to investigate the processes involved in lymphomagenesis (A. W. Harris et al., 1988).

We investigated the impact of XIAP- and USP9X-silencing on a cellular level via flow cytometry (Figure 19.).

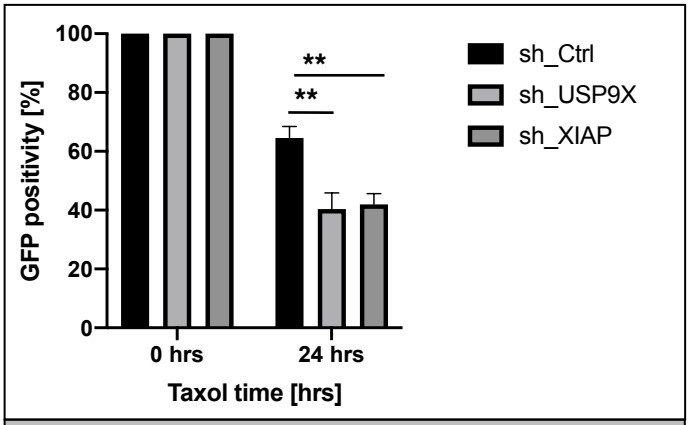

Figure 19. FACS analysis (propidium iodide, PI) of Eμ-myc cells transfected with sh_Ctrl (non-targeted shRNA), sh_USP9X, or sh_XIAP and treated with taxol. Results were derived from three independent experiments (n= 3, ±SD). **P = <0.005; Student's t-test.

Eμ-myc cells were transfected with the sh_Ctrl, sh_USP9X, or sh_XIAP plasmid, as described above. Afterward, taxol (500 uM) was added to the Eμ-myc cells. Lastly, flow cytometry was employed at several time points to assess GFP positivity, which is equivalent to cell viability. XIAP- and USP9X-silenced cells showed a significantly increased loss of GFP positivity compared to the control cells. These findings indicate that low levels of XIAP and USP9X cause increased sensitivity to taxol treatment.

Figure 20 shows an immunoblot time course (0 hrs, 8 hrs, 12 hrs, 24 hrs, 36 hrs, 48 hrs) after treatment with taxol in Eμ-myc cells, which were transfected with a Lipofectamine® 2000 protocol (chapter 3.2.3.2.) with sh_Ctrl (non-targeted shRNA),

sh_USP9X and sh_XIAP. The sh_Ctrl cells show an increased expression of cleaved PARP and cleaved caspase 3 (CC-3) starting 8 hours after taxol application, which reflects an increase of apoptosis. The sh_XIAP cells showed low levels of cleaved PARP but increased levels of CC-3 directly after taxol application. The increased CC-3 levels could indicate that the XIAP silenced Eμ-myc cells go into apoptosis earlier since they lack the anti-apoptotic effect of XIAP. In contrast to what we anticipated, the sh_USP9X cells did not show higher levels of cleaved PARP or CC-3. Additionally, the expression of USP9X and XIAP increased in the USP9X-silenced cells over time, potentially indicating a loss of the USP9X knockdown.

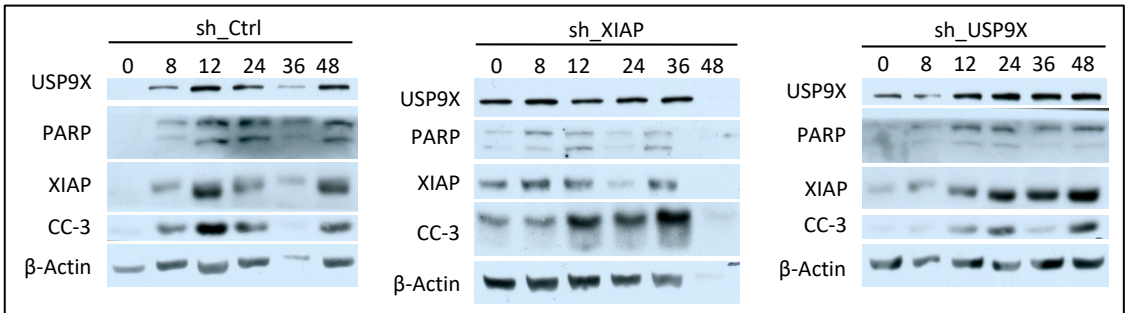

Figure 20. Immunoblot time course of Eμ-myc cells transfected with sh_Ctrl (scramble shRNA), sh_XIAP and sh_USP9X after treatment with taxol (in hrs).

Cell viability upon taxol treatment was not impacted by XIAP overexpression. Figure 21 shows no significant difference between MigR1_XIAP transfected cells and MigR1_Ctrl cells after taxol treatment (Figure 21.). Although three sets of independent experiments were performed, there were differences between the individual sets regarding the rate of GFP positivity. Therefore, the data is limited in terms of explanatory power.

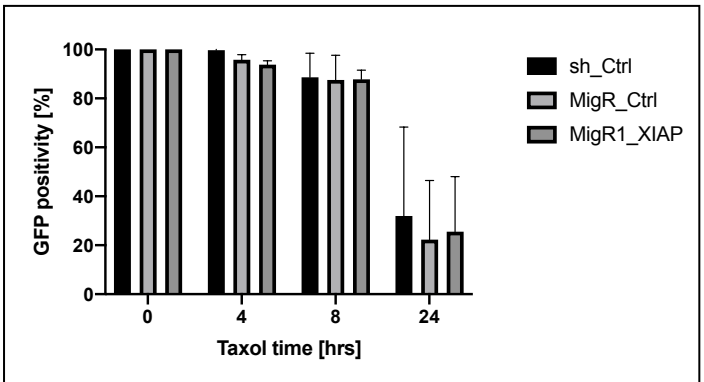

Figure 21. FACS analysis (propidium iodide, PI) of Eμ-myc cells transfected with sh_Ctrl (non-targeted shRNA), MigR1_Ctrl, or MigR1_XIAP and treated with taxol. The results come from three independent experiments (n= 3, ±SD, P= 0.7507). *P = <0.05; Student's t-test.

Since Schwickart et al. had stated that anti-apoptotic MCL1 is a substrate of USP9X (Schwickart et al., 2010) and MCL1 was shown to be degraded via APC/CCdc20 and

SCF (FBW7) at the start of mitosis (Harley, Allan, Sanderson, & Clarke, 2010; Inuzuka et al., 2011; Wertz et al., 2011), our group wanted to exclude that USP9X exerted its mitosis-specific effects only by stabilizing MCL1. The knockdown of Usp9X increased mitotic cell death independently from its MCL1 status (MCL1-/- vs. MCL1-WT, data not shown).

4.5. Lymphomagenesis is delayed in USP9X- and XIAP-silenced Eμ-Myc lymphoma cells *in vivo*

Eμ-myc lymphoma cells carry the c-myc gene that is under the control of the IgH enhancer, which leads to an increased expression of genes involved in cell proliferation. Transgenic Eμ-myc mice rapidly develop lymphomas with the lethality of 90% in the first five months of life. The tumors typically present as rapidly progressing lymphadenopathy (Adams et al., 1985; Dang, 2012; A. W. Harris et al., 1988). Therefore, the Eμ-myc model can be used to study lymphomagenesis in vivo.

We hypothesized that USP9X and the resulting XIAP overexpression would accelerate lymphomagenesis in the Eμ-Myc mouse model. On the other hand, USP9X and XIAP knockdown should slow down lymphoma development. We used lentivirus-infected Eμ-Myc lymphoma cells, which were injected into syngeneic C57BL mice. We anticipated that it would be difficult to differentiate an accelerated lymphomagenesis since Eμ-myc lymphomas develop quickly and a significant difference between an already highly proliferative state and an additional XIAP overexpression would be challenging to show. Additionally, Eμ-myc cells with an XIAP overexpression (MigR1-XIAP) did not show a significantly slower loss of GFP positivity (indicating apoptosis) upon taxol treatment in comparison to the control cells (MigR1_Ctrl) (chapter 4.4., Figure 21.). Therefore, we focused on XIAP- and USP9X-silenced Eμ-myc cells.

Figure 22 shows the immunoblots of the Eμ-myc cells that were used for the mouse experiments. The Eμ-myc cells were sorted for PI-negativity and GFP-positivity using flow cytometry. The sh_USP9X Eμ-myc cells show a clear USP9X knockdown, while the sh_XIAP Eμ-myc cells display an efficient XIAP knockdown.

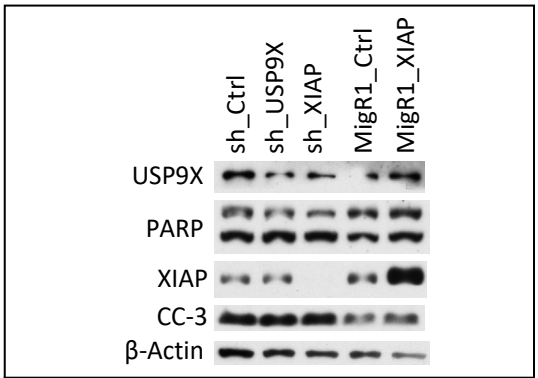

Figure 22. Immunoblot analysis of sorted Eμ-myc cells that were transduced with the indicated shRNA-constructs.

The expression of cleaved PARP and cleaved caspase 3 (CC-3), which reflects the rate of apoptosis, does not differ between the sh_Ctrl and sh_USP9X and sh_XIAP Eμ-myc cells. Accordingly, MigR1_XIAP Eμ-myc cells show an increased XIAP expression in comparison to the MigR1_Ctrl Eμ-myc cells. CC-3 and cleaved PARP expression did not differ between the groups. As mentioned above, we did not perform the following mouse experiments with the MigR1_XIAP Eμ-Myc cells.

Then, the transfected Eμ-myc cells (sh_USP9X, sh_XIAP, sh_Ctrl) were injected into syngeneic, female, and ten weeks old C57BL mice. Figure 23 shows the Kaplan-Meier survival curves of the sh_Ctrl mice in comparison to the sh_USP9X mice. Lymphoma onset was significantly delayed in mice receiving USP9X-silenced cells. Accordingly, XIAP-silencing also significantly prolongated the onset of lymphoma (Figure 24.).

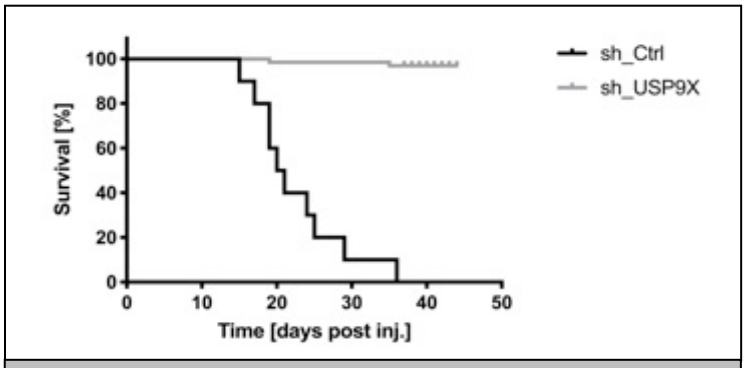

Figure 23. Kaplan–Meier survival curves of mice after injection with syngenic USP9X-silenced Eμ-Myc lymphoma cells (scramble shRNA, dark grey, n = 5; USP9X shRNA, light grey, n = 5). **P = <0.0001; Mantel-Cox test.

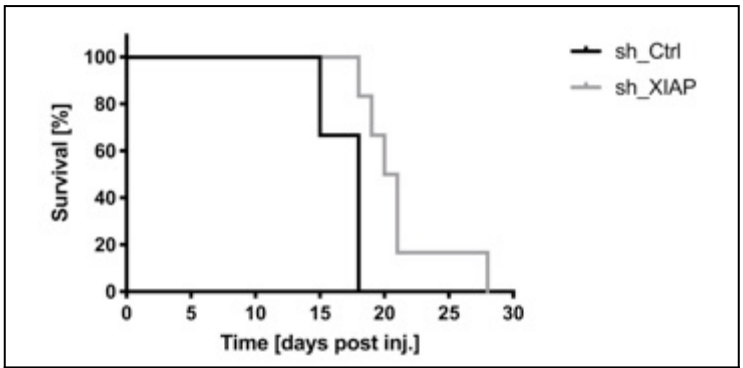

Figure 24. Kaplan–Meier survival curves of mice after injection with syngenic XIAP-silenced Eμ-Myc lymphoma cells (scramble shRNA, dark grey, n = 5; XIAP shRNA, light grey, n = 5). *P = 0.0048; Mantel–Cox test.

Our group could also confirm the B-cell origin of the lymphoma lesions that were biopsied after sacrificing the mice. The lesions also showed increased apoptosis at necropsy (Figure 25.).

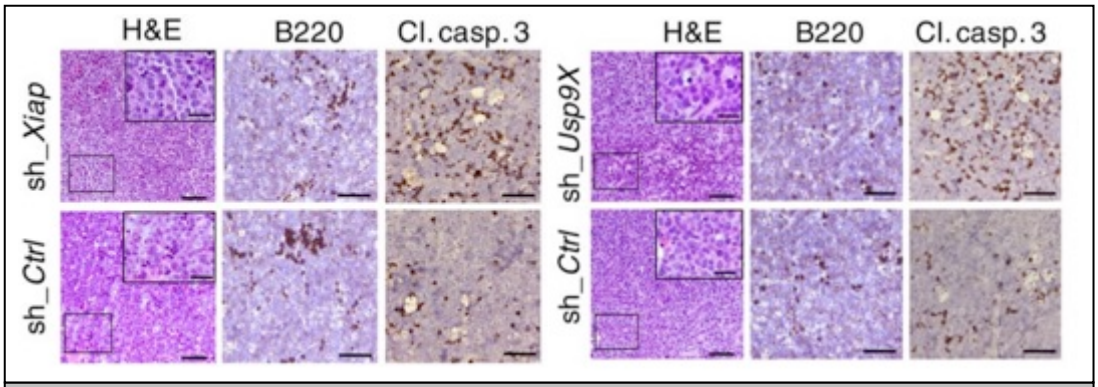

Figure 25. Histopathology of lymph nodes derived from mice injected with XIAP and USP9X-silenced Eμ-Myc cells. Histomorphology visualized by hematoxylin/eosin (H&E), B-cell origin (B220), and apoptosis (cleaved caspase-3). Scale bars denote 50 lm and 20 lm for insets. From Engel K et al. (2016).

5. Discussion

This study shows that DLBCL cells express different levels of XIAP and USP9X. DLBCL cells with low levels of both proteins display increased chemosensitivity to spindle poison-induced apoptosis. Furthermore, USP9X- and XIAP-silenced lymphoma cells show a delayed onset of disease in vivo.

Furthermore, our group also showed that USP9X deubiquitylates and stabilizes the anti-apoptotic XIAP. The up-regulation of USP9X and, consequently, of XIAP promotes mitotic survival and increased chemoresistance to mitotic spindle poisons in DLBCL. Patients with high USP9X/XIAP expression demonstrate significantly reduced event-free survival after chemotherapeutic treatment (Engel et al., 2016).

5.1. XIAP and USP9X levels correlate with chemoresistance in DLBCL cell lines

This study characterizes different DLBCL cell lines regarding their USP9X and XIAP levels. It shows that the cell lines differ in their expression and that high levels of USP9X and XIAP cause resistance to spindle poisons like taxol, which activates the DNA damage response and induces G2/M arrest in tumor cells.

Our findings fall in line with the results of other studies: Yamamoto et al. showed that XIAP overexpression inhibits chelerythrine-induced apoptosis in cardiac myocytes (Yamamoto, Seta, Morisco, Vatner, & Sadoshima, 2001). On the other hand, downregulation of XIAP induced caspase activation and sensitized leukemic cells for cell death (Carter et al., 2003). The presence of the XIAP-inhibitor Smac restored the ability of cytochrome C to activate caspase 3 and apoptosis in Hodgkin's lymphoma-derived B-cells (Kashkar et al., 2003). Additionally, the inactivation of the E3-ligase activity of XIAP inhibits tumorigenesis and prolongs survival in a mouse model of lymphoma (Schile, Garcia-Fernandez, & Steller, 2008).

USP9X has also previously been described as a pro-survival factor and a potential driver of chemoresistance. Harris et al. found that USP9X-deficient colorectal cancer cells have increased chemosensitivity to 5-fluorouracil (D. R. Harris, Mims, & Bunz, 2012). RNAi-mediated silencing of USP9X induced resistance to the selective estrogen receptor modulator tamoxifen in breast cancer cells (Oosterkamp et al., 2014).

Zhou et al. found that USP9X was overexpressed in B-ALL cell lines and patients and that USP9X knockdown significantly reduced leukemic cell growth and increased apoptosis (Zhou et al., 2015). Schwickart et al. stated that anti-apoptotic MCL1 is a substrate of USP9X and that USP9X overexpression is associated with a poorer prognosis in certain hematological malignancies, e.g., multiple myeloma (Schwickart et al., 2010).

The up-regulation of USP9X was also found to play an essential role in the formation and progression of precancerous lesions in esophageal squamous cell carcinoma

(ESCC). Increased USP9X expression levels were also correlated with poor survival of ESCC patients after radical surgery (J. Peng et al., 2013).

Liu et al. showed that the knockdown of USP9X enhanced the doxorubicin cytotoxicity in certain human liver cancer cells (H. Liu et al., 2015).

In contrast, a decrease of USP9X mRNA was associated with a poorer prognosis in pancreatic cancer, indicating an anti-apoptotic role. USP9X levels were also inversely associated with a metastatic burden in advanced disease. The loss of USP9X promoted the transformation of pancreatic cancer cells (W. Liu et al., 2018; Perez-Mancera et al., 2012). Li *et al.* XIAP levels were decreased USP9X−/− cells compared to HEK293T WT cells. USP9X−/− cells, their USP9X, and XIAP expression could be rescued. Interestingly, the XIAP mRNA levels in WT and USP9X−/− cells did not differ, indicating that USP9X is involved in the regulation of translation(Li et al., 2018).

USP9X was also found to regulate autophagy in a pro-survival pathway in pancreatic cells (Grasso et al., 2011).

Other DUBs have also been associated with tumorigenesis, e.g., USP1 and Fanconi anemia (Nijman, Huang, et al., 2005), USP2 and prostate cancer (Graner et al., 2004), and USP15 and glioblastoma (Eichhorn et al., 2012).

The proteasome inhibitor bortezomib (Velcade®) was approved by the U.S. Food and Drug Administration (FDA) for the treatment of refractory multiple myeloma. However, bortezomib inhibits the proteasome nonspecifically, so that the treatment is associated with increased toxicity and drug resistance (Chauhan et al., 2005; Kane, Farrell, Sridhara, & Pazdur, 2006). The development of DUB inhibitors could be a breakthrough for the treatment of cancer. Several DUB inhibitors have shown substantial antitumor activity in preclinical testing, but no clinical trials have been performed to date (Chauhan et al., 2012; D'Arcy & Linder, 2014; Gutierrez-Diaz, Gu, & Ntziachristos, 2020; Kategaya et al., 2017; Wang et al., 2016).

In summary, many data indicate that USP9X plays a pro-survival role and its overexpression is associated with a poorer prognosis in human cancer. Its role and mode of action are not fully understood yet and the apparent contradictions also need to be solved, e.g., acting pro- and anti-apoptotic and having oncogenic and tumor suppressor function.

5.2. Increased chemosensitivity in Eμ-myc cells with USP9X and XIAP knockdown

USP9X- and XIAP-silenced Eμ-myc cells show higher levels of PARP and CC-3 in the immunoblot and die more rapidly after taxol treatment in the flow cytometry. Consequently, the cells are more sensitive to spindle poisons. The increase of mitotic cell death was independent of the MCL1 status, which is demonstrably stabilized by USP9X and inhibits apoptosis (Schwickart et al., 2010). This means that USP9X overexpression could inhibit apoptosis by the deubiquitylation of XIAP alone.

Moreover, XIAP overexpression did not cause an increased GFP loss and, therefore, cell death, as seen in the following mouse experiments.

5.3. Lymphomagenesis is delayed in USP9X- and XIAP-silenced Eμ-Myc lymphoma cells *in vivo*

In this study, we could show that lymphomagenesis is significantly delayed in USP9X- and XIAP-silenced Eμ-Myc cells. The lymphomas were of a B cell origin and had shown signs of increased apoptosis. These findings indicate that USP9X and subsequently XIAP play an essential role in lymphomagenesis. Our group also analyzed the samples of patients with aggressive B-cell lymphoma and found overexpression of USP9X/XIAP in a significant number of patients (Engel et al., 2016). These data indicate that USP9X/XIAP might be a prognostic marker in DLBCL patients. USP9X/XIAP overexpression could define a clinical subgroup of patients with a more aggressive clinical course and a higher chance for the development of resistance to spindle poisons.

Additionally, USP9X and XIAP could be used as target structures for anti-cancer drugs for various types of cancers. Several broad-spectrum DUB inhibitors and specific DUB inhibitors have been described. However, more extensive research needs to be conducted to explore the specific mechanisms and targets of DUBs and to study and design small-molecule USP inhibitors (Yuan et al., 2018). For example, the small molecule inhibitor WP1130 is a potent DUB inhibitor and can target and several deubiquitinases (USP5, USP9X, USP14, and UCHL5), that all regulate the stability of the protein substrates and the function of the proteasome (D'Arcy, Wang, & Linder, 2015). Peterson et al. found that WP1130 induced apoptosis and blocked tumor growth in multiple myeloma via inhibition of USP9X and USP24 (Peterson et al., 2015). A study also screened for WP1130-like compounds against B-cell malignancy cell lines and found two compounds that inhibited USP9X activity in vitro and in cell culture. These compounds might be promising new therapeutic agents (Z. Peng et al., 2014).

Targeting XIAP might also be a promising therapeutic option. Small-molecule inhibitors have been designed to neutralize inhibitor of apoptosis (IAP) proteins. Mimetics of the endogenous mitochondrial protein Second mitochondria-derived activator of caspase (Smac) inhibit different IAPs and are under evaluation in clinical trials (Fulda, 2015; Fulda & Vucic, 2012). The combination of the SMAC mimetic BV6 and Bortezomib induced cell death in B-cell NHL cells (Bhatti, Abhari, & Fulda, 2017). Several groups also showed that Smac mimetics sensitize cancer cells to various cytotoxic therapies but might not be a potent anti-cancer drug alone (Belz et al., 2014; Fakler et al., 2009).

In summary, further investigations might elucidate new treatment options for these patients with DLBCL and USP9X/XIAP overexpression.

6. Summary

Diffuse large B-cell lymphoma (DLBCL) is the most common aggressive Non-Hodgkin lymphoma in adults. The R-CHOP regimen is the standard first-line therapy for all DLBCL patients. This regimen can be adapted to the patient's age and performance status. However, 30% to 40% of patients will relapse or be refractory after first-line therapy and have a poor prognosis. New, more specific therapies are needed for patients with relapsed or refractory DLBCL. Besides, new prognostic biomarkers at the time of initial diagnosis and in case of relapse or refractory disease could help to individualize and optimize therapy.

Several studies have shown that USP9X plays a pro-survival role in different human cancers and its overexpression is associated with a poorer prognosis (D. R. Harris et al., 2012; H. Liu et al., 2015; Oosterkamp et al., 2014; J. Peng et al., 2013; Zhou et al., 2015). However, its mode of action is not fully elucidated. This study demonstrates that USP9X stabilizes XIAP and leads to increased resistance toward mitotic spindle poisons. Additionally, aggressive B-cell lymphoma lines with USP9X and XIAP overexpression exhibit increased chemoresistance, which can be reversed by silencing USP9X or XIAP. The knockdown of USP9X or XIAP significantly delays lymphoma development in a Eμ-Myc lymphoma mouse model. USP9X and XIAP seem to have an impact on the cell fate decision in mitosis. The findings indicate that USP9X and XIAP might be potential prognostic biomarkers in patients with CD20+ aggressive B-cell lymphoma. In these patients, USP9X/XIAP overexpression could define a clinical subgroup of DLBCL patients with a more aggressive clinical course and a higher chance for the development of resistance to spindle poisons. USP9X and XIAP may be attractive new therapeutic targets in aggressive B-cell lymphoma. This work also indicates that the additional use of SMAC mimetics in the standard spindle poison-containing chemotherapy regimens may further improve the outcome of patients mentioned above.

7. Literature

Abramson, J., Palomba, M. L., Gordon, L., Lunning, M., Arnason, J., Wang, M., . . . Siddiqi, T. (2017). HIGH CR RATES IN RELAPSED/REFRACTORY (R/R) AGGRESSIVE B-NHL TREATED WITH THE CD19-DIRECTED CAR T CELL PRODUCT JCAR017 (TRANSCEND NHL 001). *Hematological Oncology, 35*(S2), 138-138. doi:10.1002/hon.2437_127

Abramson, J. S., Hellmann, M., Barnes, J. A., Hammerman, P., Toomey, C., Takvorian, T., . . . Hochberg, E. P. (2010). Intravenous methotrexate as central nervous system (CNS) prophylaxis is associated with a low risk of CNS recurrence in high-risk patients with diffuse large B-cell lymphoma. *Cancer, 116*(18), 4283-4290. doi:10.1002/cncr.25278

Adams, J. M., Harris, A. W., Pinkert, C. A., Corcoran, L. M., Alexander, W. S., Cory, S., . . . Brinster, R. L. (1985). The c-myc oncogene driven by immunoglobulin enhancers induces lymphoid malignancy in transgenic mice. *Nature, 318*(6046), 533-538.

Advani, R. H., Buggy, J. J., Sharman, J. P., Smith, S. M., Boyd, T. E., Grant, B., . . . Fowler, N. H. (2013). Bruton tyrosine kinase inhibitor ibrutinib (PCI-32765) has significant activity in patients with relapsed/refractory B-cell malignancies. *J Clin Oncol, 31*(1), 88-94. doi:10.1200/JCO.2012.42.7906

Akyurek, N., Ren, Y., Rassidakis, G. Z., Schlette, E. J., & Medeiros, L. J. (2006). Expression of inhibitor of apoptosis proteins in B-cell non-Hodgkin and Hodgkin lymphomas. *Cancer, 107*(8), 1844-1851. doi:10.1002/cncr.22219

Alizadeh, A. A., Eisen, M. B., Davis, R. E., Ma, C., Lossos, I. S., Rosenwald, A., . . . Staudt, L. M. (2000). Distinct types of diffuse large B-cell lymphoma identified by gene expression profiling. *Nature, 403*(6769), 503-511. doi:10.1038/35000501

Amerik, A. Y., & Hochstrasser, M. (2004). Mechanism and function of deubiquitinating enzymes. *Biochim Biophys Acta, 1695*(1-3), 189-207. doi:10.1016/j.bbamcr.2004.10.003

Armitage, J. O. (2005). Staging Non-Hodgkin Lymphoma. *CA: A Cancer Journal for Clinicians, 55*(6), 368-376. doi:10.3322/canjclin.55.6.368

Azakir, B. A., & Angers, A. (2009). Reciprocal regulation of the ubiquitin ligase Itch and the epidermal growth factor receptor signaling. *Cell Signal, 21*(8), 1326-1336. doi:10.1016/j.cellsig.2009.03.020

Barnes, J. A., Jacobsen, E., Feng, Y., Freedman, A., Hochberg, E. P., LaCasce, A. S., . . . Abramson, J. S. (2013). Everolimus in combination with rituximab induces complete responses in heavily pretreated diffuse large B-cell lymphoma. *Haematologica, 98*(4), 615-619. doi:10.3324/haematol.2012.075184

Barrans, S., Crouch, S., Smith, A., Turner, K., Owen, R., Patmore, R., . . . Jack, A. (2010). Rearrangement of MYC is associated with poor prognosis in patients with diffuse large B-cell lymphoma treated in the era of rituximab. *J Clin Oncol, 28*(20), 3360-3365. doi:10.1200/JCO.2009.26.3947

Barrington, S. F., Mikhaeel, N. G., Kostakoglu, L., Meignan, M., Hutchings, M., Mueller, S. P., . . . Cheson, B. D. (2014). Role of imaging in the staging and response assessment of lymphoma: consensus of the International Conference on Malignant Lymphomas Imaging Working Group. *J Clin Oncol, 32*(27), 3048-3058. doi:10.1200/JCO.2013.53.5229

Bassermann, F., Eichner, R., & Pagano, M. (2014). The ubiquitin proteasome system - implications for cell cycle control and the targeted treatment of cancer. *Biochim Biophys Acta, 1843*(1), 150-162. doi:10.1016/j.bbamcr.2013.02.028

Bassermann, F., Frescas, D., Guardavaccaro, D., Busino, L., Peschiaroli, A., & Pagano, M. (2008). The Cdc14B-Cdh1-Plk1 axis controls the G2 DNA-damage-response checkpoint. *Cell, 134*(2), 256-267. doi:10.1016/j.cell.2008.05.043

Belz, K., Schoeneberger, H., Wehner, S., Weigert, A., Bonig, H., Klingebiel, T., . . . Fulda, S. (2014). Smac mimetic and glucocorticoids synergize to induce apoptosis in childhood ALL by promoting ripoptosome assembly. *Blood, 124*(2), 240-250. doi:10.1182/blood-2013-05-500918

Bhatti, I. A., Abhari, B. A., & Fulda, S. (2017). Identification of a synergistic combination of Smac mimetic and Bortezomib to trigger cell death in B-cell non-Hodgkin lymphoma cells. *Cancer Lett, 405*, 63-72. doi:10.1016/j.canlet.2017.07.008

Blinder, V., Fisher, S. G., & Lymphoma Research Foundation, N. Y. (2008). The role of environmental factors in the etiology of lymphoma. *Cancer Invest, 26*(3), 306-316. doi:10.1080/07357900701805686

Bosly, A., Coiffier, B., Gisselbrecht, C., Tilly, H., Auzanneau, G., Andrien, F., . . . et al. (1992). Bone marrow transplantation prolongs survival after relapse in aggressive-lymphoma patients treated with the LNH-84 regimen. *J Clin Oncol, 10*(10), 1615-1623. doi:10.1200/JCO.1992.10.10.1615

Brito, D. A., & Rieder, C. L. (2006). Mitotic checkpoint slippage in humans occurs via cyclin B destruction in the presence of an active checkpoint. *Curr Biol, 16*(12), 1194-1200. doi:10.1016/j.cub.2006.04.043

Bu, R., Hussain, A. R., Al-Obaisi, K. A., Ahmed, M., Uddin, S., & Al-Kuraya, K. S. (2014). Bortezomib inhibits proteasomal degradation of IkappaBalpha and induces mitochondrial dependent apoptosis in activated B-cell diffuse large B-cell lymphoma. *Leuk Lymphoma, 55*(2), 415-424. doi:10.3109/10428194.2013.806799

Buchschacher, G. L., Jr., & Wong-Staal, F. (2000). Development of lentiviral vectors for gene therapy for human diseases. *Blood, 95*(8), 2499-2504.

Campo, E., Swerdlow, S. H., Harris, N. L., Pileri, S., Stein, H., & Jaffe, E. S. (2011). The 2008 WHO classification of lymphoid neoplasms and beyond: evolving concepts and practical applications. *Blood, 117*(19), 5019-5032. doi:10.1182/blood-2011-01-293050

Carter, B. Z., Milella, M., Tsao, T., McQueen, T., Schober, W. D., Hu, W., . . . Andreeff, M. (2003). Regulation and targeting of antiapoptotic XIAP in acute myeloid leukemia. *Leukemia, 17*(11), 2081-2089. doi:10.1038/sj.leu.2403113

Chai, J., Shiozaki, E., Srinivasula, S. M., Wu, Q., Datta, P., Alnemri, E. S., & Shi, Y. (2001). Structural basis of caspase-7 inhibition by XIAP. *Cell, 104*(5), 769-780.

Chan, K. S., Koh, C. G., & Li, H. Y. (2012). Mitosis-targeted anti-cancer therapies: where they stand. *Cell death & disease, 3*(10), e411-e411. doi:10.1038/cddis.2012.148

Chauhan, D., Catley, L., Li, G., Podar, K., Hideshima, T., Velankar, M., . . . Anderson, K. C. (2005). A novel orally active proteasome inhibitor induces apoptosis in multiple myeloma cells with mechanisms distinct from Bortezomib. *Cancer Cell, 8*(5), 407-419. doi:10.1016/j.ccr.2005.10.013

Chauhan, D., Tian, Z., Nicholson, B., Kumar, K. G., Zhou, B., Carrasco, R., . . . Anderson, K. C. (2012). A small molecule inhibitor of ubiquitin-specific protease-7 induces apoptosis in multiple myeloma cells and overcomes bortezomib resistance. *Cancer Cell, 22*(3), 345-358. doi:10.1016/j.ccr.2012.08.007

Chavez, J. C., & Locke, F. L. (2018). CAR T cell therapy for B-cell lymphomas. *Best Pract Res Clin Haematol, 31*(2), 135-146. doi:10.1016/j.beha.2018.04.001

Cheah, C. Y., Herbert, K. E., O'Rourke, K., Kennedy, G. A., George, A., Fedele, P. L., . . . Seymour, J. F. (2014). A multicentre retrospective comparison of central nervous system prophylaxis strategies among patients with high-risk diffuse large B-cell lymphoma. *Br J Cancer, 111*(6), 1072-1079. doi:10.1038/bjc.2014.405

Chen, Z. J., & Sun, L. J. (2009). Nonproteolytic functions of ubiquitin in cell signaling. *Mol Cell, 33*(3), 275-286. doi:10.1016/j.molcel.2009.01.014

Cheson, B. D., Fisher, R. I., Barrington, S. F., Cavalli, F., Schwartz, L. H., Zucca, E., . . . United Kingdom National Cancer Research, I. (2014). Recommendations for initial evaluation, staging, and response assessment of Hodgkin and non-Hodgkin lymphoma: the Lugano classification. *J Clin Oncol, 32*(27), 3059-3068. doi:10.1200/JCO.2013.54.8800

Cheson, B. D., Pfistner, B., Juweid, M. E., Gascoyne, R. D., Specht, L., Horning, S. J., . . . International Harmonization Project on, L. (2007). Revised response criteria for malignant lymphoma. *J Clin Oncol, 25*(5), 579-586. doi:10.1200/JCO.2006.09.2403

Chiappella, A., Martelli, M., Angelucci, E., Brusamolino, E., Evangelista, A., Carella, A. M., . . . Vitolo, U. (2017). Rituximab-dose-dense chemotherapy with or without high-dose chemotherapy plus autologous stem-cell transplantation in high-risk diffuse large B-cell lymphoma (DLCL04): final results of a multicentre, open-label, randomised, controlled, phase 3 study. *Lancet Oncol, 18*(8), 1076-1088. doi:10.1016/s1470-2045(17)30444-8

Chiappella, A., Tucci, A., Castellino, A., Pavone, V., Baldi, I., Carella, A. M., . . . Fondazione Italiana, L. (2013). Lenalidomide plus cyclophosphamide, doxorubicin, vincristine, prednisone and rituximab is safe and effective in untreated, elderly patients with diffuse large B-cell lymphoma: a phase I study by the Fondazione Italiana Linfomi. *Haematologica, 98*(11), 1732-1738. doi:10.3324/haematol.2013.085134

Choi, W. W., Weisenburger, D. D., Greiner, T. C., Piris, M. A., Banham, A. H., Delabie, J., . . . Chan, W. C. (2009). A new immunostain algorithm classifies diffuse large B-cell lymphoma

into molecular subtypes with high accuracy. *Clin Cancer Res, 15*(17), 5494-5502. doi:10.1158/1078-0432.CCR-09-0113
Ciechanover, A. (2013). Intracellular protein degradation: from a vague idea through the lysosome and the ubiquitin-proteasome system and onto human diseases and drug targeting. *Bioorg Med Chem, 21*(12), 3400-3410. doi:10.1016/j.bmc.2013.01.056
Ciechanover, A., Elias, S., Heller, H., & Hershko, A. (1982). "Covalent affinity" purification of ubiquitin-activating enzyme. *J Biol Chem, 257*(5), 2537-2542.
Coiffier, B., Lepage, E., Briere, J., Herbrecht, R., Tilly, H., Bouabdallah, R., . . . Gisselbrecht, C. (2002). CHOP chemotherapy plus rituximab compared with CHOP alone in elderly patients with diffuse large-B-cell lymphoma. *N Engl J Med, 346*(4), 235-242. doi:10.1056/NEJMoa011795
Colomo, L., Lopez-Guillermo, A., Perales, M., Rives, S., Martinez, A., Bosch, F., . . . Campo, E. (2003). Clinical impact of the differentiation profile assessed by immunophenotyping in patients with diffuse large B-cell lymphoma. *Blood, 101*(1), 78-84. doi:10.1182/blood-2002-04-1286
Couto, L. B., & High, K. A. (2010). Viral vector-mediated RNA interference. *Curr Opin Pharmacol, 10*(5), 534-542. doi:10.1016/j.coph.2010.06.007
Cunningham, D., Hawkes, E. A., Jack, A., Qian, W., Smith, P., Mouncey, P., . . . Linch, D. (2013). Rituximab plus cyclophosphamide, doxorubicin, vincristine, and prednisolone in patients with newly diagnosed diffuse large B-cell non-Hodgkin lymphoma: a phase 3 comparison of dose intensification with 14-day versus 21-day cycles. *Lancet, 381*(9880), 1817-1826. doi:10.1016/S0140-6736(13)60313-X
D'Arcy, P., & Linder, S. (2014). Molecular pathways: translational potential of deubiquitinases as drug targets. *Clin Cancer Res, 20*(15), 3908-3914. doi:10.1158/1078-0432.ccr-14-0568
D'Arcy, P., Wang, X., & Linder, S. (2015). Deubiquitinase inhibition as a cancer therapeutic strategy. *Pharmacol Ther, 147*, 32-54. doi:10.1016/j.pharmthera.2014.11.002
Dalby, B., Cates, S., Harris, A., Ohki, E. C., Tilkins, M. L., Price, P. J., & Ciccarone, V. C. (2004). Advanced transfection with Lipofectamine 2000 reagent: primary neurons, siRNA, and high-throughput applications. *Methods, 33*(2), 95-103. doi:10.1016/j.ymeth.2003.11.023
Dang, C. V. (2012). MYC on the path to cancer. *Cell, 149*(1), 22-35. doi:10.1016/j.cell.2012.03.003
Davies, A., Cummin, T. E., Barrans, S., Maishman, T., Mamot, C., Novak, U., . . . Johnson, P. W. M. (2019). Gene-expression profiling of bortezomib added to standard chemoimmunotherapy for diffuse large B-cell lymphoma (REMoDL-B): an open-label, randomised, phase 3 trial. *Lancet Oncol, 20*(5), 649-662. doi:10.1016/s1470-2045(18)30935-5
Davis, H. E., Morgan, J. R., & Yarmush, M. L. (2002). Polybrene increases retrovirus gene transfer efficiency by enhancing receptor-independent virus adsorption on target cell membranes. *Biophys Chem, 97*(2-3), 159-172.
Davis, R. E., Brown, K. D., Siebenlist, U., & Staudt, L. M. (2001). Constitutive nuclear factor kappaB activity is required for survival of activated B cell-like diffuse large B cell lymphoma cells. *J Exp Med, 194*(12), 1861-1874.
de Jong, D., Rosenwald, A., Chhanabhai, M., Gaulard, P., Klapper, W., Lee, A., . . . Lunenburg Lymphoma Biomarker, C. (2007). Immunohistochemical prognostic markers in diffuse large B-cell lymphoma: validation of tissue microarray as a prerequisite for broad clinical applications--a study from the Lunenburg Lymphoma Biomarker Consortium. *J Clin Oncol, 25*(7), 805-812. doi:10.1200/JCO.2006.09.4490
Delarue, R., Tilly, H., Mounier, N., Petrella, T., Salles, G., Thieblemont, C., . . . Bosly, A. (2013). Dose-dense rituximab-CHOP compared with standard rituximab-CHOP in elderly patients with diffuse large B-cell lymphoma (the LNH03-6B study): a randomised phase 3 trial. *Lancet Oncol, 14*(6), 525-533. doi:10.1016/S1470-2045(13)70122-0
Deveraux, Q. L., Leo, E., Stennicke, H. R., Welsh, K., Salvesen, G. S., & Reed, J. C. (1999). Cleavage of human inhibitor of apoptosis protein XIAP results in fragments with distinct specificities for caspases. *EMBO J, 18*(19), 5242-5251. doi:10.1093/emboj/18.19.5242
Deveraux, Q. L., Takahashi, R., Salvesen, G. S., & Reed, J. C. (1997). X-linked IAP is a direct inhibitor of cell-death proteases. *Nature, 388*(6639), 300-304. doi:10.1038/40901
Dupont, S., Mamidi, A., Cordenonsi, M., Montagner, M., Zacchigna, L., Adorno, M., . . . Piccolo, S. (2009). FAM/USP9x, a deubiquitinating enzyme essential for TGFbeta signaling, controls Smad4 monoubiquitination. *Cell, 136*(1), 123-135. doi:10.1016/j.cell.2008.10.051

Eichhorn, P. J., Rodon, L., Gonzalez-Junca, A., Dirac, A., Gili, M., Martinez-Saez, E., . . . Seoane, J. (2012). USP15 stabilizes TGF-beta receptor I and promotes oncogenesis through the activation of TGF-beta signaling in glioblastoma. *Nat Med, 18*(3), 429-435. doi:10.1038/nm.2619

Elstrom, R. L., Andemariam, B., Martin, P., Ruan, J., Shore, T. B., Coleman, M., . . . Furman, R. R. (2012). Bortezomib in combination with rituximab, dexamethasone, ifosfamide, cisplatin and etoposide chemoimmunotherapy in patients with relapsed and primary refractory diffuse large B-cell lymphoma. *Leuk Lymphoma, 53*(8), 1469-1473. doi:10.3109/10428194.2012.656629

Engel, K., Rudelius, M., Slawska, J., Jacobs, L., Ahangarian Abhari, B., Altmann, B., . . . Bassermann, F. (2016). USP9X stabilizes XIAP to regulate mitotic cell death and chemoresistance in aggressive B-cell lymphoma. *EMBO Mol Med, 8*(8), 851-862. doi:10.15252/emmm.201506047

Evens, A. M., Rosen, S. T., Helenowski, I., Kline, J., Larsen, A., Colvin, J., . . . Smith, S. M. (2013). A phase I/II trial of bortezomib combined concurrently with gemcitabine for relapsed or refractory DLBCL and peripheral T-cell lymphomas. *Br J Haematol, 163*(1), 55-61. doi:10.1111/bjh.12488

Fakler, M., Loeder, S., Vogler, M., Schneider, K., Jeremias, I., Debatin, K. M., & Fulda, S. (2009). Small molecule XIAP inhibitors cooperate with TRAIL to induce apoptosis in childhood acute leukemia cells and overcome Bcl-2-mediated resistance. *Blood, 113*(8), 1710-1722. doi:10.1182/blood-2007-09-114314

Fernandez-Saiz, V., Targosz, B. S., Lemeer, S., Eichner, R., Langer, C., Bullinger, L., . . . Bassermann, F. (2013). SCFFbxo9 and CK2 direct the cellular response to growth factor withdrawal via Tel2/Tti1 degradation and promote survival in multiple myeloma. *Nat Cell Biol, 15*(1), 72-81. doi:10.1038/ncb2651

Feugier, P., Van Hoof, A., Sebban, C., Solal-Celigny, P., Bouabdallah, R., Ferme, C., . . . Coiffier, B. (2005). Long-term results of the R-CHOP study in the treatment of elderly patients with diffuse large B-cell lymphoma: a study by the Groupe d'Etude des Lymphomes de l'Adulte. *J Clin Oncol, 23*(18), 4117-4126. doi:10.1200/JCO.2005.09.131

Feugier, P., Virion, J. M., Tilly, H., Haioun, C., Marit, G., Macro, M., . . . Coiffier, B. (2004). Incidence and risk factors for central nervous system occurrence in elderly patients with diffuse large-B-cell lymphoma: influence of rituximab. *Ann Oncol, 15*(1), 129-133.

Fisher, R. I., Gaynor, E. R., Dahlberg, S., Oken, M. M., Grogan, T. M., Mize, E. M., . . . Miller, T. P. (1993). Comparison of a standard regimen (CHOP) with three intensive chemotherapy regimens for advanced non-Hodgkin's lymphoma. *N Engl J Med, 328*(14), 1002-1006. doi:10.1056/NEJM199304083281404

Friedberg, J. W. (2010). PET positive, PET negative, or PET peeve? *Blood, 115*(4), 752-753. doi:10.1182/blood-2009-09-244947

Friedberg, J. W. (2011). Relapsed/refractory diffuse large B-cell lymphoma. *Hematology Am Soc Hematol Educ Program, 2011*, 498-505. doi:10.1182/asheducation-2011.1.498

Friedberg, J. W. (2015). Using the pathology report in initial treatment decisions for diffuse large B-cell lymphoma: time for a precision medicine approach. *Hematology Am Soc Hematol Educ Program, 2015*, 618-624. doi:10.1182/asheducation-2015.1.618

Friedberg, J. W. (2017). How I treat double-hit lymphoma. *Blood, 130*(5), 590-596. doi:10.1182/blood-2017-04-737320

Fu, K., Weisenburger, D. D., Choi, W. W., Perry, K. D., Smith, L. M., Shi, X., . . . Vose, J. M. (2008). Addition of rituximab to standard chemotherapy improves the survival of both the germinal center B-cell-like and non-germinal center B-cell-like subtypes of diffuse large B-cell lymphoma. *J Clin Oncol, 26*(28), 4587-4594. doi:10.1200/JCO.2007.15.9277

Fulda, S. (2015). Promises and Challenges of Smac Mimetics as Cancer Therapeutics. *Clin Cancer Res, 21*(22), 5030-5036. doi:10.1158/1078-0432.ccr-15-0365

Fulda, S., & Vucic, D. (2012). Targeting IAP proteins for therapeutic intervention in cancer. *Nat Rev Drug Discov, 11*(2), 109-124. doi:10.1038/nrd3627

Gascoyne, R. D., Adomat, S. A., Krajewski, S., Krajewska, M., Horsman, D. E., Tolcher, A. W., . . . Connors, J. M. (1997). Prognostic significance of Bcl-2 protein expression and Bcl-2 gene rearrangement in diffuse aggressive non-Hodgkin's lymphoma. *Blood, 90*(1), 244-251.

Ghielmini, M., Vitolo, U., Kimby, E., Montoto, S., Walewski, J., Pfreundschuh, M., . . . Panel Members of the 1st, E. C. C. o. M. L. (2013). ESMO Guidelines consensus conference on malignant lymphoma 2011 part 1: diffuse large B-cell lymphoma (DLBCL), follicular

lymphoma (FL) and chronic lymphocytic leukemia (CLL). *Ann Oncol, 24*(3), 561-576. doi:10.1093/annonc/mds517
Gisselbrecht, C., Glass, B., Mounier, N., Singh Gill, D., Linch, D. C., Trneny, M., . . . Schmitz, N. (2010). Salvage regimens with autologous transplantation for relapsed large B-cell lymphoma in the rituximab era. *J Clin Oncol, 28*(27), 4184-4190. doi:10.1200/jco.2010.28.1618
Glickman, M. H., & Ciechanover, A. (2002). The ubiquitin-proteasome proteolytic pathway: destruction for the sake of construction. *Physiol Rev, 82*(2), 373-428. doi:10.1152/physrev.00027.2001
Glotzer, M., Murray, A. W., & Kirschner, M. W. (1991). Cyclin is degraded by the ubiquitin pathway. *Nature, 349*(6305), 132-138. doi:10.1038/349132a0
Goldman, A., Ursitti, J. A., Mozdzanowski, J., & Speicher, D. W. (2015). Electroblotting from Polyacrylamide Gels. *Current Protocols in Protein Science, 82*(1), 10.17.11-10.17.16. doi:10.1002/0471140864.ps1007s82
Gouill, S. L., Milpied, N. J., Lamy, T., Delwail, V., Gressin, R., Guyotat, D., . . . Sauvezie, M. (2011). First-line rituximab (R) high-dose therapy (R-HDT) versus R-CHOP14 for young adults with diffuse large B-cell lymphoma: Preliminary results of the GOELAMS 075 prospective multicenter randomized trial. *Journal of Clinical Oncology, 29*(15_suppl), 8003-8003. doi:10.1200/jco.2011.29.15_suppl.8003
Graner, E., Tang, D., Rossi, S., Baron, A., Migita, T., Weinstein, L. J., . . . Loda, M. (2004). The isopeptidase USP2a regulates the stability of fatty acid synthase in prostate cancer. *Cancer Cell, 5*(3), 253-261.
Grasso, D., Ropolo, A., Lo Re, A., Boggio, V., Molejon, M. I., Iovanna, J. L., . . . Vaccaro, M. I. (2011). Zymophagy, a novel selective autophagy pathway mediated by VMP1-USP9x-p62, prevents pancreatic cell death. *J Biol Chem, 286*(10), 8308-8324. doi:10.1074/jbc.M110.197301
Gutierrez-Diaz, B. T., Gu, W., & Ntziachristos, P. (2020). Deubiquitinases: Pro-oncogenic Activity and Therapeutic Targeting in Blood Malignancies. *Trends Immunol, 41*(4), 327-340. doi:10.1016/j.it.2020.02.004
Gyrd-Hansen, M., & Meier, P. (2010). IAPs: from caspase inhibitors to modulators of NF-kappaB, inflammation and cancer. *Nat Rev Cancer, 10*(8), 561-574. doi:10.1038/nrc2889
Hannon, G. J. (2002). RNA interference. *Nature, 418*(6894), 244-251. doi:10.1038/418244a
Hans, C. P., Weisenburger, D. D., Greiner, T. C., Gascoyne, R. D., Delabie, J., Ott, G., . . . Chan, W. C. (2004). Confirmation of the molecular classification of diffuse large B-cell lymphoma by immunohistochemistry using a tissue microarray. *Blood, 103*(1), 275-282. doi:10.1182/blood-2003-05-1545
Harada, S., Suzuki, R., Uehira, K., Yatabe, Y., Kagami, Y., Ogura, M., . . . Seto, M. (1999). Molecular and immunological dissection of diffuse large B cell lymphoma: CD5+, and CD5- with CD10+ groups may constitute clinically relevant subtypes. *Leukemia, 13*(9), 1441-1447.
Harley, M. E., Allan, L. A., Sanderson, H. S., & Clarke, P. R. (2010). Phosphorylation of Mcl-1 by CDK1-cyclin B1 initiates its Cdc20-dependent destruction during mitotic arrest. *EMBO J, 29*(14), 2407-2420. doi:10.1038/emboj.2010.112
Harris, A. W., Pinkert, C. A., Crawford, M., Langdon, W. Y., Brinster, R. L., & Adams, J. M. (1988). The E mu-myc transgenic mouse. A model for high-incidence spontaneous lymphoma and leukemia of early B cells. *J Exp Med, 167*(2), 353-371.
Harris, D. R., Mims, A., & Bunz, F. (2012). Genetic disruption of USP9X sensitizes colorectal cancer cells to 5-fluorouracil. *Cancer Biol Ther, 13*(13), 1319-1324. doi:10.4161/cbt.21792
Hermine, O., Haioun, C., Lepage, E., d'Agay, M. F., Briere, J., Lavignac, C., . . . Gaulard, P. (1996). Prognostic significance of bcl-2 protein expression in aggressive non-Hodgkin's lymphoma. Groupe d'Etude des Lymphomes de l'Adulte (GELA). *Blood, 87*(1), 265-272.
Hernandez-Ilizaliturri, F. J., Deeb, G., Zinzani, P. L., Pileri, S. A., Malik, F., Macon, W. R., . . . Czuczman, M. S. (2011). Higher response to lenalidomide in relapsed/refractory diffuse large B-cell lymphoma in nongerminal center B-cell-like than in germinal center B-cell-like phenotype. *Cancer, 117*(22), 5058-5066. doi:10.1002/cncr.26135
Hershko, A., & Ciechanover, A. (1998). The ubiquitin system. *Annu Rev Biochem, 67*, 425-479. doi:10.1146/annurev.biochem.67.1.425
Hershko, A., Heller, H., Elias, S., & Ciechanover, A. (1983). Components of ubiquitin-protein ligase system. Resolution, affinity purification, and role in protein breakdown. *J Biol Chem, 258*(13), 8206-8214.

Herzenberg, L. A., Sweet, R. G., & Herzenberg, L. A. (1976). Fluorescence-activated cell sorting. *Sci Am, 234*(3), 108-117.
Higuchi, R., Fockler, C., Dollinger, G., & Watson, R. (1993). Kinetic PCR analysis: real-time monitoring of DNA amplification reactions. *Biotechnology (N Y), 11*(9), 1026-1030.
Hill, M. E., MacLennan, K. A., Cunningham, D. C., Vaughan Hudson, B., Burke, M., Clarke, P., . . . Linch, D. C. (1996). Prognostic significance of BCL-2 expression and bcl-2 major breakpoint region rearrangement in diffuse large cell non-Hodgkin's lymphoma: a British National Lymphoma Investigation Study. *Blood, 88*(3), 1046-1051.
Hill, Q. A., & Owen, R. G. (2006). CNS prophylaxis in lymphoma: who to target and what therapy to use. *Blood Rev, 20*(6), 319-332. doi:10.1016/j.blre.2006.02.001
Hofmann, H. S., Simm, A., Hammer, A., Silber, R. E., & Bartling, B. (2002). Expression of inhibitors of apoptosis (IAP) proteins in non-small cell human lung cancer. *J Cancer Res Clin Oncol, 128*(10), 554-560. doi:10.1007/s00432-002-0364-z
Horn, H., Ziepert, M., Becher, C., Barth, T. F., Bernd, H. W., Feller, A. C., . . . German High-Grade Non-Hodgkin Lymphoma Study, G. (2013). MYC status in concert with BCL2 and BCL6 expression predicts outcome in diffuse large B-cell lymphoma. *Blood, 121*(12), 2253-2263. doi:10.1182/blood-2012-06-435842
Horwitz, S. M., Negrin, R. S., Blume, K. G., Breslin, S., Stuart, M. J., Stockerl-Goldstein, K. E., . . . Horning, S. J. (2004). Rituximab as adjuvant to high-dose therapy and autologous hematopoietic cell transplantation for aggressive non-Hodgkin lymphoma. *Blood, 103*(3), 777-783. doi:10.1182/blood-2003-04-1257
Howlader N, N. A., Krapcho M, Miller D, Bishop K, Altekruse SF, Kosary CL, Yu M, Ruhl J, Tatalovich Z, Mariotto A, Lewis DR, Chen HS, Feuer EJ, Cronin KA. (1975-2013). SEER Cancer Statistics Factsheets: Non-Hodgkin Lymphoma. .
Hunt, K. E., & Reichard, K. K. (2008). Diffuse large B-cell lymphoma. *Arch Pathol Lab Med, 132*(1), 118-124. doi:10.1043/1543-2165(2008)132[118:DLBL]2.0.CO;2
Inuzuka, H., Shaik, S., Onoyama, I., Gao, D., Tseng, A., Maser, R. S., . . . Wei, W. (2011). SCF(FBW7) regulates cellular apoptosis by targeting MCL1 for ubiquitylation and destruction. *Nature, 471*(7336), 104-109. doi:10.1038/nature09732
Jacobson, A. D., Zhang, N. Y., Xu, P., Han, K. J., Noone, S., Peng, J., & Liu, C. W. (2009). The lysine 48 and lysine 63 ubiquitin conjugates are processed differently by the 26 s proteasome. *J Biol Chem, 284*(51), 35485-35494. doi:10.1074/jbc.M109.052928
Jain, P., Fayad, L. E., Rosenwald, A., Young, K. H., & O'Brien, S. (2013). Recent advances in de novo CD5+ diffuse large B cell lymphoma. *Am J Hematol, 88*(9), 798-802. doi:10.1002/ajh.23467
Johnson, N. A., Savage, K. J., Ludkovski, O., Ben-Neriah, S., Woods, R., Steidl, C., . . . Horsman, D. E. (2009). Lymphomas with concurrent BCL2 and MYC translocations: the critical factors associated with survival. *Blood, 114*(11), 2273-2279. doi:10.1182/blood-2009-03-212191
Johnston, P. B., LaPlant, B., McPhail, E., Habermann, T. M., Inwards, D. J., Micallef, I. N., . . . Witzig, T. E. (2016). Everolimus combined with R-CHOP-21 for new, untreated, diffuse large B-cell lymphoma (NCCTG 1085 [Alliance]): safety and efficacy results of a phase 1 and feasibility trial. *Lancet Haematol, 3*(7), e309-316. doi:10.1016/S2352-3026(16)30040-0
Jonathan, E. C., Bernhard, E. J., & McKenna, W. G. (1999). How does radiation kill cells? *Curr Opin Chem Biol, 3*(1), 77-83. doi:10.1016/s1367-5931(99)80014-3
Juweid, M. E., Stroobants, S., Hoekstra, O. S., Mottaghy, F. M., Dietlein, M., Guermazi, A., . . . Imaging Subcommittee of International Harmonization Project in, L. (2007). Use of positron emission tomography for response assessment of lymphoma: consensus of the Imaging Subcommittee of International Harmonization Project in Lymphoma. *J Clin Oncol, 25*(5), 571-578. doi:10.1200/JCO.2006.08.2305
Kane, R. C., Farrell, A. T., Sridhara, R., & Pazdur, R. (2006). United States Food and Drug Administration approval summary: bortezomib for the treatment of progressive multiple myeloma after one prior therapy. *Clin Cancer Res, 12*(10), 2955-2960. doi:10.1158/1078-0432.CCR-06-0170
Kashkar, H., Haefs, C., Shin, H., Hamilton-Dutoit, S. J., Salvesen, G. S., Kronke, M., & Jurgensmeier, J. M. (2003). XIAP-mediated caspase inhibition in Hodgkin's lymphoma-derived B cells. *J Exp Med, 198*(2), 341-347. doi:10.1084/jem.20021279
Kategaya, L., Di Lello, P., Rouge, L., Pastor, R., Clark, K. R., Drummond, J., . . . Wertz, I. E. (2017). USP7 small-molecule inhibitors interfere with ubiquitin binding. *Nature, 550*(7677), 534-538. doi:10.1038/nature24006

Kewalramani, T., Zelenetz, A. D., Nimer, S. D., Portlock, C., Straus, D., Noy, A., . . . Moskowitz, C. H. (2004). Rituximab and ICE as second-line therapy before autologous stem cell transplantation for relapsed or primary refractory diffuse large B-cell lymphoma. *Blood, 103*(10), 3684-3688. doi:10.1182/blood-2003-11-3911

Kingston, R. E., Chen, C. A., & Rose, J. K. (2003). Calcium phosphate transfection. *Curr Protoc Mol Biol, Chapter 9*, Unit 9 1. doi:10.1002/0471142727.mb0901s63

Klapper, W., Stoecklein, H., Zeynalova, S., Ott, G., Kosari, F., Rosenwald, A., . . . German High-Grade Non-Hodgkin's Lymphoma Study, G. (2008). Structural aberrations affecting the MYC locus indicate a poor prognosis independent of clinical risk factors in diffuse large B-cell lymphomas treated within randomized trials of the German High-Grade Non-Hodgkin's Lymphoma Study Group (DSHNHL). *Leukemia, 22*(12), 2226-2229. doi:10.1038/leu.2008.230

Komander, D., Clague, M. J., & Urbe, S. (2009). Breaking the chains: structure and function of the deubiquitinases. *Nat Rev Mol Cell Biol, 10*(8), 550-563. doi:10.1038/nrm2731

Kops, G. J., Weaver, B. A., & Cleveland, D. W. (2005). On the road to cancer: aneuploidy and the mitotic checkpoint. *Nat Rev Cancer, 5*(10), 773-785. doi:10.1038/nrc1714

Kridel, R., & Dietrich, P. Y. (2011). Prevention of CNS relapse in diffuse large B-cell lymphoma. *Lancet Oncol, 12*(13), 1258-1266. doi:10.1016/S1470-2045(11)70140-1

Kuppers, R. (2005). Mechanisms of B-cell lymphoma pathogenesis. *Nat Rev Cancer, 5*(4), 251-262. doi:10.1038/nrc1589

Laemmli, U. K. (1970). Cleavage of structural proteins during the assembly of the head of bacteriophage T4. *Nature, 227*(5259), 680-685.

Lara-Gonzalez, P., Westhorpe, F. G., & Taylor, S. S. (2012). The spindle assembly checkpoint. *Curr Biol, 22*(22), R966-980. doi:10.1016/j.cub.2012.10.006

Larouche, J. F., Berger, F., Chassagne-Clement, C., Ffrench, M., Callet-Bauchu, E., Sebban, C., . . . Coiffier, B. (2010). Lymphoma recurrence 5 years or later following diffuse large B-cell lymphoma: clinical characteristics and outcome. *J Clin Oncol, 28*(12), 2094-2100. doi:10.1200/JCO.2009.24.5860

Lenz, G., & Staudt, L. M. (2010). Aggressive lymphomas. *N Engl J Med, 362*(15), 1417-1429. doi:10.1056/NEJMra0807082

Lenz, G., Wright, G., Dave, S. S., Xiao, W., Powell, J., Zhao, H., . . . Lymphoma/Leukemia Molecular Profiling, P. (2008). Stromal gene signatures in large-B-cell lymphomas. *N Engl J Med, 359*(22), 2313-2323. doi:10.1056/NEJMoa0802885

Leonard, J. P., Kolibaba, K. S., Reeves, J. A., Tulpule, A., Flinn, I. W., Kolevska, T., . . . de Vos, S. (2017). Randomized Phase II Study of R-CHOP With or Without Bortezomib in Previously Untreated Patients With Non-Germinal Center B-Cell-Like Diffuse Large B-Cell Lymphoma. *J Clin Oncol, 35*(31), 3538-3546. doi:10.1200/jco.2017.73.2784

LePecq, J. B., & Paoletti, C. (1967). A fluorescent complex between ethidium bromide and nucleic acids. Physical-chemical characterization. *J Mol Biol, 27*(1), 87-106.

Li, Z., Cheng, Z., Raghothama, C., Cui, Z., Liu, K., Li, X., . . . Dang, Y. (2018). USP9X controls translation efficiency via deubiquitination of eukaryotic translation initiation factor 4A1. *Nucleic Acids Res, 46*(2), 823-839. doi:10.1093/nar/gkx1226

Lin, Z., Luo, X., & Yu, H. (2016). Structural basis of cohesin cleavage by separase. *Nature, 532*(7597), 131-134. doi:10.1038/nature17402

Lister, T. A., Crowther, D., Sutcliffe, S. B., Glatstein, E., Canellos, G. P., Young, R. C., . . . Tubiana, M. (1989). Report of a committee convened to discuss the evaluation and staging of patients with Hodgkin's disease: Cotswolds meeting. *J Clin Oncol, 7*(11), 1630-1636. doi:10.1200/JCO.1989.7.11.1630

Liu, H., Chen, W., Liang, C., Chen, B. W., Zhi, X., Zhang, S., . . . Liang, T. (2015). WP1130 increases doxorubicin sensitivity in hepatocellular carcinoma cells through usp9x-dependent p53 degradation. *Cancer Lett, 361*(2), 218-225. doi:10.1016/j.canlet.2015.03.001

Liu, W., Huo, Y., Yang, J., Fu, X., Yang, M., Tao, L., . . . Sun, Y. (2018). Decreased expression of USP9X is associated with poor prognosis in Chinese pancreatic ductal adenocarcinoma patients. *Oncol Lett, 15*(6), 9287-9292. doi:10.3892/ol.2018.8452

Lu, M., Lin, S. C., Huang, Y., Kang, Y. J., Rich, R., Lo, Y. C., . . . Wu, H. (2007). XIAP induces NF-kappaB activation via the BIR1/TAB1 interaction and BIR1 dimerization. *Mol Cell, 26*(5), 689-702. doi:10.1016/j.molcel.2007.05.006

MacFarlane, M., Merrison, W., Bratton, S. B., & Cohen, G. M. (2002). Proteasome-mediated degradation of Smac during apoptosis: XIAP promotes Smac ubiquitination in vitro. *J Biol Chem, 277*(39), 36611-36616. doi:10.1074/jbc.M200317200

Mansouri, A., Zhang, Q., Ridgway, L. D., Tian, L., & Claret, F. X. (2003). Cisplatin resistance in an ovarian carcinoma is associated with a defect in programmed cell death control through XIAP regulation. *Oncol Res, 13*(6-10), 399-404.

Martelli, M., Ferreri, A. J., Agostinelli, C., Di Rocco, A., Pfreundschuh, M., & Pileri, S. A. (2013). Diffuse large B-cell lymphoma. *Crit Rev Oncol Hematol, 87*(2), 146-171. doi:10.1016/j.critrevonc.2012.12.009

Marx, C., Held, J. M., Gibson, B. W., & Benz, C. C. (2010). ErbB2 trafficking and degradation associated with K48 and K63 polyubiquitination. *Cancer Res, 70*(9), 3709-3717. doi:10.1158/0008-5472.CAN-09-3768

Meyer, P. N., Fu, K., Greiner, T. C., Smith, L. M., Delabie, J., Gascoyne, R. D., . . . Weisenburger, D. D. (2011). Immunohistochemical methods for predicting cell of origin and survival in patients with diffuse large B-cell lymphoma treated with rituximab. *J Clin Oncol, 29*(2), 200-207. doi:10.1200/JCO.2010.30.0368

Mikhaeel, N. G., Timothy, A. R., Hain, S. F., & O'Doherty, M. J. (2000). 18-FDG-PET for the assessment of residual masses on CT following treatment of lymphomas. *Ann Oncol, 11 Suppl 1*, 147-150.

Mori, S., Rempel, R. E., Chang, J. T., Yao, G., Lagoo, A. S., Potti, A., . . . Nevins, J. R. (2008). Utilization of pathway signatures to reveal distinct types of B lymphoma in the Emicro-myc model and human diffuse large B-cell lymphoma. *Cancer Res, 68*(20), 8525-8534. doi:10.1158/0008-5472.can-08-1329

Morizane, Y., Honda, R., Fukami, K., & Yasuda, H. (2005). X-linked inhibitor of apoptosis functions as ubiquitin ligase toward mature caspase-9 and cytosolic Smac/DIABLO. *J Biochem, 137*(2), 125-132. doi:10.1093/jb/mvi029

Morton, L. M., Wang, S. S., Devesa, S. S., Hartge, P., Weisenburger, D. D., & Linet, M. S. (2006). Lymphoma incidence patterns by WHO subtype in the United States, 1992-2001. *Blood, 107*(1), 265-276. doi:10.1182/blood-2005-06-2508

Moskowitz, C. H., Zelenetz, A. D., Kewalramani, T., Hamlin, P., Lessac-Chenen, S., Houldsworth, J., . . . Teruya-Feldstein, J. (2005). Cell of origin, germinal center versus nongerminal center, determined by immunohistochemistry on tissue microarray, does not correlate with outcome in patients with relapsed and refractory DLBCL. *Blood, 106*(10), 3383-3385. doi:10.1182/blood-2005-04-1603

Mounier, N., Briere, J., Gisselbrecht, C., Emile, J. F., Lederlin, P., Sebban, C., . . . Coiffier, B. (2003). Rituximab plus CHOP (R-CHOP) overcomes bcl-2--associated resistance to chemotherapy in elderly patients with diffuse large B-cell lymphoma (DLBCL). *Blood, 101*(11), 4279-4284. doi:10.1182/blood-2002-11-3442

Mounier, N., El Gnaoui, T., Tilly, H., Canioni, D., Sebban, C., Casasnovas, R. O., . . . Haioun, C. (2013). Rituximab plus gemcitabine and oxaliplatin in patients with refractory/relapsed diffuse large B-cell lymphoma who are not candidates for high-dose therapy. A phase II Lymphoma Study Association trial. *Haematologica, 98*(11), 1726-1731. doi:10.3324/haematol.2013.090597

Murray, R. Z., Jolly, L. A., & Wood, S. A. (2004). The FAM deubiquitylating enzyme localizes to multiple points of protein trafficking in epithelia, where it associates with E-cadherin and beta-catenin. *Mol Biol Cell, 15*(4), 1591-1599. doi:10.1091/mbc.E03-08-0630

Murtaza, M., Jolly, L. A., Gecz, J., & Wood, S. A. (2015). La FAM fatale: USP9X in development and disease. *Cell Mol Life Sci, 72*(11), 2075-2089. doi:10.1007/s00018-015-1851-0

Musacchio, A., & Salmon, E. D. (2007). The spindle-assembly checkpoint in space and time. *Nat Rev Mol Cell Biol, 8*(5), 379-393. doi:10.1038/nrm2163

Nakatani, Y., Kleffmann, T., Linke, K., Condon, S. M., Hinds, M. G., & Day, C. L. (2013). Regulation of ubiquitin transfer by XIAP, a dimeric RING E3 ligase. *Biochem J, 450*(3), 629-638. doi:10.1042/BJ20121702

Naldini, L., Blomer, U., Gallay, P., Ory, D., Mulligan, R., Gage, F. H., . . . Trono, D. (1996). In vivo gene delivery and stable transduction of nondividing cells by a lentiviral vector. *Science, 272*(5259), 263-267.

Nalepa, G., Rolfe, M., & Harper, J. W. (2006). Drug discovery in the ubiquitin-proteasome system. *Nat Rev Drug Discov, 5*(7), 596-613. doi:10.1038/nrd2056
Navarro, E., Serrano-Heras, G., Castano, M. J., & Solera, J. (2015). Real-time PCR detection chemistry. *Clin Chim Acta, 439*, 231-250. doi:10.1016/j.cca.2014.10.017
Neelapu, S. S., Locke, F. L., Bartlett, N. L., Lekakis, L. J., Miklos, D. B., Jacobson, C. A., . . . Go, W. Y. (2017). Axicabtagene Ciloleucel CAR T-Cell Therapy in Refractory Large B-Cell Lymphoma. *N Engl J Med, 377*(26), 2531-2544. doi:10.1056/NEJMoa1707447
Nijman, S. M., Huang, T. T., Dirac, A. M., Brummelkamp, T. R., Kerkhoven, R. M., D'Andrea, A. D., & Bernards, R. (2005). The deubiquitinating enzyme USP1 regulates the Fanconi anemia pathway. *Mol Cell, 17*(3), 331-339. doi:10.1016/j.molcel.2005.01.008
Nijman, S. M., Luna-Vargas, M. P., Velds, A., Brummelkamp, T. R., Dirac, A. M., Sixma, T. K., & Bernards, R. (2005). A genomic and functional inventory of deubiquitinating enzymes. *Cell, 123*(5), 773-786. doi:10.1016/j.cell.2005.11.007
Nowakowski, G. S., LaPlant, B., Macon, W. R., Reeder, C. B., Foran, J. M., Nelson, G. D., . . . Witzig, T. E. (2015). Lenalidomide combined with R-CHOP overcomes negative prognostic impact of non-germinal center B-cell phenotype in newly diagnosed diffuse large B-Cell lymphoma: a phase II study. *J Clin Oncol, 33*(3), 251-257. doi:10.1200/JCO.2014.55.5714
Oosterkamp, H. M., Hijmans, E. M., Brummelkamp, T. R., Canisius, S., Wessels, L. F., Zwart, W., & Bernards, R. (2014). USP9X downregulation renders breast cancer cells resistant to tamoxifen. *Cancer Res, 74*(14), 3810-3820. doi:10.1158/0008-5472.can-13-1960
Paddison, P. J., Caudy, A. A., Bernstein, E., Hannon, G. J., & Conklin, D. S. (2002). Short hairpin RNAs (shRNAs) induce sequence-specific silencing in mammalian cells. *Genes Dev, 16*(8), 948-958. doi:10.1101/gad.981002
Paddison, P. J., Cleary, M., Silva, J. M., Chang, K., Sheth, N., Sachidanandam, R., & Hannon, G. J. (2004). Cloning of short hairpin RNAs for gene knockdown in mammalian cells. *Nat Methods, 1*(2), 163-167. doi:10.1038/nmeth1104-163
Pantaleon, M., Kanai-Azuma, M., Mattick, J. S., Kaibuchi, K., Kaye, P. L., & Wood, S. A. (2001). FAM deubiquitylating enzyme is essential for preimplantation mouse embryo development. *Mech Dev, 109*(2), 151-160.
Panwalkar, A., Verstovsek, S., & Giles, F. J. (2004). Mammalian target of rapamycin inhibition as therapy for hematologic malignancies. *Cancer, 100*(4), 657-666. doi:10.1002/cncr.20026
Pasqualucci, L., & Dalla-Favera, R. (2015). The genetic landscape of diffuse large B-cell lymphoma. *Semin Hematol, 52*(2), 67-76. doi:10.1053/j.seminhematol.2015.01.005
Pedersen, M. O., Gang, A. O., Poulsen, T. S., Knudsen, H., Lauritzen, A. F., Nielsen, S. L., . . . Norgaard, P. (2014). MYC translocation partner gene determines survival of patients with large B-cell lymphoma with MYC- or double-hit MYC/BCL2 translocations. *Eur J Haematol, 92*(1), 42-48. doi:10.1111/ejh.12212
Peng, J., Hu, Q., Liu, W., He, X., Cui, L., Chen, X., . . . Wang, H. (2013). USP9X expression correlates with tumor progression and poor prognosis in esophageal squamous cell carcinoma. *Diagn Pathol, 8*, 177. doi:10.1186/1746-1596-8-177
Peng, Z., Maxwell, D. S., Sun, D., Bhanu Prasad, B. A., Schuber, P. T., Jr., Pal, A., . . . Bornmann, W. G. (2014). Degrasyn-like symmetrical compounds: possible therapeutic agents for multiple myeloma (MM-I). *Bioorg Med Chem, 22*(4), 1450-1458. doi:10.1016/j.bmc.2013.12.048
Perez-Mancera, P. A., Rust, A. G., van der Weyden, L., Kristiansen, G., Li, A., Sarver, A. L., . . . Tuveson, D. A. (2012). The deubiquitinase USP9X suppresses pancreatic ductal adenocarcinoma. *Nature, 486*(7402), 266-270. doi:10.1038/nature11114
Peters, J. M. (2006). The anaphase promoting complex/cyclosome: a machine designed to destroy. *Nat Rev Mol Cell Biol, 7*(9), 644-656. doi:10.1038/nrm1988
Petersen, F. B., Appelbaum, F. R., Hill, R., Fisher, L. D., Bigelow, C. L., Sanders, J. E., . . . et al. (1990). Autologous marrow transplantation for malignant lymphoma: a report of 101 cases from Seattle. *J Clin Oncol, 8*(4), 638-647. doi:10.1200/JCO.1990.8.4.638
Peterson, L. F., Sun, H., Liu, Y., Potu, H., Kandarpa, M., Ermann, M., . . . Donato, N. J. (2015). Targeting deubiquitinase activity with a novel small-molecule inhibitor as therapy for B-cell malignancies. *Blood, 125*(23), 3588-3597. doi:10.1182/blood-2014-10-605584
Pfreundschuh, M., Schubert, J., Ziepert, M., Schmits, R., Mohren, M., Lengfelder, E., . . . German High-Grade Non-Hodgkin Lymphoma Study, G. (2008). Six versus eight cycles of bi-weekly CHOP-14 with or without rituximab in elderly patients with aggressive CD20+ B-cell lymphomas: a randomised controlled trial (RICOVER-60). *Lancet Oncol, 9*(2), 105-116. doi:10.1016/S1470-2045(08)70002-0

Pfreundschuh, M., Trumper, L., Osterborg, A., Pettengell, R., Trneny, M., Imrie, K., . . . MabThera International Trial, G. (2006). CHOP-like chemotherapy plus rituximab versus CHOP-like chemotherapy alone in young patients with good-prognosis diffuse large-B-cell lymphoma: a randomised controlled trial by the MabThera International Trial (MInT) Group. *Lancet Oncol, 7*(5), 379-391. doi:10.1016/S1470-2045(06)70664-7

Philip, T., Armitage, J. O., Spitzer, G., Chauvin, F., Jagannath, S., Cahn, J. Y., . . . et al. (1987). High-dose therapy and autologous bone marrow transplantation after failure of conventional chemotherapy in adults with intermediate-grade or high-grade non-Hodgkin's lymphoma. *N Engl J Med, 316*(24), 1493-1498. doi:10.1056/NEJM198706113162401

Phillips, G. L., Fay, J. W., Herzig, R. H., Lazarus, H. M., Wolff, S. N., Lin, H. S., . . . et al. (1990). The treatment of progressive non-Hodgkin's lymphoma with intensive chemoradiotherapy and autologous marrow transplantation. *Blood, 75*(4), 831-838.

Pines, J. (2011). Cubism and the cell cycle: the many faces of the APC/C. *Nat Rev Mol Cell Biol, 12*(7), 427-438. doi:10.1038/nrm3132

Poeschel, V., Held, G., Ziepert, M., Altmann, B., Witzens-Harig, M., Holte, H., . . . Pfreundschuh, M. (2018). Excellent Outcome of Young Patients (18-60 years) with Favourable-Prognosis Diffuse Large B-Cell Lymphoma (DLBCL) Treated with 4 Cycles CHOP Plus 6 Applications of Rituximab: Results of the 592 Patients of the Flyer Trial of the Dshnhl/GLA. *Blood, 132*(Supplement 1), 781-781. doi:10.1182/blood-2018-99-112403

Possinger, K. R., A. C. (2015). Aggressive (hoch maligne) Non-Hodgkin-Lymphome. In K. Possinger (Ed.), *Facharztwissen Hämatologie Onkologie* (3. Auflage ed., Vol. 3. Auflage, pp. 461 - 485). Munich: Elsevier, Urban & Fischer

A predictive model for aggressive non-Hodgkin's lymphoma. The International Non-Hodgkin's Lymphoma Prognostic Factors Project. (1993). *N Engl J Med, 329*(14), 987-994. doi:10.1056/NEJM199309303291402

Rajcan-Separovic, E., Liston, P., Lefebvre, C., & Korneluk, R. G. (1996). Assignment of human inhibitor of apoptosis protein (IAP) genes xiap, hiap-1, and hiap-2 to chromosomes Xq25 and 11q22-q23 by fluorescence in situ hybridization. *Genomics, 37*(3), 404-406. doi:10.1006/geno.1996.0579

Ramp, U., Krieg, T., Caliskan, E., Mahotka, C., Ebert, T., Willers, R., . . . Gerharz, C. D. (2004). XIAP expression is an independent prognostic marker in clear-cell renal carcinomas. *Hum Pathol, 35*(8), 1022-1028.

Récher, C., Coiffier, B., Haioun, C., Molina, T. J., Fermé, C., Casasnovas, O., . . . Tilly, H. (2011). Intensified chemotherapy with ACVBP plus rituximab versus standard CHOP plus rituximab for the treatment of diffuse large B-cell lymphoma (LNH03-2B): an open-label randomised phase 3 trial. *Lancet, 378*(9806), 1858-1867. doi:10.1016/s0140-6736(11)61040-4

Rieder, C. L., & Maiato, H. (2004). Stuck in division or passing through: what happens when cells cannot satisfy the spindle assembly checkpoint. *Dev Cell, 7*(5), 637-651. doi:10.1016/j.devcel.2004.09.002

Riedl, S. J., Renatus, M., Schwarzenbacher, R., Zhou, Q., Sun, C., Fesik, S. W., . . . Salvesen, G. S. (2001). Structural basis for the inhibition of caspase-3 by XIAP. *Cell, 104*(5), 791-800.

Rigaud, S., Fondaneche, M. C., Lambert, N., Pasquier, B., Mateo, V., Soulas, P., . . . Latour, S. (2006). XIAP deficiency in humans causes an X-linked lymphoproliferative syndrome. *Nature, 444*(7115), 110-114. doi:10.1038/nature05257

Rosenwald, A., Wright, G., Chan, W. C., Connors, J. M., Campo, E., Fisher, R. I., . . . Lymphoma/Leukemia Molecular Profiling, P. (2002). The use of molecular profiling to predict survival after chemotherapy for diffuse large-B-cell lymphoma. *N Engl J Med, 346*(25), 1937-1947. doi:10.1056/NEJMoa012914

Ruan, J., Martin, P., Furman, R. R., Lee, S. M., Cheung, K., Vose, J. M., . . . Leonard, J. P. (2011). Bortezomib plus CHOP-rituximab for previously untreated diffuse large B-cell lymphoma and mantle cell lymphoma. *J Clin Oncol, 29*(6), 690-697. doi:10.1200/JCO.2010.31.1142

Salles, G., de Jong, D., Xie, W., Rosenwald, A., Chhanabhai, M., Gaulard, P., . . . Weller, E. (2011). Prognostic significance of immunohistochemical biomarkers in diffuse large B-cell lymphoma: a study from the Lunenburg Lymphoma Biomarker Consortium. *Blood, 117*(26), 7070-7078. doi:10.1182/blood-2011-04-345256

Sant, M., Allemani, C., Tereanu, C., De Angelis, R., Capocaccia, R., Visser, O., . . . Group, H. W. (2010). Incidence of hematologic malignancies in Europe by morphologic subtype:

results of the HAEMACARE project. *Blood, 116*(19), 3724-3734. doi:10.1182/blood-2010-05-282632
Savage, K. J., Johnson, N. A., Ben-Neriah, S., Connors, J. M., Sehn, L. H., Farinha, P., . . . Gascoyne, R. D. (2009). MYC gene rearrangements are associated with a poor prognosis in diffuse large B-cell lymphoma patients treated with R-CHOP chemotherapy. *Blood, 114*(17), 3533-3537. doi:10.1182/blood-2009-05-220095
Schile, A. J., Garcia-Fernandez, M., & Steller, H. (2008). Regulation of apoptosis by XIAP ubiquitin-ligase activity. *Genes Dev, 22*(16), 2256-2266. doi:10.1101/gad.1663108
Schmitz, N., Nickelsen, M., Ziepert, M., Haenel, M., Borchmann, P., Schmidt, C., . . . Glass, B. (2012). Conventional chemotherapy (CHOEP-14) with rituximab or high-dose chemotherapy (MegaCHOEP) with rituximab for young, high-risk patients with aggressive B-cell lymphoma: an open-label, randomised, phase 3 trial (DSHNHL 2002-1). *Lancet Oncol, 13*(12), 1250-1259. doi:10.1016/s1470-2045(12)70481-3
Schuster, S. J., Bishop, M. R., Tam, C. S., Waller, E. K., Borchmann, P., McGuirk, J. P., . . . Maziarz, R. T. (2017). Primary Analysis of Juliet: A Global, Pivotal, Phase 2 Trial of CTL019 in Adult Patients with Relapsed or Refractory Diffuse Large B-Cell Lymphoma. *Blood, 130*(Supplement 1), 577-577. doi:10.1182/blood.V130.Suppl_1.577.577
Schwickart, M., Huang, X., Lill, J. R., Liu, J., Ferrando, R., French, D. M., . . . Dixit, V. M. (2010). Deubiquitinase USP9X stabilizes MCL1 and promotes tumour cell survival. *Nature, 463*(7277), 103-107. doi:10.1038/nature08646
Scott, D. W., Mottok, A., Ennishi, D., Wright, G. W., Farinha, P., Ben-Neriah, S., . . . Gascoyne, R. D. (2015). Prognostic Significance of Diffuse Large B-Cell Lymphoma Cell of Origin Determined by Digital Gene Expression in Formalin-Fixed Paraffin-Embedded Tissue Biopsies. *J Clin Oncol, 33*(26), 2848-2856. doi:10.1200/JCO.2014.60.2383
Sehn, L. H. (2012). Paramount prognostic factors that guide therapeutic strategies in diffuse large B-cell lymphoma. *Hematology Am Soc Hematol Educ Program, 2012*, 402-409. doi:10.1182/asheducation-2012.1.402
Sehn, L. H., Donaldson, J., Chhanabhai, M., Fitzgerald, C., Gill, K., Klasa, R., . . . Connors, J. M. (2005). Introduction of combined CHOP plus rituximab therapy dramatically improved outcome of diffuse large B-cell lymphoma in British Columbia. *J Clin Oncol, 23*(22), 5027-5033. doi:10.1200/JCO.2005.09.137
Shaffer, A. L., 3rd, Young, R. M., & Staudt, L. M. (2012). Pathogenesis of human B cell lymphomas. *Annu Rev Immunol, 30*, 565-610. doi:10.1146/annurev-immunol-020711-075027
Shaltiel, I. A., Krenning, L., Bruinsma, W., & Medema, R. H. (2015). The same, only different - DNA damage checkpoints and their reversal throughout the cell cycle. *J Cell Sci, 128*(4), 607-620. doi:10.1242/jcs.163766
Shin, H., Renatus, M., Eckelman, B. P., Nunes, V. A., Sampaio, C. A., & Salvesen, G. S. (2005). The BIR domain of IAP-like protein 2 is conformationally unstable: implications for caspase inhibition. *Biochem J, 385*(Pt 1), 1-10. doi:10.1042/bj20041107
Shiozaki, E. N., Chai, J., Rigotti, D. J., Riedl, S. J., Li, P., Srinivasula, S. M., . . . Shi, Y. (2003). Mechanism of XIAP-mediated inhibition of caspase-9. *Mol Cell, 11*(2), 519-527.
Shivakumar, L., & Armitage, J. O. (2006). Bcl-2 gene expression as a predictor of outcome in diffuse large B-cell lymphoma. *Clin Lymphoma Myeloma, 6*(6), 455-457. doi:10.3816/CLM.2006.n.025
Silke, J., & Vucic, D. (2014). IAP family of cell death and signaling regulators. *Methods Enzymol, 545*, 35-65. doi:10.1016/B978-0-12-801430-1.00002-0
Skaar, J. R., & Pagano, M. (2009). Control of cell growth by the SCF and APC/C ubiquitin ligases. *Curr Opin Cell Biol, 21*(6), 816-824. doi:10.1016/j.ceb.2009.08.004
Spaepen, K., Stroobants, S., Dupont, P., Van Steenweghen, S., Thomas, J., Vandenberghe, P., . . . Verhoef, G. (2001). Prognostic value of positron emission tomography (PET) with fluorine-18 fluorodeoxyglucose ([18F]FDG) after first-line chemotherapy in non-Hodgkin's lymphoma: is [18F]FDG-PET a valid alternative to conventional diagnostic methods? *J Clin Oncol, 19*(2), 414-419. doi:10.1200/JCO.2001.19.2.414
Spina, M., Balzarotti, M., Uziel, L., Ferreri, A. J., Fratino, L., Magagnoli, M., . . . Tirelli, U. (2012). Modulated chemotherapy according to modified comprehensive geriatric assessment in 100 consecutive elderly patients with diffuse large B-cell lymphoma. *Oncologist, 17*(6), 838-846. doi:10.1634/theoncologist.2011-0417

Stiff, P. J., Unger, J. M., Cook, J. R., Constine, L. S., Couban, S., Stewart, D. A., . . . Fisher, R. I. (2013). Autologous transplantation as consolidation for aggressive non-Hodgkin's lymphoma. *N Engl J Med, 369*(18), 1681-1690. doi:10.1056/NEJMoa1301077

Swerdlow, S. H., Campo, E., Harris, N.L., Jaffe, E.S., Pileri, S.A., Stein, H., Thiele, J., Vardiman, J.W. (2008). *World Health Organization Classification of Tumours of Haematopoietic and Lymphoid Tissues, Fourth Edition* (Fourth Edition ed.). Lyon: World Health Organization; Auflage: 4th ed., 2008. (3. Januar 2008).

Tamm, I., Kornblau, S. M., Segall, H., Krajewski, S., Welsh, K., Kitada, S., . . . Reed, J. C. (2000). Expression and prognostic significance of IAP-family genes in human cancers and myeloid leukemias. *Clin Cancer Res, 6*(5), 1796-1803.

Taya, S., Yamamoto, T., Kanai-Azuma, M., Wood, S. A., & Kaibuchi, K. (1999). The deubiquitinating enzyme Fam interacts with and stabilizes beta-catenin. *Genes Cells, 4*(12), 757-767.

Tilly, H., Gomes da Silva, M., Vitolo, U., Jack, A., Meignan, M., Lopez-Guillermo, A., . . . Committee, E. G. (2015). Diffuse large B-cell lymphoma (DLBCL): ESMO Clinical Practice Guidelines for diagnosis, treatment and follow-up. *Ann Oncol, 26 Suppl 5*, v116-125. doi:10.1093/annonc/mdv304

Topham, C. H., & Taylor, S. S. (2013). Mitosis and apoptosis: how is the balance set? *Curr Opin Cell Biol, 25*(6), 780-785. doi:10.1016/j.ceb.2013.07.003

van Imhoff, G. W., Boerma, E. J., van der Holt, B., Schuuring, E., Verdonck, L. F., Kluin-Nelemans, H. C., & Kluin, P. M. (2006). Prognostic impact of germinal center-associated proteins and chromosomal breakpoints in poor-risk diffuse large B-cell lymphoma. *J Clin Oncol, 24*(25), 4135-4142. doi:10.1200/JCO.2006.05.5897

Vaux, D. L., & Silke, J. (2005). IAPs--the ubiquitin connection. *Cell Death Differ, 12*(9), 1205-1207. doi:10.1038/sj.cdd.4401696

Vitolo, U., Chiappella, A., Franceschetti, S., Carella, A. M., Baldi, I., Inghirami, G., . . . Fondazione Italiana, L. (2014). Lenalidomide plus R-CHOP21 in elderly patients with untreated diffuse large B-cell lymphoma: results of the REAL07 open-label, multicentre, phase 2 trial. *Lancet Oncol, 15*(7), 730-737. doi:10.1016/S1470-2045(14)70191-3

Vong, Q. P., Cao, K., Li, H. Y., Iglesias, P. A., & Zheng, Y. (2005). Chromosome alignment and segregation regulated by ubiquitination of survivin. *Science, 310*(5753), 1499-1504. doi:10.1126/science.1120160

Vose, J. M., Sharp, G., Chan, W. C., Nichols, C., Loh, K., Inwards, D., . . . Armitage, J. O. (2002). Autologous transplantation for aggressive non-Hodgkin's lymphoma: results of a randomized trial evaluating graft source and minimal residual disease. *J Clin Oncol, 20*(9), 2344-2352. doi:10.1200/JCO.2002.09.138

Wang, X., Mazurkiewicz, M., Hillert, E. K., Olofsson, M. H., Pierrou, S., Hillertz, P., . . . D'Arcy, P. (2016). The proteasome deubiquitinase inhibitor VLX1570 shows selectivity for ubiquitin-specific protease-14 and induces apoptosis of multiple myeloma cells. *Sci Rep, 6*, 26979. doi:10.1038/srep26979

Weissman, A. M., Shabek, N., & Ciechanover, A. (2011). The predator becomes the prey: regulating the ubiquitin system by ubiquitylation and degradation. *Nat Rev Mol Cell Biol, 12*(9), 605-620. doi:10.1038/nrm3173

Wertz, I. E., Kusam, S., Lam, C., Okamoto, T., Sandoval, W., Anderson, D. J., . . . Dixit, V. M. (2011). Sensitivity to antitubulin chemotherapeutics is regulated by MCL1 and FBW7. *Nature, 471*(7336), 110-114. doi:10.1038/nature09779

Wiernik, P. H., Lossos, I. S., Tuscano, J. M., Justice, G., Vose, J. M., Cole, C. E., . . . Habermann, T. M. (2008). Lenalidomide monotherapy in relapsed or refractory aggressive non-Hodgkin's lymphoma. *J Clin Oncol, 26*(30), 4952-4957. doi:10.1200/JCO.2007.15.3429

Witzig, T. E., LaPlant, B., Habermann, T. M., McPhail, E., Inwards, D. J., Micallef, I. N., . . . Johnston, P. B. (2017). High rate of event-free survival at 24 months with everolimus/RCHOP for untreated diffuse large B-cell lymphoma: updated results from NCCTG N1085 (Alliance). *Blood Cancer J, 7*(6), e576. doi:10.1038/bcj.2017.57

Witzig, T. E., Reeder, C. B., LaPlant, B. R., Gupta, M., Johnston, P. B., Micallef, I. N., . . . Habermann, T. M. (2011). A phase II trial of the oral mTOR inhibitor everolimus in relapsed aggressive lymphoma. *Leukemia, 25*(2), 341-347. doi:10.1038/leu.2010.226

Xi, G., Hu, X., Wu, B., Jiang, H., Young, C. Y., Pang, Y., & Yuan, H. (2011). Autophagy inhibition promotes paclitaxel-induced apoptosis in cancer cells. *Cancer Lett, 307*(2), 141-148. doi:10.1016/j.canlet.2011.03.026

Yamaguchi, M., Nakamura, N., Suzuki, R., Kagami, Y., Okamoto, M., Ichinohasama, R., . . . Nakamura, S. (2008). De novo CD5+ diffuse large B-cell lymphoma: results of a detailed clinicopathological review in 120 patients. *Haematologica, 93*(8), 1195-1202. doi:10.3324/haematol.12810

Yamamoto, S., Seta, K., Morisco, C., Vatner, S. F., & Sadoshima, J. (2001). Chelerythrine rapidly induces apoptosis through generation of reactive oxygen species in cardiac myocytes. *J Mol Cell Cardiol, 33*(10), 1829-1848. doi:10.1006/jmcc.2001.1446

Younes, A., Sehn, L. H., Johnson, P., Zinzani, P. L., Hong, X., Zhu, J., . . . Wilson, W. (2019). Randomized Phase III Trial of Ibrutinib and Rituximab Plus Cyclophosphamide, Doxorubicin, Vincristine, and Prednisone in Non-Germinal Center B-Cell Diffuse Large B-Cell Lymphoma. *J Clin Oncol, 37*(15), 1285-1295. doi:10.1200/jco.18.02403

Younes, A., Thieblemont, C., Morschhauser, F., Flinn, I., Friedberg, J. W., Amorim, S., . . . Oki, Y. (2014). Combination of ibrutinib with rituximab, cyclophosphamide, doxorubicin, vincristine, and prednisone (R-CHOP) for treatment-naive patients with CD20-positive B-cell non-Hodgkin lymphoma: a non-randomised, phase 1b study. *Lancet Oncol, 15*(9), 1019-1026. doi:10.1016/S1470-2045(14)70311-0

Yuan, T., Yan, F., Ying, M., Cao, J., He, Q., Zhu, H., & Yang, B. (2018). Inhibition of Ubiquitin-Specific Proteases as a Novel Anticancer Therapeutic Strategy. *Front Pharmacol, 9*, 1080. doi:10.3389/fphar.2018.01080

Zelenetz, A. D. (2014). Guidelines for NHL: updates to the management of diffuse large B-cell lymphoma and new guidelines for primary cutaneous CD30+ T-cell lymphoproliferative disorders and T-cell large granular lymphocytic leukemia. *J Natl Compr Canc Netw, 12*(5 Suppl), 797-800.

Zhang, S., Ding, F., Luo, A., Chen, A., Yu, Z., Ren, S., . . . Zhang, L. (2007). XIAP is highly expressed in esophageal cancer and its downregulation by RNAi sensitizes esophageal carcinoma cell lines to chemotherapeutics. *Cancer Biol Ther, 6*(6), 973-980.

Zhou, M., Wang, T., Lai, H., Zhao, X., Yu, Q., Zhou, J., & Yang, Y. (2015). Targeting of the deubiquitinase USP9X attenuates B-cell acute lymphoblastic leukemia cell survival and overcomes glucocorticoid resistance. *Biochem Biophys Res Commun, 459*(2), 333-339. doi:10.1016/j.bbrc.2015.02.115

Ziepert, M., Hasenclever, D., Kuhnt, E., Glass, B., Schmitz, N., Pfreundschuh, M., & Loeffler, M. (2010). Standard International prognostic index remains a valid predictor of outcome for patients with aggressive CD20+ B-cell lymphoma in the rituximab era. *J Clin Oncol, 28*(14), 2373-2380. doi:10.1200/JCO.2009.26.2493

Zinzani, P. L., Dirnhofer, S., Sabattini, E., Alinari, L., Piccaluga, P. P., Stefoni, V., . . . Pileri, S. A. (2005). Identification of outcome predictors in diffuse large B-cell lymphoma. Immunohistochemical profiling of homogeneously treated de novo tumors with nodal presentation on tissue micro-arrays. *Haematologica, 90*(3), 341-347.

Zinzani, P. L., Pellegrini, C., Argnani, L., & Broccoli, A. (2016). Prolonged disease-free survival in elderly relapsed diffuse large B-cell lymphoma patients treated with lenalidomide plus rituximab. *Haematologica, 101*(9), e385-386. doi:10.3324/haematol.2016.147256

Zinzani, P. L., Pellegrini, C., Gandolfi, L., Stefoni, V., Quirini, F., Derenzini, E., . . . Baccarani, M. (2011). Combination of lenalidomide and rituximab in elderly patients with relapsed or refractory diffuse large B-cell lymphoma: a phase 2 trial. *Clin Lymphoma Myeloma Leuk, 11*(6), 462-466. doi:10.1016/j.clml.2011.02.00

8. List of figures and tables

8.1. List of figures

8.2. List of tables

9. Publications

Katharina Engel, Martina Rudelius, Jolanta Slawska, Laura Jacobs, Behnaz, Ahangarian Abhari, Bettina Altmann, Julia Kurutz, Abirami Rathakrishnan, Vanesa Fernández‐Sáiz, Andrä Brunner, Bianca‐Sabrina Targosz, Felicia Loewecke, Christian Johannes Gloeckner, Marius Ueffing, Simone Fulda, Michael Pfreundschuh, Lorenz Trümper, Wolfram Klapper, Ulrich Keller, Philipp J Jost, Andreas Rosenwald, Christian Peschel, Florian Bassermann: *USP9X stabilizes XIAP to regulate mitotic cell death and chemoresistance in aggressive B‐cell lymphoma.* EMBO Molecular Medicine (2016).

10. Acknowledgement

I would like to thank Prof. Dr. med. Florian Bassermann, who gave me the opportunity to work in his laboratory and on this exciting project. I am especially grateful to him for his feedback, his great ideas and his thriving motivation. I would also like to thank Dr. med. Katharina Engel, who was my mentor during the project. She introduced me to the various laboratory techniques and I am grateful for her constant feedback. My thanks also go to all other laboratory members for their constant support and advice.

I would also like to thank my husband Arvid for his incredible patience, understanding und support at all times. Finally, I am also deeply grateful to my parents and my aunt for supporting me and believing in me, especially in times when I did not believe in myself.